# Neurotoxic impact of protein fragmentation and aggregation in tauopathy mouse models

**Inauguraldissertation**

zur

Erlangung der Würde eines Doktors der Philosophie

vorgelegt der

Philosophisch-Naturwissenschaftlichen Fakultät

der Universität Basel

von

**Frederik Sprenger**

Aus Salzkotten, Deutschland

Basel, 2017

Genehmigt von der Philosophisch-Naturwissenschaftlichen Fakultät

auf Antrag von

| | |
|---|---|
| Fakultätsverantwortlicher: | Prof. Dr. Markus Rüegg |
| Dissertationsleiter: | PD Dr. Dr. David T. Winkler |
| Koreferent: | Prof. Dr. Bernhard Bettler |

Basel, den 18.04.2017

_____

*Unterschrift des Fakultätsverantwortlichen*

Prof. Dr. Martin Spiess

(Dekan)

# Preface

The following dissertation was written by the author. The “Introduction” is based on an extended version of a review manuscript in preparation (Sprenger, Winkler, 2017 expected). The “Results” section consists of two published manuscripts and additional preliminary data. In the co-first-authorship publication (Ozcelik, Sprenger et al., 2016) the author significantly contributed to experiments, analysis, and writing process. In the second co-author publication (Skachokova , Sprenger et al., 2015) the author contributed to some analysis and final writing. The additional data section is the result of own work.

# Acknowledgements

My most heartfelt thanks go to my boss, David Winkler, for his valuable mentoring and his substantial support.

I would like to express my deep gratitude to Markus Tolnay and Stephan Frank for their support of my work.

I am grateful to our collaborators, in particular Michel Goedert and Graham Fraser, for their expertise.

I particularly wish to thank colleagues and technicians, for their useful discussions, advices, and practical support throughout my work. My special thanks are extended to the staff at the ZLF animal facility for their support.

Finally, I wish to thank my family, my wife Lima and my son Sam. Thank you for everything that make this possible.

# Abstract

The microtubule-associated protein tau and its pathological modification constitute the central pathology of various human neurodegenerative diseases, including Alzheimer's disease (AD), collectively termed 'tauopathies'. Abundant hyperphosphorylation and aggregation of tau is a disease-defining hallmark, yet the underlying pathogenic and pathophysiological processes have remained only partly understood. In addition, protein fragmentation is a frequently observed phenomenon in the course of various neurodegenerative diseases; however, the contribution of tau fragmentation to the pathogenesis of tauopathies is still a matter of debate.

In our novel inducible mouse model, co-expression of truncated and full-length human tau provokes axonal transport failure, mitochondrial mislocalization, disruption of the Golgi apparatus and dysregulation of synaptic proteins associated with extensive nerve cell loss and a severe neurological phenotype as early as 3 weeks of age. Of note, this was paralleled only by the formation of soluble oligomeric tau species, and no insoluble filamentous tau aggregates; therewith, identifying oligomeric tau species as toxic key players in tau pathology. Despite continuous full-length tau expression, mice recovered from the neurotoxic insult once truncated tau expression was halted. The induction of drastic but reversible neurotoxicity highlights the neurotoxic potential of tau fragments as pathogenic mediators in neurodegenerative disorders.

The present work implicates the complexity of protein fragmentation and oligomerization and their neurotoxic impact in the context of tauopathies and aims for a better understanding of the cellular mechanisms underlying tau toxicity.

# Index

# 1 Introduction

## 1.1 Chapter 1

## Tau protein and neurodegeneration

### 1.1.1 Neurodegeneration

In human beings, neurodegenerative diseases are commonly characterized by progressive dysfunction and decease of neurons associated with pathological deposits of altered proteins in the brain as well as in peripheral organs. In patients with neurological disorders, the clinical manifestations caused by malfunction of individual gene expression products correlate with the affected brain regions, linking a particular disease-type to its predominant phenotype. Unique pathological conformers or misfolded proteins with modified native physiological properties are integral parts and the core concept of diverse human 'proteinopathies'; nevertheless, the understanding of the cellular and molecular bases underlying the pathogenesis of neurodegenerative diseases gradually widened over the years, yet being far from fully disclosed.

The pathological conformation and subsequent aggregation of proteins is not solely responsible for neuronal degeneration, rather a complex network of **molecular events** ultimately leading to progressive neuronal dysfunction and death. For instance, the **ubiquitine**

**proteasome system** (UPS) and **autophagy-lysosomal pathways**, as major mechanisms for degradation of numerous proteins, have been found to be relevant for the genesis and progression of several neurodegenerative diseases (Keller et al., 2000; Nixon, 2007; reviewed in Oddo, 2008; Pickford et al., 2008). Indeed, various aggregated proteins as well as induction of proteasome inhibitors have been shown to interfere with the highly regulated cell physiology by impairing UPS function (Bence et al., 2001; David et al., 2002; Gregori et al., 1995; Keck et al., 2003; Lee et al., 2010; Snyder et al., 2003; Tseng et al., 2007). In contrast to their ability of non-aggregated and soluble unfolded protein degradation, oligomeric or aggregated species are rather inaccessible to the catalytic core of the UPS; an efficient autophagy-lysosomal machinery is needed to degrade aggregation-prone proteins, thereby preventing neuropathological processes (Anglade et al., 1997; Boland et al., 2008; Qin et al., 2003). In addition, stimulation of autophagy has been shown to reduce the generation of pathological protein inclusions in nerve cells (Ozcelik et al., 2013; Schaeffer et al., 2012; Wang et al., 2009b).

Aside further neurodegenerative disease-causing processes such as glutamate-induced **exocytoxic insults** (Marchetti et al., 2004) or **neuroinflammatory processes** (Harry et al., 2000), another event detrimental to neuronal homeostasis is **mitochondrial injury** by neurodegeneration-associated proteins; mitochondrial dysfunction, i.e. in terms of impaired mitochondrial trafficking inside neurons (Rui et al., 2010; Rui et al., 2006) or alterations in mitochondrial dynamics (Wang et al., 2009a), is crucially linked to **oxidative** and **nitrosativ stress** (Cho et al., 2009; Hirai et al., 2001; Lustbader et al., 2004), contributing to neuropathological processes.

### 1.1.2 Protein fragmentation and neurodegeneration

Protein fragmentation is a frequently observed phenomenon in the course of various neurodegenerative processes. Indeed, small, aggregation prone cleaved proteins are integral parts of a plethora of disorders including Alzheimer's diseases (AD); familial British and Danish dementia (FBD, FDD); Parkinson's diseases (PD); TDP-43 related disorders; and in other triplet expansion disorders such as Huntington disease (HD) and spinocerebellar-ataxias (SCAs). The initiation of fragmentation remains mostly elusive; mutations represent the cause of altered

cleavage in some hereditary variants of neurodegenerative diseases such as presenilin mutations in AD or the frame shift mutations in FBD; by contrast, in most sporadic forms the cause for increased or aberrant fragmentation is simply not known.

However, the contribution of protein fragmentation to the pathogenesis of proteinopathies is not always evident and the neurotoxic potential of cleavage products is still a matter of debate. Cleavage occurs at multiple sites of single large proteins with researchers consider the question of a causal relationship between protein fragmentation and disease, or whether fragmentation just being an epiphenomenon. Protein aggregates in neurodegenerative disorders may either consist of (I) fragments alone derived from larger precursor proteins: as in case of amyloid-β (Aβ) in AD or amyloid-Bri (ABri) in FBD (Vidal et al., 1999); or they comprise (II) full-length and fragmented proteins in parallel: as in case of α-synuclein (α-Syn) in PD (Dufty et al., 2007; Liu et al., 2005) or in TDP-43 related disorders (Neumann et al., 2006; Zhang et al., 2009b).

Neurodegeneration-associated proteins can be substrate to a plethora of proteolytic enzymes including members of the α-, β-, and $\gamma$-secretase families as well as cysteine proteases. Aside thrombin (Arai et al., 2005), cathepsins (Kenessey et al., 1997) and puromycin-sensitive aminopeptidase (PSA) (Sengupta et al., 2006), members of the caspase and calpain family are the most prominent enzymes involved in tau protein cleavage and therefore of particular interest in the present work.

### 1.1.3 Caspases and calpains and neurodegeneration

**Caspases** are intracellular **c**ysteine-**asp**artatic-specific prote**ases** that cleave their substrates at specific sites. First expressed as latent zymogens, these pro-caspases get post-translationally activated that either can lead to the inactivation of the substrate or to a toxic gain of function in the form of active protein fragments in the proteolytic process. Aside other non-apoptotic and pro-inflammatory members, apoptotic caspases can be subdivided into (I) initiator caspases (caspases-2, 8, 9 and 10) that, in response to a stimulus, direct the signal to (II) executioner caspases (caspases-3, 6, and 7) (Pop and Salvesen, 2009). These caspase candidates are associated with programmed apoptotic cell death in various neurodegenerative disorders including AD, HD, and PD. Also, **calpains** are intracellular

**cal**cium-activated (pa**pain**-like) neutral proteases and have been implicated in the pathogenesis of neurodegenerative diseases such as AD or PD; although their calcium-induced apoptotic role is less characterized compared to that of apoptotic caspases.

Multiple neurodegeneration-related proteins are substrate to caspase- and calpain-mediated cleavage. Indeed, caspases-3 (Metcalfe et al., 2012), caspase-6, and calpains are the main enzymes involved in **tau protein fragmentation**, with the Asp421 being the most prominent caspase cleavage site (for review see Avila, 2010; Fasulo et al., 2005; Guillozet-Bongaarts et al., 2005; Guo et al., 2004) (Figure 1.1). Furthermore, site-directed mutagenesis at two caspase-7 cleavage sites of neurotoxic ataxin-7 protein in Spinocerebellar ataxia type 7 (SCA7) polyglutamine (polyQ) disorder results in a non-cleavable form of polyQ-expanded ataxin-7 displaying attenuated neuronal death, aggregate formation, and transcriptional interference (Young et al., 2007). Of note, caspase-3 and caspase-6 have been implicated in cytoskeletal disintegration through actin and tubulin cleavage ultimately leading to axonal degeneration *in vitro* and *in vivo* (Sokolowski et al., 2014). Aside, calpain activation has been demonstrated to play a crucial role in Aβ-triggered pathological cascade in AD (Higuchi et al., 2012). Moreover, N-terminal calpain cleaved ataxin-3 fragment has been shown to provoke altered behavioural and motor phenotype associated with pathological protein inclusions and nerve cell death *in vivo* (Hubener et al., 2011).

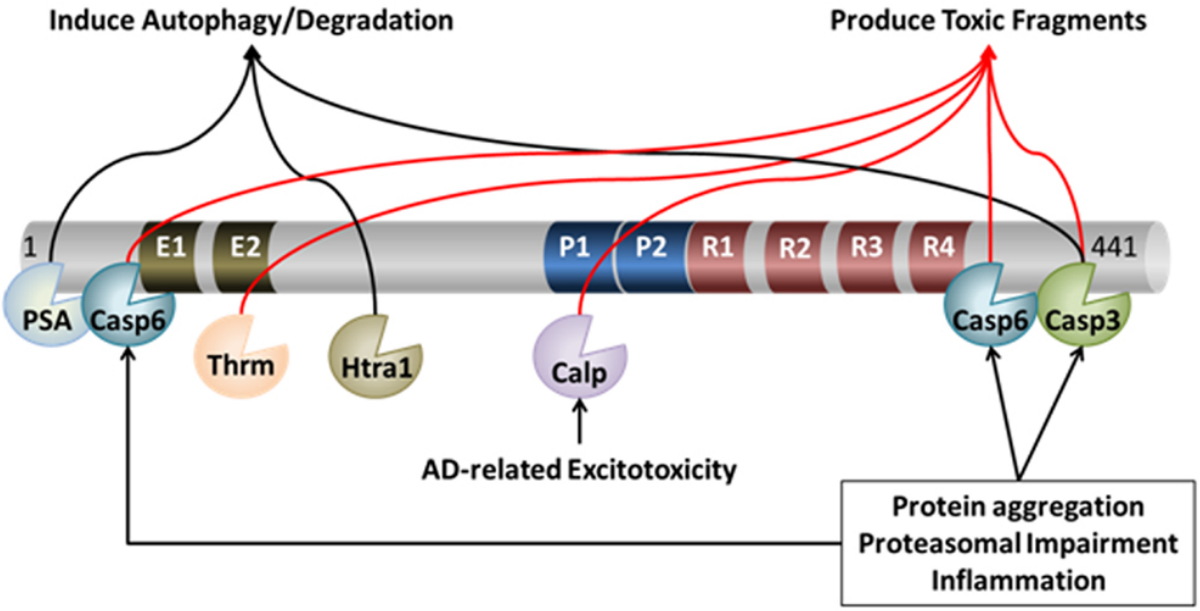


**Figure 1.1 Proteolytic processing of tau.** Caspase and calpains are the main proteases involved in tau protein cleavage. Truncation of tau at distinct proteolytic cleavage sites can either lead to preservation of neuronal structure and/or function, and/or exacerbation of tau toxicity. (Chesser et al., 2013)

### 1.1.4 Neurodegenerative disease-associated proteins

A wide variety of cellular and molecular events can be ascribed to the individual pathological profile of a vast number of neurodegenerative diseases. However, pathologically altered proteins including their characteristic structure and morphology remain to be the most prominent entity. Proteins that undergo fragmentation in parallel to pathological aggregation are not only found in neurodegenerative proteopathies, but also in systemic amyloidosis. Proteinopathies with associated protein fragmentation include:

(I) The microtubule-associated protein **tau** that is encoded by a gene (*MAPT*) located on chromosome 17 (Weingarten et al., 1975);

(II) The **amyloid-beta** peptide (Aβ) that is encoded by a gene (*APP*) located in chromosome 21 (Alzheimer, 1906, 1907; Kang et al., 1987; Tanzi et al., 1987);

(III) The **amyloid-Bri** (ABri) and **amyloid-Dan** (ADan) peptides that are both encoded by a gene (*BRI*) located on chromosome 13 (Vidal et al., 1999; Vidal et al., 2000);

(IV) The neuronal protein **alpha-synuclein** (α-Syn) that is encoded by a gene (*SNCA*) located on chromosome 4 (Spillantini et al., 1997);

(V) Proteins encoded by genes linked to cytosine-adenine-guanine (CAG) trinucleotide repeats including **huntingtin** (Htt), **ataxins** (1, 2, 3, 6, 7, and 17), and **atrophin-1** (Fan et al., 2014);

(VI) **Prion protein** (PrP) that is encoded by a gene (*PRNP*) located on chromosome 20 (Aguzzi and O'Connor, 2010);

(VII) Transactive response (**TAR) DNA-binding protein 43** (TDP-43) that is encoded by a gene (*TARDBP)* located on chromosome 1 (Ou et al., 1995);

(VIII) And others including proteins that belong to the **FET** family including (**F)used in sarcoma protein** (FUS), (**E)wing's sarcoma protein** (EWS), (**T)ATA-binding protein-associated factor 15** (TAF15) (Kwiatkowski et al., 2009; Law et al., 2006); **charged multivescular body protein 2B** (CHMP2B) (Ghazi-Noori et al., 2012) ; glycoprotein **reelin** (D'Arcangelo et al., 1997); globular protein **transthyretin** (TTR) (Conceicao et al., 2016); actin binding protein **gelsolin** (Chen et al., 2001; Solomon et al., 2012); hormone **islet** amyloid peptide (IAPP) (Akter et al., 2016); and human **serum amyloid A** (SAA) (Egashira et al., 2011).

The most notable neurodegeneration-associated proteins will be addressed in the following paragraphs; however, the tau protein and its role in tauopathies and the neuropathological relevance of protein fragmentation will be of particular interest.

### 1.1.5 Tau protein

Tau belongs to the natively unfolded microtubule-associated protein family (MAP) and is abundant in the central and peripheral nervous system. In the 1970s, a microtubule binding activity of tau protein has first been shown by Weingarten et al., who isolated a heat stable protein most abundantly found to promote microtubule assembly and stability in cell-free conditions (Weingarten et al., 1975). Microtubules are protein polymers and a major component of the cytoskeleton with an essential role in regulated motor-driven axonal transport. Later, evidence from brains of patients with AD suggested that tau is actual an integral part of the pathology in neurodegenerative disorders (Goedert et al., 1988; Grundke-Iqbal et al., 1986; Kondo et al., 1988; Kosik et al., 1986; Wischik et al., 1988a). Efforts for a better understanding of the physiological role and identity of tau protein have been intensified since.

#### 1.1.5.1 Cellular localization and domain organization of tau

The tau protein, synthesized and produced in all neurons, is predominantly found in axons (Binder et al., 1985). However, it also has been shown to be located in the dendritic compartment albeit in lower concentration as well as under pathological conditions in the somatodendritic domain (Ittner et al., 2010). Structurally, tau is a naturally unfolded protein that contains **four major regions**. Once tau is bound to multiple tubulin dimers, the **N-terminal acidic projection region** protrudes outward from the surface of the microtubule and in this way, being able to serve as a spacer between the individual components within the microtubule network (Chen et al., 1992; Frappier et al., 1994). Furthermore, it was found that this region appears to interact with membrane-binding proteins such as annexin A2 (AnxA2) and thus retain the tau protein at the distal tip of neurites (Brandt et al., 1995; Gauthier-

Kemper et al., 2011; Weissmann et al., 2009). The **proline-rich region** (PRR) harbours many phosphorylation sites and contributes to the microtubule-binding affinity of tau (Augustinack et al., 2002; Biernat et al., 1992; Brandt and Lee, 1993; Goode et al., 1997). Moreover, it enables interaction with other proteins such as the SH3 domain containing tyrosine kinase Fyn (Lee et al., 1998). The **C-terminal region** of tau contains a microtubule binding domain (MTB) composed of 18-amino acid (aa) tandem repeats separated by sequences of 13- or 14-aa that encourage tau to bind to the microtubules and a **short tail sequence**, which is involved in the regulation of microtubule polymerization (Brandt and Lee, 1993; Lee et al., 1988; Lee et al., 1989).

#### 1.1.5.2 Tau isoforms

The tau protein is encoded by a single gene that contains a total of 16 exons (Andreadis et al., 1992). **Six isoforms** of tau are expressed in the adult human brain (Goedert et al., 1989). Produced by complex alternative mRNA splicing of the *MAPT* gene located on chromosome 17q21.31, each isoform differs in its specific representation as such in the presence or absence of both, **amino-terminal inserts** (0N, 1N, 2N) and **carboxy-terminal microtubule-binding repeat domains** (3R, 4R). Thus, splicing of the neuron-specific tau transcript at two 29- or 58-aa inserts and one 31-aa repeat domain encoded by exons 2, 3 and 10, respectively, results in a set of proteins with the range from 352-aa in length for 3R0N, 381 for 3R1N and 410 for 3R2N to 383-aa in length for 4R0N, 412 for 4R1N and 441 for 4R2N (Figure 1.2).

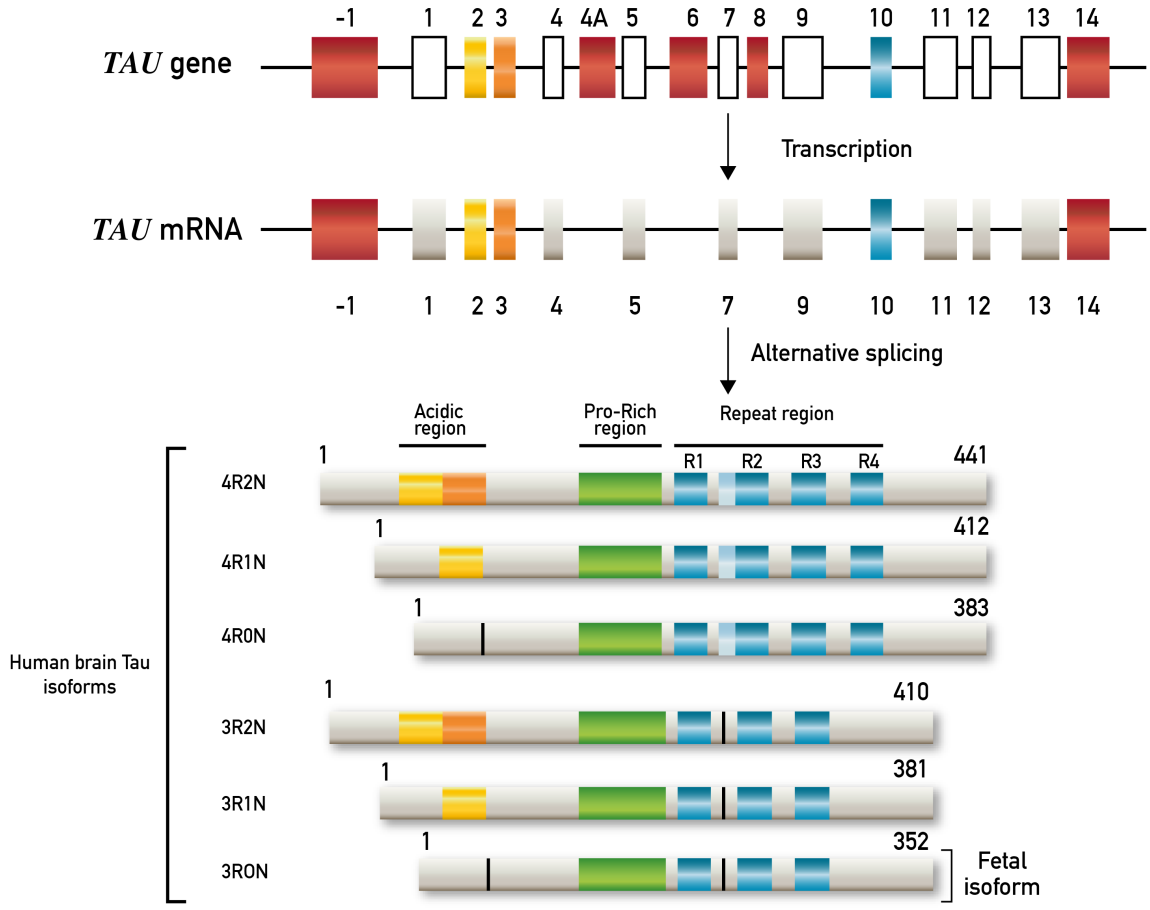


**Figure 1.2 Schematic representation of the human TAU gene, TAU mRNA, and the six tau protein isoforms.** Six isoforms are generated through alternative splicing in the adult human brain. (Adapted from Buee et al., 2000)

### 1.1.5.3 Tau function

Tau, as a natively unfolded protein, lacks a well-defined secondary or tertiary structure that allows the protein to interact with a variety of partners in the environment of a cell (Schweers et al., 1994). The main physiological function of tau is **stabilization of the microtubule network** by promoting the polymerization of tubulin and thus the maintenance of normal axonal transport (Bohm et al., 1990; Brandt and Lee, 1993; Cleveland et al., 1977; Shahani and Brandt, 2002; Weingarten et al., 1975). As a main cytoskeleton component, microtubules contribute to morphogenesis, division and intracellular trafficking in the cell (Mitchison and Kirschner, 1984).

At any given moment, about 80% of tau is in direct interaction with microtubules (Weissmann et al., 2009). Tau binding to microtubules is regulated by a delicate equilibrium of kinases and phosphatases and both, over-stabilization by tau or detached tau from the microtubule can impair cell viability (Bramblett et al., 1993; Panda et al., 2003; Thies and Mandelkow, 2007; Wang et al., 2007).

In fact, neuronal function is critically dependent on an intact microtubule network. Specific cellular compartments such as the pre- and post-synaptic cell structures have high energy requirements and accumulated waste products to manage; therefore, cellular motors of the kinesin and dynein superfamily utilize energy derived from ATP hydrolysis to transport cargo-filled vesicles over long distances on microtubule tracks in the axon (De Vos et al., 2008). In this way, mitochondria (Hollenbeck and Saxton, 2005), lysosomes (Harada et al., 1998), peroxisomes (Wali et al., 2016) and various other organelles can be localized to distinct areas in the neuronal realm in order to accomplish their very own function. The tight binding of tau alters the intracellular traffic as well as ensures the dynamic instability of microtubules (Mitchison and Kirschner, 1984; Trinczek et al., 1995). The latter is distinguished by their capability to switch between slow growth and rapid shrinking during microtubule growth (Binder et al., 1985; Mitchison and Kirschner, 1984). Aside from its predominant neurophysiological activity – binding to microtubule – numerous functions have been attributed to tau. Among them, modulation of biochemical cascades, such that tau can act as a protein scaffold (Brandt et al., 1995; Ittner et al., 2010; Reynolds et al., 2008) or direct enzyme inhibitor (Perez et al., 2009). In parallel, tau appears to interact with nucleic acids as well as mitochondria (Jancsik et al., 1989; Kampers et al., 1996; Loomis et al., 1990; Sultan et al., 2011); suggesting a role as a multifunctional communication instrument within the cell.

#### 1.1.5.4 Post-translational modifications of tau

In physiological conditions and untypically for most cytosolic proteins, tau resists a compact folded structure; the entire tau molecule is considered to be intrinsically disordered and its function is tightly regulated by a host of post-translational modification such as phosphorylation (Grundke-Iqbal et al., 1986), acetylation (Cohen et al., 2011), glycosylation (Gong et al., 2005), glycation (Ledesma et al., 1994), sumoylation (Dorval and Fraser, 2006),

ubiquitination (Mori et al., 1987), nitration (Reynolds et al., 2006), and truncation (Gamblin et al., 2003; Wischik et al., 1988b). The contribution of various cellular mechanisms to tau pathogenesis are not known and it has yet remained unclear, which modification is crucial for the development of tauopathies.

The individual post-translational modifications of tau can only be outlined in the present work; however, **tau phosphorylation** (I) and **tau truncation** (II) will be discussed in detail in the following paragraph.

#### 1.1.5.4.1 Tau phosphorylation

Tau phosphorylation occurs in both pathological and physiological conditions. It was found that isolated tau molecules from healthy human brains contained roughly two moles of phosphate per mole of tau, whereas tau proteins associated with paired helical filaments (PHFs) of patients with AD contained six to eight moles of phosphate per mole of tau (Ksiezak-Reding et al., 1992).

Given the loose disordered character of tau, many known potential phosphorylation sites are sensitive to numerous protein kinases and phosphatases; indeed, these phosphorylatable domains consist of 80 serine and threonine residues and five tyrosine residues are key players in the regulation of the microtubule binding activity of tau (Figure 1.3). The most prominent candidate **kinases** for tau phosphorylation include proline-directed kinases glycogen synthase kinase 3 (**GSK3**), cyclin-dependent protein kinase (**cdk5**), the **p38** mitogen-activated protein kinase (**MAPK**); or c-Jun N-terminal kinases (**JNK**) families, as well as other stress activated kinases, such as **cdc2**; and non-proline-directed kinases such as protein kinase A (**PKA**), protein kinase C (**PKC**), calmodulin (**CaM**) kinase II, microtubule-affinity regulating kinase (**MARK**), and casein kinase II (**CKII**) (Correas et al., 1992).

Aside from kinases, various **phosphatases** (PP) have been identified to dephosphorylate tau protein (Sergeant et al., 2005). It has been shown that **PP1**, **PP2A** and **PP2B**, predominantly dephosphorylate tau *in vitro* (Wang et al., 1995; Yamamoto et al., 1988); moreover, PP2A expression and activity was found to be reduced in the brains of AD patients, suggesting that dephosphorylation defects play a vital role in the pathological cascade in tau mediated neurodegenerative disorders (Gong et al., 1993).

Indeed, abnormal tau phosphorylation is considered as an early event in the pathology of tau (Bramblett et al., 1993). As mentioned above, the adult human brain tau harbours more than 80 potential phosphorylation sites and a disequilibrium in candidate protein kinase and phosphatase activity results in tau hyperphosphorylation with subsequently increased amount of tau detached from microtubule.

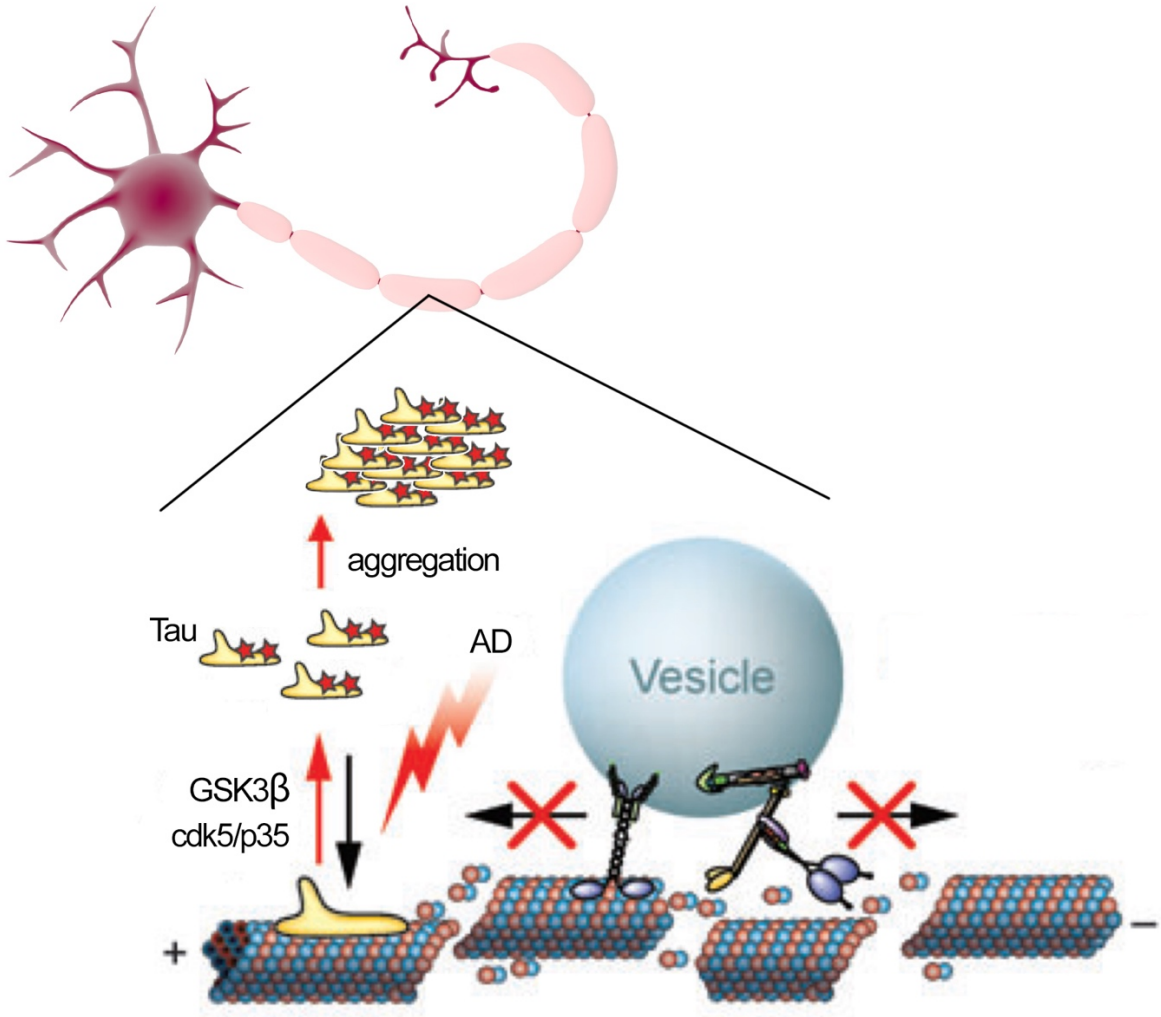


**Figure 1.3 Dysregulation of axonal transport**. Destabilization of microtubules by decreased kinase activity results in hyperphoshorylated and aggregated tau. Subsequent disintegration of the microtubule tracks leads to kinesin-mediated anterograde and dynein-mediated retrograde axonal transport dysfunction. (Adapted from De Vos et al., 2008)

#### 1.1.5.4.2 Tau truncation

Phosphorylation is typically regarded as one of the most relevant modification responsible for changes of tau protein. Alternatively, **proteolytic processing** of tau by a variety of endogenous

**proteases** has been postulated to be involved in the pathological cascade in tau mediated neurodegenerative disorders (Gamblin et al., 2003; Rissman et al., 2004).

Tau protein exhibit a physiological random coil structure; however, it is able to assemble into ordered filamentous aggregates by the formation of β-sheet structural elements (von Bergen et al., 2005). Given that the aggregation of tau correlates with its propensity for β-sheet structure, an altered shape of tau protein by proteolytic fragmentation potentially affect its aggregation capacity. The architecture of paired helical and straight filaments of AD is predominantly defined by all six full-length isoforms of tau (Goedert et al., 1992); nevertheless, studies on tau aggregation had revealed that truncated forms of tau are, in fact, present in the core of PHFs (Gamblin et al., 2003; Mena et al., 1996; Rissman et al., 2004). Likewise, fragmented tau has been reported to facilitate and promote faster polymerization into fibrils, in this way, highlight a greater aggregation propensity compared to full-length tau (Abraha et al., 2000).

In Alzheimer's disease, tau truncation was found to be an early event and appears before neurofibrillary tangle (NFT) formation albeit after hyperphophorylation of tau (Guillozet-Bongaarts et al., 2005; Mondragon-Rodriguez et al., 2008; Rohn et al., 2002; Saito et al., 2010). Various types of tau fragmentation have been reported in cells and brain tissue; cysteine proteases such as caspases and calpains have been implicated in proteolysis of tau during apoptosis (Canu et al., 1998). *In vitro* and *in vivo* experiments predicted multiple putative cleavage sites of tau at both, its C-terminal as well as N-terminal domain by a variety of caspases (Delobel et al., 2008; Gamblin et al., 2003; Guillozet-Bongaarts et al., 2005; Horowitz et al., 2004). However, not all proteolytic cleavage sites can be assigned to a distinct protease: C-terminal truncated tau at glutamic acid$^{391}$ (E391) is linked to clinical dementia yet catalyzed by an unknown proteolytic enzyme (Basurto-Islas et al., 2008; Novak et al., 1993).

However, presently the most studied, caspases cleave tau preferentially at aspartatic acid$^{421}$ (**D421**); both, **caspase 3** and **caspase 6** have been found to be involved in this cleavage at the C-terminal domain of tau (Guo et al., 2004; Rissman et al., 2004; Zhang et al., 2009a). Moreover, accumulation of caspase-cleaved C-terminal fragments have been reported to correlate with the progression in AD and *in vivo* mouse models of tauopathy (Basurto-Islas et al., 2008; Cente et al., 2006; de Calignon et al., 2010; Delobel et al., 2008; Guillozet-Bongaarts et al., 2005).

### 1.1.6 Tauopathies

The term "Tauopathy" summarizes a heterogeneous group of disorders with hyperphosphorylated, insoluble, filamentous tau protein inclusions in neurons and glial cells (Spillantini and Goedert, 2013) (Figure 1.4). These human neurodegenerative diseases are in most cases sporadic, and clinically characterized by dementia, often associated with movement impairment. Most frequent tauopathies include AD (see paragraph 1.2.2.1), Progressive supranuclear palsy (PSP) (Steele et al., 1964), Corticobasal degeneration (CBD) (Rebeiz et al., 1968), Pick's disease (PiD) (Constantinidis et al., 1974), Argyrophilic grain disease (AgD) (Braak and Braak, 1989), and Frontotemporal dementia and parkinsonism linked to chromosome 17 (FTDP-17T) (Wilhelmsen et al., 1994).

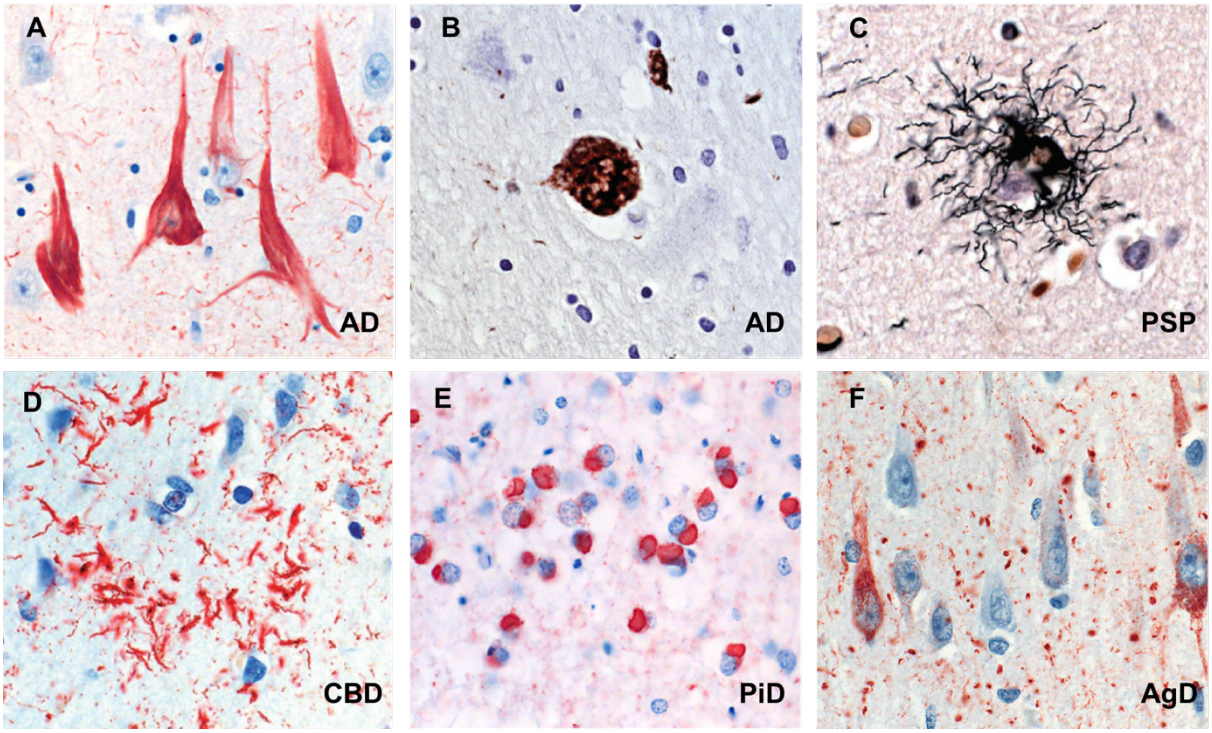


**Figure 1.4 Different types of tau immunoreactivity in tauopathies**. Hyperphosphorylated tau, AD (**A**); gallyas positive globose tangle, AD (**B**); gallyas positive tufted astrocyte, PSP (**C**); hyperphosphorylated tau in astrocytic plaques, CBD (**D**); hyperphosphorylated tau from pick bodies, PiD (**E**); hyperphosphorylated tau, AgD (**F**). (Adapted from Neumann et al., 2009)

### 1.1.7 Prion-like seeding in neurodegenerative proteinopathies

**Prion-like** seeding or transmission is a general mechanism observed in neurodegeneration proteinopathies including Creutzfeldt-Jakob disease (CjD), kuru, and scrapie. In this process involved are misfolded and aggregated proteins that potentially act as **infectious agents** by structurally corrupting other proteins, and thus trigger their pathogenic aggregation (Jucker and Walker, 2013). Various neurodegeneration-associated proteins including **Aβ**, **tau**, **α-Syn**, and **TDP-43** are increasingly emerging as considerable candidates with potential prion-like properties (Figure 1.5). In case of potential Aβ seeding, this is reflected in studies on mouse models, where brain tissues from AD patients of APP transgenic mice can indeed seed amyloidosis *in vivo*, indicating a prion-like behavior of pathologic Aβ (Kane et al., 2000; Meyer-Luehmann et al., 2006). Moreover, inoculation of brain homogenates derived from human tauopathy patients and NFTs bearing P301S tau transgenic mice into wild-type tau expressing ALZ17 host mice demonstrated a prion-like spreading potential of insoluble tau aggregates (Clavaguera et al., 2013; Clavaguera et al., 2009).

#### 1.1.7.1 CSF Aβ

Previously it has been shown that small and soluble Aβ species found in the brain of APP23 transgenic mice exhibit prion-like behaviour (Langer et al., 2011). Given that Aβ is also present in the cerebrospinal fluid (CSF), CSF biomarkers constitute a valuable tool for early AD diagnosis (Cummings, 2004; McKhann et al., 2011); current CSF analysis, though, suffers from measurements variabilities (Scheltens et al., 2016). Studies on post-mortem CSF have been demonstrated that $A\beta_{42}$ levels inversely correlate with cortical plaque deposition (Tapiola et al., 2009). Further, in parallel to the progression of senile plaques, $A\beta_{40}$ and $A\beta_{42}$ levels in the CSF appear to decrease with age (Maia et al., 2013). However, the potency of human CSF for amyloid aggregation induction in mouse models of dementia remains elusive.

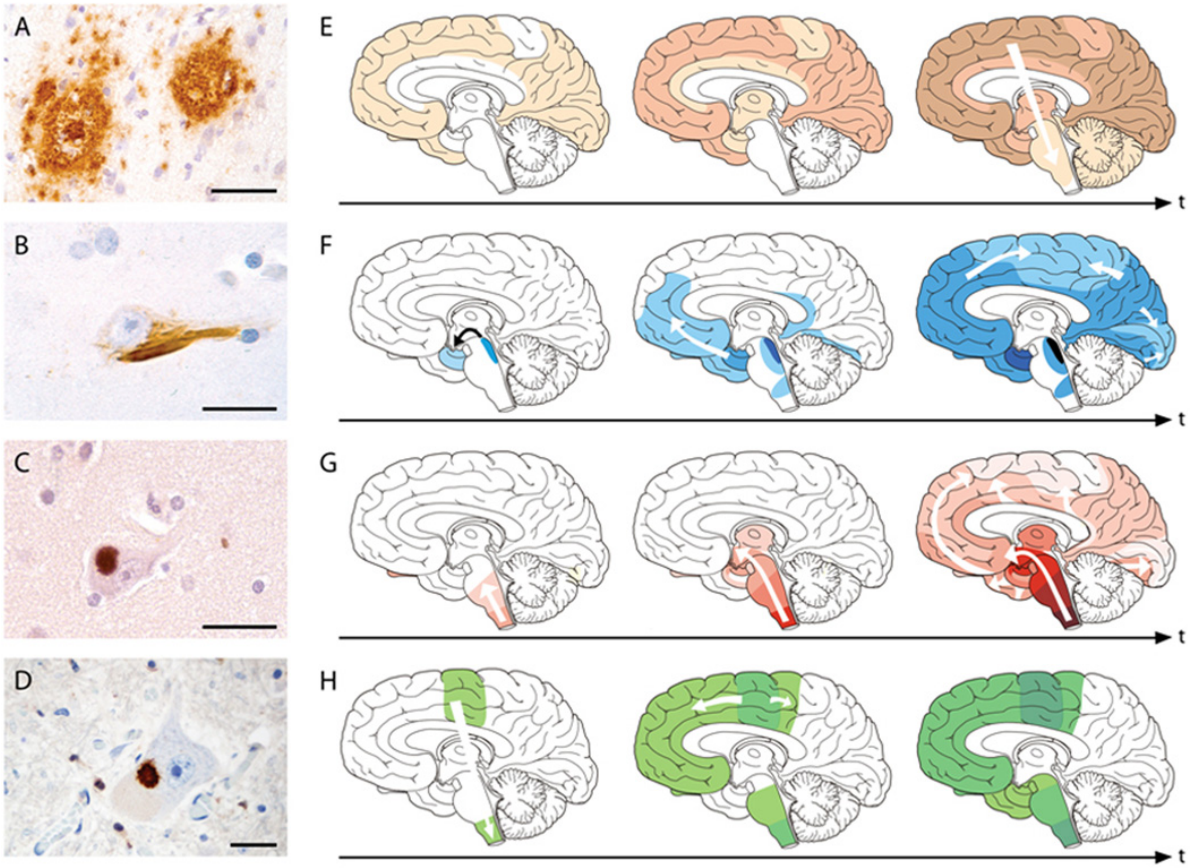


**Figure 1.5 Spreading of neurodegeneration-associated proteins.** Progressive prion-like propagation and spreading of Aβ (**A**), tau (**B**), α-Syn (**C**), and TDP-43 (**D**) based on brain autopsy studies of human disease patients. (Adapted from Jucker and Walker, 2013)

## 1.2 Chapter 2:

## Protein fragmentation in neurodegenerative disorders

**Frederik Sprenger**, David T. Winkler

*Review in preparation*

### 1.2.1 Neurodegenerative disorders

The majority of neurodegenerative disorders is associated with pathological protein aggregation. The term “proteinopathies” has therefore been established for these diseases. The mechanisms underlying protein aggregation in proteinopathies has in many cases only been partially understood. Different factors may eventually lead to pathological protein aggregation. First of all, an increased aggregation propensity of a given protein can induce pathological folding and aggregation. Proteins can be rendered aggregation prone by patholocigal mutations, e.g. in the case of hereditary forms of proteinopathies, or by truncation. In sporadic diseases, factors i.e. decreased protein clearance, e.g. by autophagy disruption, are furthermore suspected to be underlying the aggregation process. These processes involve protein cleavage and may thereby not only be beneficial by removing misfolding proteins, but also indirectly contribute to render the aggregation propensity by cutting proteins into small peptides with seed-like character. In most cases, the aggregating proteins are rather small, often derived of a precursor protein. All this points towards a unifying characteristic of protein cleavage as a key factor leading to aggregation prone fragments. Such fragments often possess an inherently higher aggregation propensity compared to their primary full-length protein of which they are derived.

Protein cleavage is a widely observed process in neurodegenerative disorders. Based on the specific neurodegeneration-associated proteins and their modifications leading to disease-typical hallmarks at the neuropathological level, various neurodegenerative diseases can be linked to one another and assigned to the following terms:

(I) **Tauopathy**; including **Alzheimer's disease** (AD), frontotemporal dementia and parkinsonism linked to chromosome 17 (FTDP-17T), progressive supranuclear palsy (PSP), cortocobasal degeneration (CBD), and argyrophilic grain disease (AGD); Pick disiease (PiD), and globular glial tauopathy (GGT) (Fasulo et al., 2005; Ferreira and Bigio, 2011; Guo et al., 2004; Park et al., 2007; Zhang et al., 2009a) (see also paragraph 1.1.6.);

(II) **Heriditary amyloidoses/Cerebral amyloid angiopathy** (CAA); including AD and familial CAA related to Aβ variants such as familial British (FBD) and Danish (FDD) dementias; gelsolin; and transthyterin (Chen et al., 2001; De Strooper et al., 1999; Ihse et al., 2013; Vidal et al., 1999; Vidal et al., 2000);

(III) **α-Synucleinopathy**; including Parkinson disease (PD), dementia with Lewy bodies (DLB), and multiple system atrophy (MSA) (Dufty et al., 2007; Kessler et al., 2003; Mishizen-Eberz et al., 2005);

(IV) **Trinucleotide repeat expansion disorder** (TRD); including Huntingtin disease (HD), and spinocerebellar-ataxia-1, 2, 3, 6, 7, 17 (SCA3 and SCA7) (Graham et al., 2006; Hubener et al., 2011; Mookerjee et al., 2009; Wellington et al., 2002);

(V) **Prion disease;** including Creutzfeldt-Jakob disease (CjD) (Altmeppen et al., 2012; Notari et al., 2008);

(VI) **TDP-43 proteinopathy;** TDP-43 related disorders including frontotemporal lobar degeneration (FTDP-TDP) (Arai et al., 2010; Igaz et al., 2009; Nonaka et al., 2009);

(VII) **FUS/FET proteinopathy**; including basophilic inclusion body disease (BIBD) (Kent et al., 2014; Rademakers and Rovelet-Lecrux, 2009).

Aggregates of aberrant modified proteins may either consist of mainly fragmented precursor protein remnants, or contain co-aggregated full-length proteins and cleaved fragments in parallel. Cleavage derived species of the most notable entities and their potential role in neurodegeneration will be addressed separately in the following paragraphs; a detailed discussion, though, of other individual protein modifications is beyond the scope of the present work.

### 1.2.2 Protein fragmentation in AD: Aβ

#### 1.2.2.1 Alzheimer's disease (AD)

In 2015, the worldwide prevalence of dementia was estimated to be 46.8 million (Prince et al., 2015). This number is forecast to double every 20 years, reaching over 130 million affected people in 2050. Over 90% of all AD cases occur sporadically; foremost among others, age constitutes the main risk factor for dementia (Blennow et al., 2006); in addition, the frequency of the apolipoprotein E4 (ApoE4) allele, a major genetic risk factor, on chromosome 19 in late-onset AD (LOAD) patients has been shown to be significantly increased (Strittmatter et al., 1993). In contrast, about 5 to 10% are familial cases (FAD) and results in aggressive early-onset progression of AD (EOAD) (Tanzi, 1999). Mutations in genes coding for amyloid precursor protein (APP; located on chromosome 21; presenilin 1 (PS1; located on chromosome 14), presenilin 2 (PS2; located on chromosome 1) have been reported in FAD (Goate et al., 1991; Sherrington et al., 1995).

Alzheimer's disease is a most probably heterogeneous neurodegenerative disorder. It is clinically characterized by progressive cognitive decline, typically delineated by short-term and long-term memory impairment, as well as loss of social abilities including symptoms like confusion, irritability, aggression and language breakdown (Tabert et al., 2005; Waldemar et al., 2007); in parallel, patients are affected by muscular deterioration and motor disabilities (Scarmeas et al., 2004). Furthermore, AD is neuropathologically defined by extracellular **β-amyloid** (Aβ; see paragraph 1.2.2.2) plaques, vascular Aβ deposits (cerebral amyloid angiopathy; CAA; see paragraph 1.2.3.) and intracellular aggregates of **tau protein** (NFTs; see paragraph 1.1.6) (Alzheimer, 1906, 1907) (Figure 1.6).

Massive neuronal and dendritic loss is the primary cause of **cortical atrophy** during the progression of AD. Atrophic changes results in cortical thinning and enlargement of the lateral cerebral ventricles. Reduced neuronal numbers in a variety of brain regions such as the temporal, parietal and enthorhinal cortex (Gomez-Isla et al., 1997), the CA1 region of the hippocampus (West et al., 1994) and amygdala (Vereecken et al., 1994) have been documented; however, the cause of neuron death is disputable.

In fact, the pathogenic mechanisms are poorly understood, with some studies suggest that

intraneuronal and/or **oligomeric Aβ-peptides** act as key mediators of neurotoxicity and cell death (Bayer and Wirths, 2010; Larson and Lesne, 2012). However, pathological tau protein increasingly gained attention in the pathogenesis of tauopathies including AD. Other studies provide evidence of an intimate coherence between neuron loss and the appearance of neurofibrillary tangles (Cras et al., 1995; Gomez-Isla et al., 1997); indeed, in contrast to the degree of Aβ pathology in form of senile plaques, the extent of tau pathology has been shown to correlate best with the clinical state of AD (Arriagada et al., 1992; Giannakopoulos et al., 2007; Landau et al., 2016; Ossenkoppele et al., 2016).

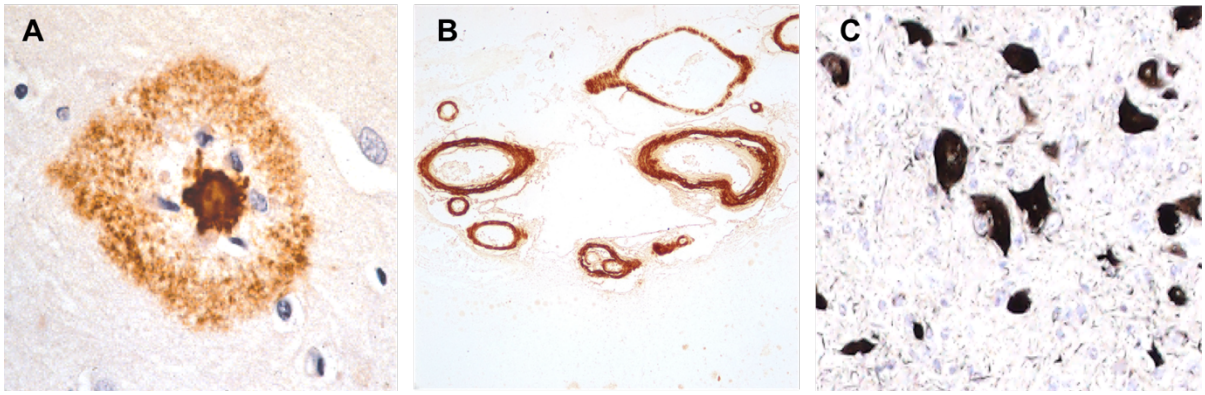


**Figure 1.6 The pathological hallmarks of AD.** Senile Aβ plaque (**A**), cerebrovascular amyloid (**B**), and neurofibrillary tangles (**C**)**.** (A and B adapted from Castellani et al., 2010)

### 1.2.2.2 Aβ

Amyloid-beta (Aβ) is generated from the **amyloid precursor protein** (APP) (Kang et al., 1987; Tanzi et al., 1987), which is a single **transmembrane** glycoprotein consisting of an exocytoplasmic domain and a short cytoplasmic tail. This large precursor protein is sequentially processed releasing distinct secreted derivatives into vesicle lumens and the extracellular space. As summarized in Figure 1.7, APP is proteolytic processed via (**I**) the non-amyloidogenic pathway; or (**II**) the amyloidogenic pathway (Selkoe, 2001b); of note, the latter is crucial for Aβ liberation and thus of neuropathological relevance.

**(I) The non-amyloidogenic pathway**

This processing prevents an accumulation of Aβ peptides by demolishing the complete amyloid sequence. APP is sequentially cleaved by α-and $\gamma$-secretases to release a smaller fragment (p3), that has no neuropathological recognized role. The α-site cleavage of APP by adamalysin protease (ADAM) cuts 12-aa at the N-terminal single transmembrane domain (Roberts et al., 1994); consequently, a C-terminally truncated form of soluble ectodomain fragment (α-sAPP) is released from the membrane. The remaining 83-residue C-terminal fragment (C83; CTFα) in the membrane is further processed by $\gamma$-secretases which then leads to the release of the short extracellular p3 fragment (Selkoe, 2001b) and the APP intracellular domain (AICD) (Zhang et al., 2011).

**(II) The amyloidogenic pathway**

Aβ protein is liberated by sequential proteolytic processing of APP involving β-and $\gamma$-secretases. Initially, proteolytic cleavage occurs 16-aa residues to the N-terminal of the α-cleavage site by the β-site APP cleaving enzyme 1 (BACE1) (Hussain et al., 1999; Sinha et al., 1999; Vassar et al., 1999), generating a soluble amino terminal APP derivate (β-sAPP) and a membrane-associated 99-residue C-terminal (C99, CTFβ). Further, $\gamma$-secretase activity at different intramembranous CTFβ sites generates Aβ species of varying length between 35- and 43-aa. Foremost among them are peptides of $A\beta_{40}$ or $A\beta_{42}$ aa in lengths, that are, together with the AICD, most abundantly produced (Citron et al., 1995; Haass et al., 1994; Selkoe, 2001a; Tang, 2009). The $\gamma$-secretase is a highly hydrophobic catalytic enzyme and composed of distinct components: presenilin proteins (PS1 or PS2), nicastrin, anterior pharynx defective 1 (APH1) and presenilin enhancer 2 (PEN-2). Aside of being involved in APP processing, $\gamma$-secretase cleaves further substrates, such as Notch, cadherins, CD44 and neuregulin (De Strooper and Annaert, 2010).

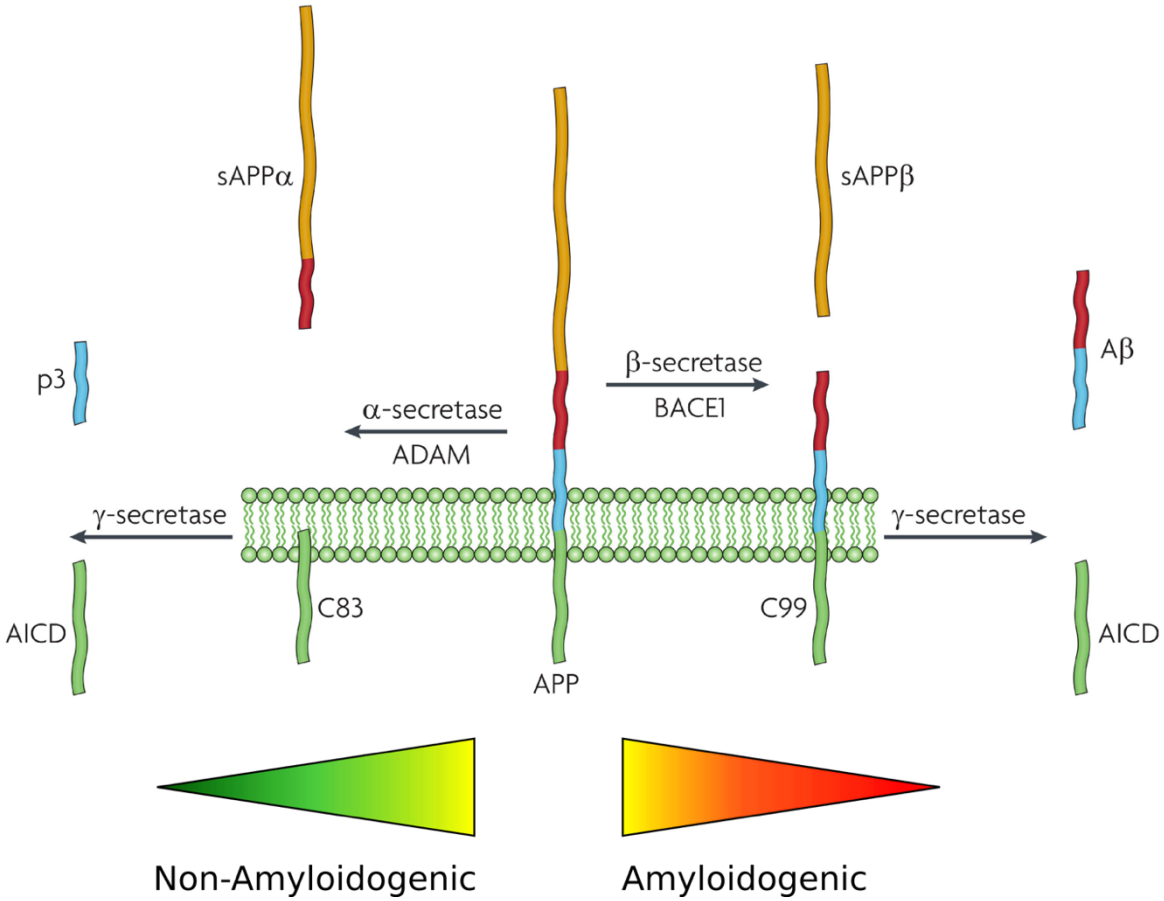


**Figure 1.7 Schematic representation of APP processing.** In non-amyloidogenic processing, APP is sequentially cleaved by α-secretase and $\gamma$-secretases to release the p3 fragment. In amyloidogenic processing, sequential cleavage by β-and $\gamma$-secretases releases the Aβ peptide. (Thathiah and De Strooper, 2011)

### 1.2.3 Protein fragmentation in familial CAA: ABri and ADan

#### 1.2.3.1 Cerebral amyloid angiopathies: familial British and Danish dementia

Cerebral amyloid angiopathy (CAA) summarizes entities with deposition of amyloid within the walls of blood vessel of the CNS (Ghiso et al., 2001; Mandybur, 1986); it occurs as sporadic and/or familial disease forms with various proteins involved including APP in AD, amyloid-Bri precursor protein (ABriPP) in familial British dementia (FBD), and amyloid-Dan precursor protein (ADanPP) in familial Danish dementia (FDD) (Rensink et al., 2003; Revesz et al., 1999; Revesz et al., 2002).

FBD and FDD are late-onset diseases and clinically characterized by progressive dementia, spastic tetraparesis, and cerebellar ataxia (Mead et al., 2000; Stromgren et al., 1970); with neuropathological hallmarks similar to those in AD including severe CAA, neuroinflammation, and neurofibrillary tangle formation (Coomaraswamy et al., 2010; Revesz et al., 2002; Rostagno and Ghiso, 2008).

### 1.2.3.2 ABri and ADan

Mutation in the integral membrane protein $BRI_2$ leads to accumulation of highly soluble ABri and ADan peptides. $BRI_2$ is a type-II single-spanning trans-membrane precursor protein of 266-aa in length. A missense mutation or decamer duplication mutation produces a frame-shift in the BRI gene sequence are generating two larger, 277-residue precursor proteins ABriPP and ADanPP, respectively (Vidal et al., 1999; Vidal et al., 2000).

The immature $BRI_2$ precursor protein is cleaved in a multi-step proteolytic process resulting in distinct intermediate- and end-products: (I) several proteases such as furin and other subtilisin/kexin-like proprotein convertases (PPCs) leads to the secretion of a 23-residue C-terminal peptide (**$Bri_2$-23**) (Kim et al., 1999). (II) the remaining membrane bound mature $BRI_2$ protein is further processed by α-secretases ADAM10 releasing the BRICHOS domain to the extracellular space (Martin et al., 2008). (III) finally, an N-terminal fragment (NTF) undergoes proteolytic cleavage by signal peptide peptidase-like 2 (SPPL2) resulting in a small extracellular $BRI_2$-C-terminal peptide and in parallel to an intracellular domain (ICD) (Martin et al., 2008). Notably, instead of $Bri_2$-23, proteolytic processing of ABriPP or ADanPP by PPCs leads to liberation of highly soluble 34-residue C-terminal peptides **ABri** and **ADan**, respectively (Figure 1.8).

Unlike the shorter wild-type peptide Bri, cleaved ABri showed an increased propensity in the formation of toxic oligomers through inter-molecule disulfide bonds *in vitro* (Cantlon et al., 2015; El-Agnaf et al., 2001). Overexpression of different amyloid peptides in the retina of *Drosophila* demonstrated that ADan appears to be more toxic compared to e.g. $Aβ_{42}$ peptides (Marcora et al., 2014). The two amyloidogenic peptides, ABri and ADan, which do not occur in nature in the absence of the disease causing changes in the respective precursor proteins, demonstrate that the de novo creation of short peptides is sufficient to induce amyloid

formation and associated neurodegeneration. ABri and ADan therefore serve as principal models for an upstream role of protein cleavage in neurodegeneration. In addition to the induction of amyloid deposits, these novel peptides also induce downstream tau pathology in FBD and FDD (Del Campo et al., 2015). In murine models, co-expression of soluble ADan and P301S tau exacerbates tau toxicity associated synaptic dysfunction, and results in increased soluble hyperphosphorylated and insoluble aggregated tau species as well as tau truncation at Asp421 (Coomaraswamy et al., 2010; Garringer et al., 2013).

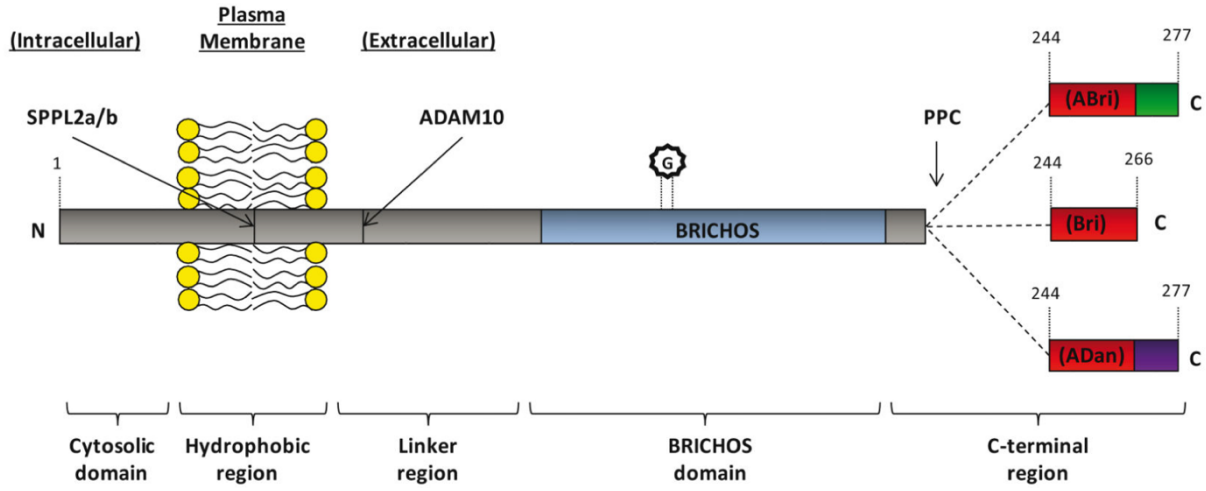


**Figure 1.8 Schematic representation of $BRI_2$ processing.** (Cantlon et al., 2015)

### 1.2.4 Protein fragmentation in PD: α-synuclein

#### 1.2.4.1 Parkinson's disease (PD)

Parkinson's disease (PD) is characterized by tremors and locomotion abnormalities and constitutes the most frequent movement disorder among **α-synucleinopathies** including dementia with Lewy body (DLB) and Multiple System Atrophy (MSA). PD is pathologically defined by the presence of aberrant **α-synuclein** (α-Syn) in intracellular deposits of Lewy bodies (LB) and Lewy neurites (LN) and by neuronal degeneration in the substantia nigra (Forno, 1996; reviewed in Tofaris and Spillantini, 2005).

### 1.2.4.2 α-synuclein

Proteolytic processing of α-synuclein is thought to be considerably relevant for the formation of fibrillogenic protein inclusions and neurotoxicity (Dufty et al., 2007) (Figure 1.9); indeed, truncated α-synuclein species have been found in brains PD and DLB patients (Baba et al., 1998; Liu et al., 2005). In fact, **C-terminally truncated α-Syn** has been found to increase the aggregation propensity of full-length α-Syn, resulting in enhanced neurotoxicity *in vivo* and *in vitro* (Giasson et al., 2002; Kanda et al., 2000; Li et al., 2005). It also has been demonstrated that C-terminal truncated α-Syn aggregates more rapidly compared to its full-length counterpart; moreover, truncated α-Syn species exhibit seeding potential of full-length α-Syn aggregation *in vitro* (Murray et al., 2003). Of note, manganese (Mn), a cofactor for homeostatic and trophic enzymes in the CNS, has been shown to induce cleavage of α-Syn protein *in vitro* and provoke toxic α-Syn oligomers, ultimately leading to neuronal injury (Xu et al., 2015). Aside, matrix metalloproteinases (MMPs) generating aggregation-enhancing α-Syn fragments *in vitro* are believed to be also relevant for PD pathogenesis *in vivo* (Levin et al., 2009). Further, **N-terminal truncation** of α-Syn protein prevents β-sheet and fibril formation (Kessler et al., 2003). Also, in transgenic mice overexpressing a calpain-specific inhibitor, reduced proteolytic cleavage of α-Syn protein lead to a decrease of α-Syn-positive aggregates and astrogliosis; indicating a crucial role of truncated α-Syn species, but also of calpains in the pathogenesis of PD (Diepenbroek et al., 2014).

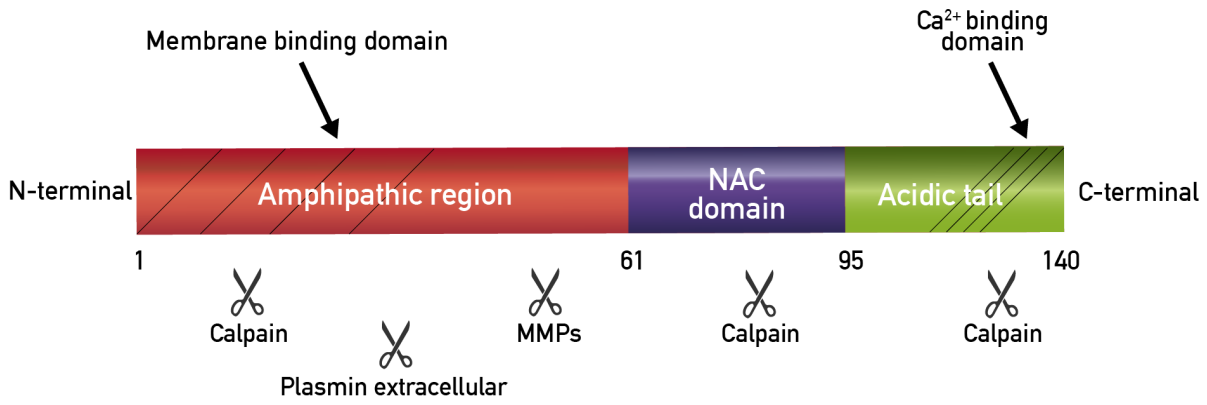


**Figure 1.9 Schematic representation of α-Syn protein processing.** (Adapted from Emanuele and Chieregatti, 2015)

### 1.2.5 Protein fragmentation in TRD: Htt, ataxin, and atrophin

#### 1.2.5.1 Huntington's disease (HD)

Huntington's disease (HD) is a late-onset, autosomal dominant, and progressive neurodegenerative disorder caused by a CAG trinucleotide repeats expansion in the coding region of the huntingtin (htt) gene, which encodes an polyglutamine (**polyQ**) stretch that alters the function of the htt protein; indeed, the mutant htt possibly affects cellular processes including mitochondrial dysfunction and vesicle transport failure (Browne, 2008). In addition, polyQ induced conformational change makes the htt protein more aggregation-prone and cause inclusions in the cytoplasm, dendrites and axon terminals of neurons (Fan et al., 2014). Interestingly, it has been shown that **wild-type huntingtin** can diminish the neurotoxicity of mutant huntingtin (Leavitt et al., 2001; Leavitt et al., 2006; Zhang et al., 2003) and also act as an **autophagy scaffold** (Rui et al., 2015).

The clinical picture of HD includes psychiatric features and dementia; progressive chorea development and other movement abnormalities. In parallel, severe degeneration occurs in the striatal medium-sized spiny neurons, and subsequently in the deep layers of the cortex (Novak and Tabrizi, 2011; Vonsattel and DiFiglia, 1998).

#### 1.2.5.2 htt

The correlation between huntingtin length and neurotoxicity is poorly understood; however, htt fragments have been found in the brains of HD patients, as well as in transgenic mouse models of HD (Kim et al., 2001; Wellington et al., 2002). Indeed, proteolytic cleavage of mutant htt by caspases, calpains and other proteases such as MMPs (Miller et al., 2010) release an **aggregation-prone polyQ tract containing N-terminal fragment**, and ultimately leading to intracellular inclusions and neuronal dysfunction (Wellington et al., 2000) (Figure 1.10); as well as to impaired mitochondrial trafficking, preceding the formation of aggregates (Orr et al., 2008). Further, mouse models transgenic for truncated forms of htt have shown a rapidly progressive and lethal phenotype (Mangiarini et al., 1996; Schilling et al., 1999); in contrast, mice expressing full-length mutant constructs exhibit only a mild pathological phenotype (Van Raamsdonk et al., 2005).

### 1.2.5.3 Other polyglutamine diseases

Other trinuleotide repeat expansion disorders, including various forms of **Spinocerebellar ataxia** (SCA types 1, 2, 3, 6, 7, and 17) and **Dentatorubral-pallidoluysian atrophy** (DRPLA) share **common properties of HD**, albeit being less frequent; mutations in polyQ expansion alters the normal function of ataxin proteins (Margolis and Ross, 2001; Palhan et al., 2005) and the transcription co-regulator atrophin-1 (Sato et al., 2009), respectively, leading to intranuclear aggregation in cerebellar Purkinje cells and cortical neurons (Rolfs et al., 2003). Among the other types, an important neuropathological role of ataxin cleavage has been shown in a *Drosophila* model of SCA3 and for SCA7 *in vitro* and *in vivo.* Specifically, polyQ-containing fragments derived from caspase-dependent cleavage of ataxin-3 have been demonstrated to induce neurotoxicity, thus contribute to SCA3 disease progression (Jung et al., 2009) In addition, it has been shown that toxic polyQ-containing fragments generated by caspase-7 mediated N-terminal cleavage of ataxin-7 are subject to regulated clearance mechanisms; however, distinct post-translational modifications such as acetylation/deacetylation appear to modulate fragment stability/clearance, and thus being crucial for mediating polyQ-fragment induced toxicity. (Mookerjee et al., 2009).


**Figure 1.10 Schematic representation of htt protein processing.** (Adapted from Ross and Tabrizi, 2011)

### 1.2.6 Protein fragmentation in Prion diseases: $PrP^C$ and $PrP^{Sc}$

#### 1.2.6.1 Prion diseases

Prion diseases are a group of neurodegenerative disorders that may occur sporadically, but also manifest familial and, infectious forms. In human beings, prion diseases such as Creutzfeldt-Jakob disease (CjD) and kuru are clinically characterized by progressive dementia and motor dysfunction (Prusiner, 1991).

Prions are infectious, pathogenic proteins that, in contrast to viruses, are encoded by a chromosomal gene (*PRNP*) and are devoid of nucleic acid; they are crucially linked to the conversion of the physiological **cellular prion protein** ($PrP^C$), a **membrane-associated extracellular glycoprotein** anchored by glycosylphosphatidylinositol (GPI), into the abnormal, self-propagating **'scrapie' prion isoform** ($PrP^{Sc}$) (Prusiner et al., 1998). The post-translational modification from a structural α-helical sheet to insoluble β-sheet structures results in an increased aggregation propensity of $PrP^{Sc}$; ultimately, polymerizing into amyloidogenic deposits and encouraging prion propagation (DeArmond et al., 1985).

#### 1.2.6.2 Prion protein

Biologically active fragments derived from proteolytic processing are thought to have implications in the course of prion diseases. $PrP^C$ is subject to diverse proteolytic events under physiological conditions: (I) **α-cleavage** within the neurotoxic domain produces soluble N1- and a membrane bound C1-fragment; (II) **β-cleavage** gives rise to a N2- and C2-fragment; and (III) **shedding** close to the plasma membrane releases almost full-length $PrP^C$ into the extracellular space (reviewed in Altmeppen et al., 2012) (Figure 1.11).

Given that the neurotoxic domain of $PrP^C$ is essential for the abnormal conversion to the $PrP^{Sc}$ isoform, **α-cleavage** and the resulting inactivation of this structural part is assumed to be a protective mechanism as to prion propagation (Lewis et al., 2009; Turnbaugh et al., 2012). In addition, α-cleaved C1-fragment has been linked to apoptotic caspase-3 activation *in vitro* (Sunyach et al., 2007). Of note, the cleavage derived N1-fragment has been demonstrated to be neuroprotective *in vitro* and *in vivo* (Guillot-Sestier et al., 2009).

The role of $PrP^{C}$ shedding by **a** **d**esintegrin **a**nd **m**etalloproteinase **10** (**ADAM10**) in neurodegenerative diseases remain unclear. However, there is evidence that shedding of not only $PrP^{C}$, but also of already misfolded $PrP^{Sc}$ leads to accumulation of anchorless $PrP^{Sc}$; thus, **encouraging neurotoxic spreading** in the brain (Chesebro et al., 2005; Rogers et al., 1993). Notably, shedded $PrP^{Sc}$ in the cerebrospinal fluid (CSF) is also thought to enhance pathological transmission (Tagliavini et al., 1992).

**N-terminally truncated PrP species** has been found to co-localized with full-length forms in infectious $PrP^{Sc}$ aggregates in mouse brains (Pan et al., 2005). Indeed, various truncated forms of full-length $PrP^{Sc}$ has been shown to be involved in prion diseases: the most common $PrP^{Sc}$ fragment PrP27-30 (Parchi et al., 1996); PrP7-8 truncated forms in Gerstmann-Sträussler-Scheinker (GSS) diseases (Parchi et al., 1998); PrP16-17 truncated species in scrapie-infected animals (Caughey et al., 1998); or PrP-CTF12/13 in sporadic CjD (Zou et al., 2003). Aside, it is thought that **non-fibrillar PrP oligomers** have implications in the process of prion diseases. However, N-terminal truncated PrP lead to non-specific aggregates, but failed to form toxic oligomeric species *in vitro* and *in vivo*; indicating that the structural N-terminus plays a key role in the infectious and neurotoxic process (Trevitt et al., 2014). Moreover, transgenic mice expressing a truncated form of mutant PrP lacking a short N-terminal segment of 9-aa displayed a neurotoxic phenotype (Westergard et al., 2011).

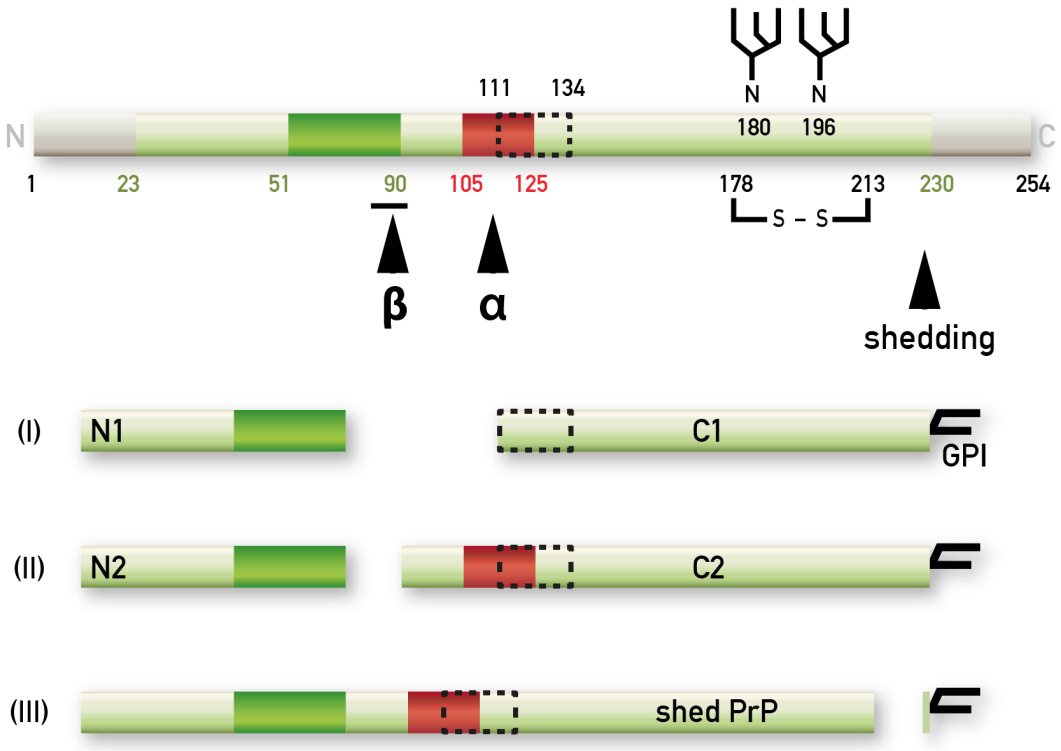


**Figure 1.11 Schematic representation of PrP processing.** (Adapted from Altmeppen et al., 2012)

### 1.2.7 Protein fragmentation in FTLD and ALS: TDP-43

#### 1.2.7.1 TDP-43 proteinopathies

TDP-43 proteinopathies including sporadic and familial frontotemporal lobar degeneration (FTLD) (Arai et al., 2006) and amyotrophic lateral sclerosis (ALS) (Neumann et al., 2006) are a group of neurodegenerative disorder caused by pathological neuritic inclusions containing transactive response (TAR) DNA-binding protein 43. Aside AD, FTLD is the most common form of progressive dementia in human beings under the age of 65 years (Neary et al., 1998). ALS, however, is the most common cause of motor neuron degeneration accompanied by progressive muscle wasting. Moreover, FTLD patients may also develop ALS; and vice versa (Murphy et al., 2007). Aside, mutation in the progranulin gene (*PGRN*) are thought to cause familial form of FTLD (Ghidoni et al., 2008).

### 1.2.7.2 TDP-43

Physiologically, TDP-43 is thought to play a role in the regulation of various cellular processes including alternate splicing, transcription, apoptosis, microRNA biogenesis, and mRNA transport and stability (reviewed in Buratti and Baralle, 2008; Ou et al., 1995). Human TDP-43 is a 414-aa **nuclear protein**, ubiquitously expressed and highly conserved; structurally, it harbors two RNA-recognition motifs (**RRM1; RRM2**) and a protein-protein interaction mediating C-terminal glycine-rich region (Wang et al., 2004). Furthermore, the TDP-43 molecule exhibit three potential caspase-3 cleavage sites (Zhang et al., 2007).

Both, hyperphosphorylated and ubiquitinated **full-length** and **N-terminally truncated TDP-43** are the major component of **neuritic inclusions** in brain tissue of FTLD and ALS patients. **Caspase 3/7-mediated proteolytic cleavage** at Asp89 and Asp220 of wild-type TDP-43 generates a 35-kDa (**CTF35**) and a 25-kDa C-terminal fragment (**CTF25**) respectively (Figure 1.12); moreover, different cleavage sites at Arg208, Asp219, and Asp247 of CTF25 were further identified (Igaz et al., 2009; Neumann et al., 2006; Nonaka et al., 2009). Moreover, each individual TDP-43 CTF has been shown to possess distinct molecular properties including intracellular distribution and phosphorylation status, contributing to the pathogenic diversity of TDP-43 proteinopathies (Furukawa et al., 2011).

So far, accumulation of truncated species might mediate toxicity, or is simply a consequence in the course of neurodegeneration; in any case, the pathological role of TDP-43 fragments remains elusive. However, several studies implicate a neurotoxic relevance of TDP-43 fragmentation. Indeed, expression of **caspase-cleaved CTF25 fragment** in human cell lines lead to cell death accompanied by the formation of **toxic insoluble aggregates**; aside, this fragment did not interact with full-length nuclear TDP-43 or affect its function, thus, indicating a toxic gain-of-function (Zhang et al., 2009b). Furthermore, this fragment showed an increased hyperphosphorylation propensity at sites not required for neurotoxic inclusion formation compared to full-length TDP-43. In contrast, another study demonstrated that TDP-43 CTFs provoke both, first, the formation of aberrant phosphorylated and ubiquitinated aggregates, and second, the incorporation of newly synthesized endogenous full-lengths species into these cytoplasmic inclusions (Nonaka et al., 2009). Interestingly, given that regulation of exon splicing is a defined function of TDP-43, aberrant splicing has been demonstrated in cultured

cells expressing TDP-43 CTFs cleaved at Arg208; thus, strengthened the pathogenic role of TDP-43 fragments in FTLD and ALS (Igaz et al., 2009).

However, there is also evidence of **fragmentation-mediated clearance** of full-length TDP-43: the activation of endoplasmatic reticulum (ER) membrane-bound caspase-4 cleavage diminishes ER stress caused by abundant accumulation of TDP-43; subsequent activation of the downstream caspase-3/7 pathway ultimately results in reduced full-length TDP-43 cytotoxicity and necrotic cell death (Li et al., 2015).

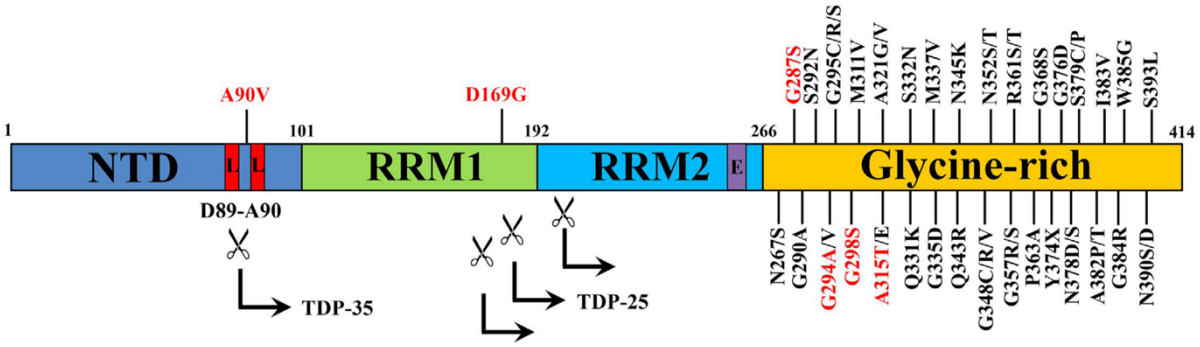


**Figure 1.12 Schematic representation of TDP-43 domain processing.** (Adapted from Chiang 2016)

We have outlined above several examples of proteinopathies, where protein cleaveage results in aggregation prone fragments, pointing towards a general pathogenic role of protein fragmentation in neurodegenerative diseases. This can't be said without mentioning the ongoing debate on the toxicity of aggregates in proteinopathies.

There exist two opposing views on amyloid lesions in most neurodegenerative diseases: high molecular, fibrillary aggregates can either be considered as inert intracellular garbage or, as specifically toxic entities. In most proteinopathies, the current evidence points towards considerable neurotoxicity of early, non-fibrillary oligomeric aggregates (Berger et al., 2007; Gerson et al., 2014; Patterson et al., 2011; Usenovic et al., 2015). This concept of oligomer toxicity in neurodegenerative disorders is compatible with a primary pathogenic role of protein fragments that induce the aggregation of proteins into oligomeric species. We have recently reported such a toxicity inducing effect of a tau fragment in tau transgenic mouse models (Ozcelik et al., 2016), providing experimental support of this hypothesis.

# 2 Aims of the work

Attributable to the increase in life expectancy, the prevalence of tauopathies including AD is continually growing with underlying pathological mechanisms partly unknown. Given that current therapeutic treatments are limited to symptomatic approaches, global society is faced with enormous socioeconomic challenges.

Yet, neurodegenerative disease research highlighted various aspects of the pathogenesis of tauopathies such as protein fragmentation and spreading.

Protein fragmentation is increasingly emerging as an integral event in the pathogenesis of neurodegenerative diseases. Numerous *in vitro* and *in vivo* studies have addressed whether cleavage of disease-associated proteins is sufficient to exacerbate an ongoing disease process. Indeed, the relevance of protein fragmentation has been highlighted in the course of a plethora of proteinopathies with an emphasis on the neurotoxic potential of protein fragments (Altmeppen et al., 2012; Furukawa et al., 2011; Masters and Selkoe, 2012; Mookerjee et al., 2009; Vidal et al., 1999; Wellington et al., 2000). As for tau protein, truncated forms have been shown to facilitate tau aggregation; and thus, appear to possess an increased neurotoxic potential compared to full-length tau species (Abraha et al., 2000). In tauopathies, the dynamics of various neurotoxic tau species is still a matter of debate. To date, it is not known which tau species is the most toxic and how the toxicity is mediated (Goedert, 2015). However, hyperphosphorylated and aggregated tau species are considered as the fundamental neurodegenerative components in tauopathies (Spillantini and Goedert, 2013).

Directly determining the pathological function of distinct tau species and cellular mechanisms underlying tau toxicity, *in vivo*, remains challenging. Numerous tau transgenic mouse models have been created to explain changes in the regulation of tau metabolism (Duyckaerts et al., 2008). Accordingly, we generated multiple transgenic mouse lines in order to study the relevance of tau fragmentation for the neurodegenerative process in tauopathies. These mice either express a truncated tau sequence (3R $\Delta tau_{151-421}$) alone or in combination with wild-type (0N3R or 2N4R) or mutant (0N4R) full-length tau isoforms. Of note, animal models that express wild-type full-length forms of tau generally stay devoid of insoluble tau inclusions, whereas models that overexpress mutated full-length tau exhibit NFTs (Allen et al., 2002; Gotz et al., 1995).

Aside tau protein, the aggregation of Aβ species generated by proteolytic cleavage of APP constitutes a key pathological hallmark of AD. Lately, a prion-like role of mouse brain derived Aβ species has been demonstrated (Langer et al., 2011); thus indicating that Aβ species present in the CSF may exhibit similar seed-like properties *in vivo*.

Within this framework, we sought, to longitudinally analyze the effects of a human tau fragment in a murine model and specifically its potential interaction with human full-length tau, and in parallel, to analyze potential seed-potent CSF derived Aβ species *in vivo*.

# 3 Results

## 3.1 Publication No. 1

### Co-expression of truncated and full-length tau induces severe neurotoxicity

Ozcelik S*, **Sprenger F***, Skachokova Z, Fraser G, Abramowski D, Clavaguera F, Probst A, Frank S, Müller M, Staufenbiel M, Goedert M, Tolnay M, Winkler DT.

** Both authors contributed equally to the work*

*Mol Psychiatry. 2016*

OPEN

Molecular Psychiatry (2016), 1–9

www.nature.com/mp

ORIGINAL ARTICLE

# Co-expression of truncated and full-length tau induces severe neurotoxicity

S Ozcelik[1,2,5], F Sprenger[1,2,5], Z Skachokova[1,2], G Fraser[3], D Abramowski[4], F Clavaguera[1], A Probst[1], S Frank[1], M Müller[4], M Staufenbiel[4], M Goedert[3], M Tolnay[1] and DT Winkler[1,2]

Abundant tau inclusions are a defining hallmark of several human neurodegenerative diseases, including Alzheimer's disease. Protein fragmentation is a widely observed event in neurodegenerative proteinopathies. The relevance of tau fragmentation for the neurodegenerative process in tauopathies has yet remained unclear. Here we found that co-expression of truncated and full-length human tau in mice provoked the formation of soluble high-molecular-weight tau, the failure of axonal transport, clumping of mitochondria, disruption of the Golgi apparatus and missorting of synaptic proteins. This was associated with extensive nerve cell dysfunction and severe paralysis by the age of 3 weeks. When the expression of truncated tau was halted, most mice recovered behaviorally and functionally. In contrast, co-expression of full-length tau isoforms did not result in paralysis. Truncated tau thus induces extensive but reversible neurotoxicity in the presence of full-length tau through the formation of nonfilamentous high-molecular-weight tau aggregates, in the absence of tau filaments. Targeting tau fragmentation may provide a novel approach for the treatment of human tauopathies.

*Molecular Psychiatry* advance online publication, 2 February 2016; doi:10.1038/mp.2015.228

## INTRODUCTION

Tau pathology is a defining characteristic of a number of human neurodegenerative diseases, including Alzheimer's disease, progressive supranuclear palsy, corticobasal degeneration, argyrophilic grain disease, chronic traumatic encephalopathy and some cases of frontotemporal dementia.[1,2] Physiologically, tau promotes microtubule assembly and stability. In tauopathies, soluble tau assembles into insoluble filaments, resulting in neurodegeneration.[2–4] It remains to be determined which tau species are the most toxic and how toxicity is mediated.

Abnormal protein aggregation underlies the vast majority of human neurodegenerative diseases.[5] In some diseases, the aggregates are made of cleavage products of larger proteins, such as Aβ in Alzheimer's disease[6] and amyloid-Bri in familial British dementia.[7] In other diseases, full-length and truncated proteins co-exist in the aggregates, as is the case of α-synuclein in Parkinson's disease and dementia with Lewy bodies[8,9] and TDP-43 in cases of frontotemporal dementia and amyotrophic lateral sclerosis.[10,11] Truncated proteins are often more aggregation prone than their full-length counterparts.[12,13]

It is being increasingly debated whether tau fragmentation may play a role in the pathogenesis of Alzheimer's disease. Cleaved tau has been detected in patient brains and in mouse models.[14–20] In Alzheimer's disease, tau fragmentation has been described as an early event. Caspases and calpains have been implicated, with the caspase 3 cleavage after D421 being the most studied.[21] More recently, asparagine endopeptidase has also been shown to cleave tau and promote pathology.[22] However, the general relevance of tau fragmentation for neurodegeneration has been questioned. Thus, in mouse lines transgenic for human mutant P301S[23] or P301L[24] tau, cleavage after D421 was a late event and only small amounts of caspase-cleaved tau were detected. Moreover, earlier studies found tau fragmentation to be primarily associated with degradation of the fuzzy filament coat.[25,26] Full-length tau is the major component of the paired helical and straight filaments of Alzheimer's disease.[27] On the other hand, truncation of tau increases its propensity to aggregate and it has been suggested that cleaved tau may seed the aggregation of the full-length protein.[28–30] Taken together, it is therefore possible that truncation of a small amount of tau can lead to its aggregation and the seeding of full-length tau.

Here we studied the interaction of truncated and full-length human tau. We generated an inducible mouse line (TAU62) overexpressing human 3R $tau_{151–421}$ (Δtau). This 239 amino acid tau protein extends from the proline-rich region to the caspase cleavage site. We co-expressed it with either wild-type full-length 3R tau or 4R tau,[31] or with mutant full-length 4R P301S tau.[32] In all double transgenic lines, high-molecular-weight tau, severe nerve cell damage and motor palsy were observed in young mice. Following cessation of truncated tau expression, functional and structural recovery was observed in mice expressing full-length 4R tau. In contrast, young mice double transgenic for full-length 3R and 4R tau were unaffected.

## MATERIALS AND METHODS

### Production of transgenic mouse lines and doxycycline treatment

An overview of the mouse lines used in this study is provided in Supplementary Table 1. For the neuron-specific, inducible expression of 3R $tau_{151–421}$ (Δtau), TAU62 transgenic mice were generated by coinjection of

[1]Institute of Pathology, University Hospital Basel, Basel, Switzerland; [2]Department of Neurology, University Hospital Basel, Basel, Switzerland; [3]MRC, Laboratory of Molecular Biology, Cambridge, UK and [4]Institute of Biomedical Research, Novartis Pharma AG, Basel, Switzerland. Correspondence: Dr DT Winkler, Institute of Pathology and Department of Neurology, University Hospital Basel, Petersgraben 4, CH-4031 Basel, Switzerland.
E-mail: winklerd@uhbs.ch
[5]These two authors contributed equally to this work.
Received 1 September 2015; revised 3 December 2015; accepted 15 December 2015

two Thy 1.2 minigene-based[33] constructs into C57BL/6J oocytes. The Thy1.2-tTS construct was obtained by inserting a tetracycline-controlled transcriptional silencer element (tTS) complementary DNA into the *Xho*I site of the murine Thy 1.2 minigene. The Thy1.2-TRE-Δtau construct contained a tetracycline-responsive element (TRE) in the *Spe*I site of the Thy1.2 cassette ~860 bp upstream of human wild-type Δtau complementary DNA encoding amino acids 151 to 421 of a 3-repeat domain spanning human wild-type tau fragment (0N3R $tau_{151-421}$) cloned in the *Xho*I site. Six transgenic founder TAU62 mice (C57BL/6J-TgN(TRE-Thy1$tau_{151-421}$ xThy1tTS)62) were identified and the inducible expression of human Δtau was assessed by western blotting and immunohistochemistry. Lines 62/2 and 62/48 expressed similar levels of Δtau ('*on*') and stopped expression following the removal of doxycycline ('*on-off*'). Most experiments were performed using the TAU62/48 line, abbreviated TAU62. TAU62/2 mice were used to rule out an insertion site effect. The production of P301S mutant 0N4R tau transgenic mice (C57BL/6J-TgN(Thy1-h$Tau_{P301S}$))[32] and full-length wild-type 2N4R tau transgenic ALZ17 mice (C57BL/6J-TgN (Thy1hTau)17) has been previously described.[31] For the generation of ALZ31 wild-type human 0N3R tau transgenic mice (C57BL/6J-TgN (Thy1hTau)31), 0N3R human tau complementary DNA was cloned into the Thy 1.2 minigene and injected into C57BL/6J oocytes. P301SxTAU62, ALZ17xTAU62 and ALZ31xTAU62 double transgenic mice were obtained by crossbreeding of the respective single transgenic lines using TAU62/48 mice if not indicated otherwise. All transgenic mice, including P301SxALZ31 and ALZ17xALZ31 mice, were heterozygous for the transgenes of interest, unless specifically mentioned otherwise. Food containing 500 mg $kg^{-1}$ doxycycline was provided *ad libitum* also during breeding to induce Δtau expression. The number of mice used was minimized according to the Swiss regulation on Animal Experimentation. All animal experiments were approved by the local ethics and animal care and use committees.

### Histology and immunohistochemistry

Mice were anesthetized with a mixture of ketamine (100 mg $kg^{-1}$) and xylazine (10 mg $kg^{-1}$) intraperitoneally and after deep sleeping, mice were injected by sodium pentobarbital (100 mg $kg^{-1}$) and transcardially perfused with cold phosphate-buffered saline (PBS). Spinal cord, sciatic nerve and the brain were quickly removed. Brain and spinal cord tissue was immersion fixed in 4% paraformaldehyde and embedded in paraffin. Sagittal and transverse serial sections (4–20 μm) were cut. Muscles were removed and snap frozen in liquid nitrogen cooled isopentane. Coronal sections (10 μm) were cut. Myofibers with or without internalized nuclei and fiber cross-sectional areas were quantified[34,35] in tissue derived from five mice per group, using ImageJ software v1.43 (NIH, Bethesda, MD, USA). Sciatic nerves were dissected and fixed for at least 2 h in 2.5% of glutaraldehyde, followed by washing of the tissues in 10 mM PBS overnight. The tissues were reduced in 1% osmium tetroxide and following dehydration, embedded in Durcupan. Semithin sections were cut. Hematoxylin–eosin, Holmes–Luxol, Thioflavin S,[36] as well as ATPase (pH 4.2), Masson's trichrom and *para*-phenylenediamine staining were performed according to standard protocols.[37] Fibrillar tau pathology was assessed by Gallyas silver staining. Antibodies used for immunohistochemistry are listed under Supplementary Experimental Procedures.

### Electron microscopy

Mice were anesthetized with a mixture of ketamine (100 mg $kg^{-1}$) and xylazine (10 mg $kg^{-1}$) intraperitoneally, injected with sodium pentobarbital (100 mg $kg^{-1}$) and transcardially perfused with PBS, followed by perfusion with 2% paraformaldehyde and 2% glutaraldehyde. Brains and spinal cords were removed and postfixed for 1 h, followed by rinsing of the tissues in 10 mM PBS. The tissues were reduced in 1% osmium tetroxide and 1.5% potassium ferrocyanide and, following dehydration, embedded in Epon. Ultrathin sections from selected areas were cut with a microtome (Ultracut E; Leica Microsystems GmbH, Wetzlar, Germany), collected on single-slot grids and stained in 6% uranyl acetate. Sections were examined and photographed with a Morgagni FEI 80kV electron microscope (FEI Company, Eindhoven, The Netherlands).

### Sarkosyl extraction and western blotting

Following PBS perfusion, one half of the mouse brain was dissected into forebrain and brainstem and frozen in liquid nitrogen. Brain tissue was homogenized 1:10 (w/v) in Tris-buffered saline Complete buffer (20 mM Tris, pH 7.5, 137 mM NaCl, 1 tablet of complete mini protease inhibitor cocktail tablets) and the samples were aliquoted. Sarkosyl extraction was performed as previously described.[23] Briefly, the brain tissue was homogenized in A68 buffer (0.5 ml of 800 mM NaCl, 10% sucrose, 10 mM Tris-HCl, pH 7.4, 1 mM EGTA) using a Kinetica polytron. Samples were centrifuged at 5000 *g* for 15 min. The supernatant was collected and sarkosyl added to 1%, followed by shaking for 1 h. The samples were then centrifuged at 80 000 *g* for 30 min and the pellet resuspended in 150 μl $g^{-1}$ of 50 mM Tris-HCl, pH 7.4. Western blots were performed under nonreducing conditions by using samples composed of an appropriate amount of protein, 5 μl NuPAGE LDS sample buffer and deionized water. Additional application of 2 μl NuPAGE reducing agent was used to obtain reducing conditions. Antibodies used for western blotting are listed under Supplementary Experimental Procedures.

### Behavioral assessment

Motor behavior, including gait ataxia, tremor and hindlimb reflexes, was assessed. Quantitative motor testing was performed by the grid test in which mice were placed on a vertical mesh grid and the latency to fall off from the grid was recorded for 3 min.

For object recognition test, mice were placed in a squared open field box (48 × 48 × 40 cm) under dim light conditions. Mice were let freely to explore the box during 3 consecutive days for 15 min, until no signs of stress were present (habituation phase). During the following 2 days, two identical objects were introduced at diagonal corners of the field for training sessions of 10 min duration (training phase). Training was halted when the mice had closely explored the objects for 20 s.[38] Next day, the animals' short-term memory was tested (test phase) by replacing one of the familiar objects with a novel one, and the time spent exploring each object during a period of 6 min was video recorded. Video scoring was done by a researcher blind to the genotype, and as exploration criteria nose sniffing/touching of the object at 2 cm or less distance[38] were used. For both training and test phases, 10 cm high objects composed of the same material were used, and the position of the novel and familiar objects were randomized across groups.

### Statistics

Statistical analysis was performed using one-way analysis of variance followed by Bonferroni's multiple comparison test and Student's *t*-tests with Graphpad Prism software Version 5.0a (GraphPad Software, La Jolla, CA, USA). *P*-values are reported and outlined as follows: $*P < 0.05$, $**P < 0.01$ and $***P < 0.001$. The mean and s.d. are indicated.

## RESULTS

### Inducible expression of Δtau results in mild motor palsy, memory dysfunction and pretangle pathology

To study the interplay of truncated and full-length human tau *in vivo*, we first generated an inducible transgenic mouse model (line TAU62) overexpressing wild-type 3R $tau_{151-421}$ (Δtau). A tetracycline-controlled, neuron-specific Thy1.2 promoter element (Figure 1a) was used to drive expression that ceased completely upon the removal of doxycycline (Figure 1b).

The Δtau expression resulted in a mild motor phenotype starting at 3–6 months of age. At higher ages, tremor and gait ataxia were followed by mild hindlimb paralysis, and TAU62 mice showed an abnormal limb flexion reflex (Figure 1c and Supplementary Figure 1). Indicative of short-term memory deficits, adult TAU62 mice explored a familiar object significantly longer ($P = 0.04$) than their C57Bl6 littermates. The latter accurately discriminated familiar from novel objects ($P = 0.02$, Figure 1d).

The Δtau was expressed throughout the central nervous system, including cerebral cortex (Figure 1e), hippocampus (Figure 1f) and brainstem (Figure 1g), comparable to the expression patterns in other transgenic lines using the Thy1.2 promoter.[32]

Pretangle pathology, defined as tau hyperphosphorylation at the AT8 epitope, persisted in aged TAU62 mice (Figure 1h). In contrast to rat models overexpressing truncated tau,[39] TAU62 mice did not develop tau tangles and showed no hyperphosphorylation of late epitopes, such as AT100, consistent with the absence of tau filaments (Figure 1i). In addition, Δtau was

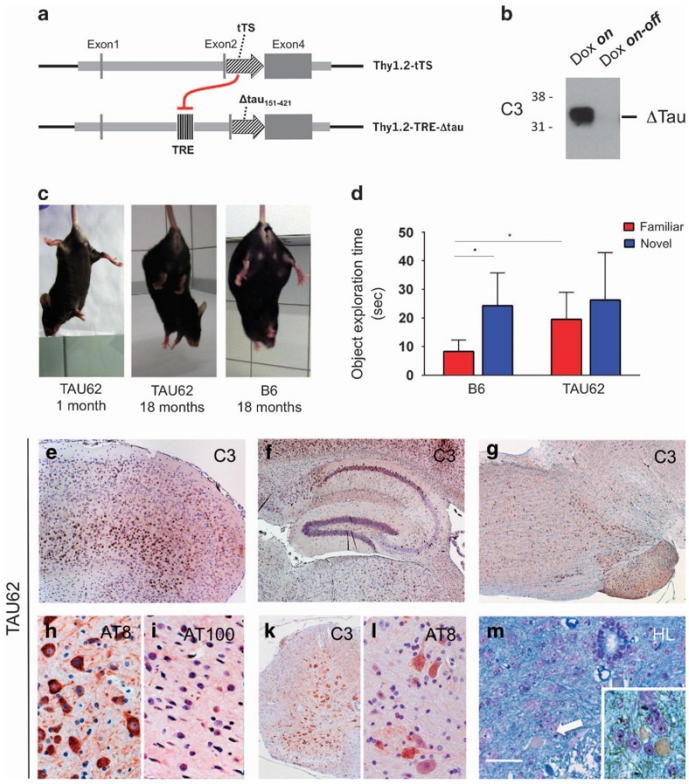


**Figure 1.** TAU62 mice express Δtau, develop a mild motor phenotype, memory deficits and pretangle pathology. (**a**) Expression constructs. In the presence of doxycycline, 3R $tau_{151–421}$ (Δtau) is expressed. In the absence of doxycycline, tTS (tetracycline-controlled transcriptional silencer) binds to TRE (tetracycline-responsive element), preventing the expression of Δtau. (**b**) Western blot of brain using anti-tau antibody C3 of a 1-month-old TAU62 mouse under doxycycline (Dox *on*) and 3 days after doxycycline withdrawal (Dox *on-off*). (**c**) Tail suspension test on young TAU62 mouse (1 month), aged B6 mouse (18 months) and aged TAU62 mouse (18 months). (**d**) Object recognition test. Object exploration time of adult TAU62 mice (aged 6 months) and their C57Bl6 littermates. (**e–m**) Histology of TAU62 mice aged 12 months (**e–g**) and 18 months (**h–m**). Immunohistochemistry with C3 of somatomotor cortex and orbital area (**e**), hippocampus (**f**), brainstem with tegmental reticular nucleus (**g**) and spinal cord (**k**). Immunohistochemistry of brainstem with AT8 (**h**) and AT100 (**i**); immunohistochemistry of spinal cord with AT8 (**l**). Holmes–Luxol (HL) staining shows the presence of spheroids in spinal cord (arrow; inset) (**m**). The scale bar in (**m**) corresponds to 60 μm in (**h**, **l** and **m**), 80 μm in (**i**), 200 μm in (**e**) and 400 μm in (**f**, **g** and **k**). $*P < 0.05$.

robustly expressed in spinal cord neurons (Figure 1k) where AT8-positive tau accumulated in motor neurons (Figure 1l). Occasional axonal spheroids were seen by Holmes–Luxol staining (Figure 1m). These findings are comparable to those obtained in aged ALZ17 mice.[31]

### Co-expression of Δtau and full-length four-repeat human mutant P301S tau causes early, but reversible, nerve cell dysfunction

We crossed TAU62 mice with tau inclusion-developing four-repeat P301S tau mice (383 amino acid tau isoform with P301S mutation).[32] Surprisingly, P301SxTAU62$^{on}$ mice showed a drastic motor phenotype at 3 weeks of age (Supplementary Video S1). In contrast, homozygous P301S tau mice developed immobilizing limb paralysis at ~5 to 7 months (Supplementary Video S2), whereas heterozygous mice remained ambulatory until up to 16 months of age. In P301SxTAU62$^{on}$ mice, motor impairment started with gait ataxia at 9 days and had evolved to a severe palsy by 3 weeks of age. Paralysis was reversible when Δtau expression was halted at 3 weeks of age. P301SxTAU62$^{on\text{-}off}$ mice recovered from severe palsy, and their gait normalized within 2–3 weeks (Figures 2a and b, Supplementary Video S3).

### Paralysis of P301SxTAU62 mice is associated with the presence of high-molecular-weight tau

In P301S tau mice, paralysis evolves in parallel to tau tangle formation.[32] It was therefore surprising that paralyzed P301SxTAU62$^{on}$ mice showed only mild pretangle pathology, in the absence of tau filaments (Figures 2c–f, for positive controls see Supplementary Figure 2a). However, the presence of soluble high-molecular-weight tau paralleled the motor impairment (Figure 2g and Supplementary Figure 2b). These tau species comprised Δtau as detected by antibody RD3 (Supplementary Figure 2c). There were

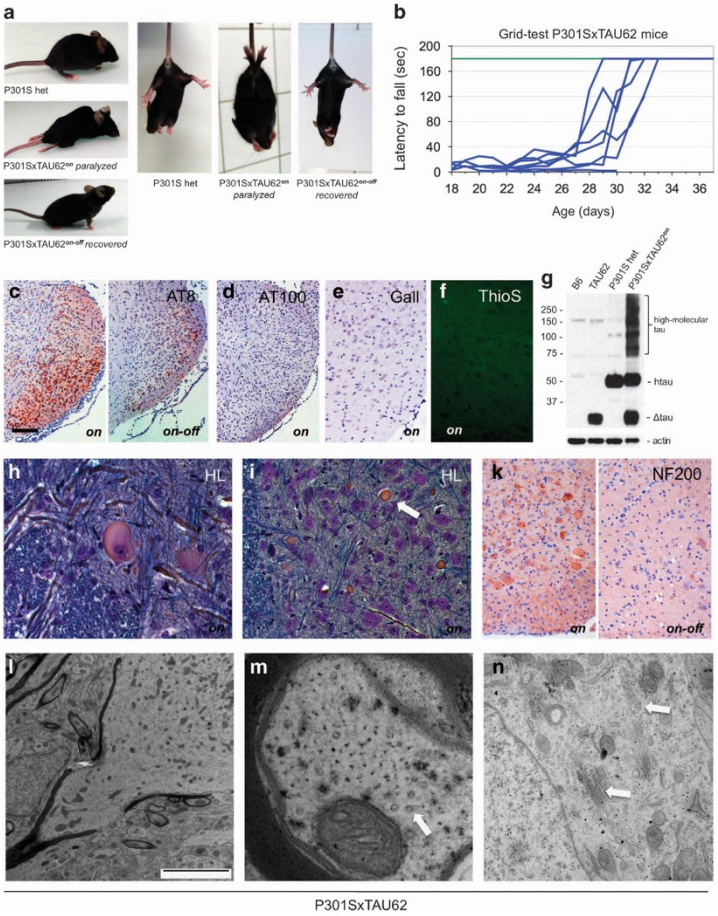


**Figure 2.** Co-expression of 4R P301S tau and Δtau (P301SxTAU62 mice) causes nerve cell dysfunction that is reversible upon cessation of Δtau expression. Paralysis is associated with the presence of soluble high-molecular-weight tau in the absence of sarkosyl-insoluble tau and tau filaments. Paralyzed mice exhibit axonal accumulations of neurofilaments and mitochondria. (**a**) Heterozygous P301S mouse (aged 3 weeks); paralyzed (aged 3 weeks) and recovered (3 weeks after cessation of Δtau expression) P301SxTAU62 mice (see also Supplementary Videos S1 and S3). (**b**) Recovery of motor function was assessed by a grid test of P301SxTAU62 mice following the removal of doxycycline at 21 days of age (blue lines). Motor function of heterozygous P301S tau littermates (green line, $n = 8$). (**c**) Immunohistochemistry with AT8 of the tegmental reticular nucleus of the brainstem of paralyzed (‘*on*’) and recovered (‘*on-off*’) P301SxTAU62 mice; immunohistochemistry with AT100 (**d**), Gallyas–Braak silver (**e**) and Thioflavin S staining (**f**) of the reticular nucleus of paralyzed mice. (**g**) Western blot with human-specific anti-tau antibody HT7 of brainstem tissue from nontransgenic (B6), TAU62, P301S and P301SxTAU62 mice. (**h** and **i**) Holmes–Luxol (HL) staining of spinal cord of paralyzed 3-week-old P301SxTAU62 mice. The arrow in (**i**) points to a spheroid; (**k**) immunohistochemistry of paralyzed (‘*on*’) and recovered (‘*on-off*’) mice using antibodies against the 200 kDa subunit of neurofilaments (NF200). The scale bar in (**c**) corresponds to 26 μm in (**h**), 40 μm in (**f** and **i**), 80 μm in (**k**), 100 μm in (**e**) and 200 μm in (**c** and **d**). (**l–n**) Electron microscopy of the spinal cord of paralyzed mice. Only a few isolated microtubules are present in axons (**m**, arrow). Fragmented Golgi material is seen in nerve cell bodies (**n**, arrows). The scale bar in (**l**) corresponds to 5 nm in (**l**), 220 nm in (**m**) and 1.4 nm in (**n**).

no tau bands in the sarkosyl-insoluble fraction (Supplementary Figure 2d). Although high-molecular-weight tau forms were absent in young heterozygous P301S tau mice, similar species were observed in aged homozygous mice (Supplementary Figure 2b). After the expression of Δtau had ceased and P301SxTAU62$^{on\text{-}off}$ mice were moving normally, high-molecular-weight tau was no longer detectable (Supplementary Figure 2b).

### Reversible axonal damage

The Δtau was widely expressed in the spinal cord of P301SxTAU62$^{on}$ mice, resulting in a reversible pretangle pathology (Supplementary Figures 2e–g). Spinal cord neurons of paralyzed mice showed signs of severe dysfunction with pathological swelling, chromatolysis (Figure 2h) and axonal damage, with extensive accumulation of neurofilaments, partly in the form of

axonal spheroids (Figures 2i and k). Neurofilament accumulation normalized upon cessation of Δtau expression (Figure 2k).

By electron microscopy, spheroids comprised massed, poorly oriented neurofilaments intermixed with multiple small, congested mitochondria (Figure 2l), compatible with axonal transport disruption. Spinal cord axons of paralyzed P301SxTAU62$^{on}$ mice contained only sparse microtubules, whereas neurofilaments were abundant (Figure 2m). Widespread fragmentation of the Golgi network was also seen (Figure 2n).

### Reversible disruption of the Golgi network, dysregulation of synaptic proteins and mitochondrial mislocalization

When aged 3 weeks, P301SxTAU62$^{on}$ mice exhibited a fragmented and swollen Golgi network in CA1 pyramidal cells (Supplementary Figures 3a, b, d and e). After Δtau expression was halted, the Golgi structure normalized (Supplementary Figures 3c and f). Synaptophysin immunoreactivity accumulated within the soma of pyramidal cells (Supplementary Figures 3g–i), indicative of transport dysfunction. VAMP2 was lost from CA1 dendrites when Δtau was co-expressed with full-length mutant tau (Supplementary Figures 3k–m). Mitochondria reversibly accumulated within the soma of pyramidal cells, as well as in axons (Supplementary Figures 3n–p).

### Reversible neuropathy and myopathy

In paralyzed mice, nerve cell damage was accompanied by an axonal neuropathy (Figures 3a–i and Supplementary Figures 4a–c). The sciatic nerve fibers exhibited vacuolated (Figure 3b) as well as collapsed myelin sheets (Figure 3e), indicating Wallerian degeneration. Neurofilament staining revealed thinned nerve fibers and spotty areas of fiber loss in paralyzed mice (Figure 3h, arrow). Upon motor recovery, myelin debris was no longer detectable and intact nerve fibers of slightly reduced diameter were seen (Figures 3c, f and i). Hindlimb paralysis was associated with muscle wasting (Figure 3k) and marked muscle fiber atrophy (Figure 3n), whereas muscle fibers of heterozygous P301S and TAU62 mice were of normal size (Figures 3k–m and Supplementary Figures 4d and e). Atrophic muscle fibers of paralyzed mice (Figure 3n) were significantly smaller compared with nonparalyzed controls (Figure 3p, $P < 0.001$). Both type 1 and 2 fibers were affected and groups of angulated atrophic fibers present, consistent with neurogenic muscle atrophy (Supplementary Figures 4d–g). In parallel with motor improvement, the muscles largely recovered macroscopically (Figure 3k). Recovered mice exhibited partly hypertrophic muscle fibers, with grouping of type 2 fibers, again indicative of neurogenic muscular atrophy (Figure 3o and Supplementary Figure 4g). Upon motor recovery, the percentage of muscle fibers with centralized nuclei was significantly increased in P301SxTAU62$^{on\text{-}off}$ mice (Figure 3q).

### Co-expression of Δtau and full-length four-repeat human wild-type tau causes early, but reversible, nerve cell dysfunction

In Alzheimer's disease, tau pathology develops in the absence of *MAPT* mutations. We therefore crossed TAU62 mice with ALZ17 transgenic mice[31] that express wild-type full-length human four-repeat tau (441 amino acid isoform). ALZ17xTAU62$^{on}$ mice showed a similar phenotype to that of P301SxTAU62$^{on}$ mice. They developed severe motor palsy within 3 weeks (Figures 4a and b and Supplementary Video S4), and soluble high-molecular-weight tau was present (Figure 4c). Pretangle pathology was accompanied by the accumulation of neurofilaments and the formation of axonal spheroids (Figures 4d–g). Peripheral nerves showed evidence of Wallerian degeneration with ovoid-shaped myelin debris (Figure 4h) with consecutive neurogenic muscle atrophy (Figure 4k). Structural and functional changes were reversible, following the cessation of Δtau expression (Figures 4b, i and l and Supplementary Video S5).

### Co-expression of Δtau and full-length three-repeat human wild-type tau causes early and largely irreversible nerve cell dysfunction

We crossed TAU62 mice with ALZ31 transgenic mice that express wild-type full-length three-repeat human tau (352 amino acid tau isoform). ALZ31xTAU62$^{on}$ mice showed severe and early paralysis (Supplementary Figures 5a and b and Supplementary Video S6), developed soluble high-molecular-weight tau (Supplementary Figure 5c) and pre-tangle pathology, as well as neuronal and muscular damage occurred (Supplementary Figures 5d–i). However, unlike what we observed before, most mice failed to recover when Δtau expression was halted.

### Co-expression of two full-length human tau isoforms causes only late nerve cell dysfunction

Slowly progressive, initially mild, motor impairment occurred in mice co-expressing two full-length human tau isoforms (Figures 5a and b). P301SxALZ31 tau mice were still ambulatory at the age of 12 months (Figure 5a and Supplementary Video S7). Similarly, ALZ17xALZ31 tau mice confirmed the absence of severe nerve cell dysfunction (Figure 5b and Supplementary Video S8). Mice from both lines showed robust tau expression, whereas no high molecular tau was detected (Figure 5c and Supplementary Figure 6). They developed only mild motor impairment at the age of 4 months and showed pretangle pathology with extensive AT8 staining (Figures 5d–l).

## DISCUSSION

Here we demonstrate the detrimental interplay between truncated and full-length human tau *in vivo*. Co-expression of truncated tau and full-length wild-type or mutant tau resulted in the formation of soluble, high-molecular-weight tau, severe nerve cell dysfunction, paralysis and marked histopathological changes. Full-length tau and tau truncated at D421 were present in the high-molecular-weight aggregates, consistent with the need for an interaction between the two species. Sarkosyl-insoluble tau or filaments were not present, indicating that nonfilamentous, sarkosyl-soluble, aggregated tau can cause extensive neurotoxicity.

These findings are in agreement with the postulated importance of oligomeric, sarkosyl-soluble tau for the pathogenesis of human tauopathies.[40–42] Tau oligomers have been detected in the brains of patients with Alzheimer's disease and progressive supranuclear palsy.[43–45] In transgenic mouse models of tauopathies, nerve cell loss and memory deficits can precede detectable filamentous tau pathology.[46–48] Moreover, nerve cell loss has been reported in the absence of filaments in tau-overexpressing *Drosophila*,[49] suggesting that the events that lead from tau accumulation to neurodegeneration may not involve filament formation. Reducing tau overexpression in mice transgenic for human mutant P301L tau has been reported to decrease nerve cell loss, despite the continued formation of tau filaments.[50]

Of the mouse lines transgenic for full-length tau, only that expressing human mutant P301S tau develops sarkosyl-insoluble tau inclusions, neurodegeneration and paralysis. However, these inclusions form only when animals heterozygous for the transgene are more than 12 months old.[51] When crossed with line TAU62, heterozygous P301S tau mice were paralyzed by the age of 3 weeks, in the absence of sarkosyl-insoluble tau. The same was true of mice transgenic for wild-type 4R tau when crossed with the TAU62 line; wild-type 4R tau-expressing mice do not develop tau inclusions or neurodegeneration.[31] Whereas soluble oligomeric tau can cause neurotoxicity, it has been reported that either

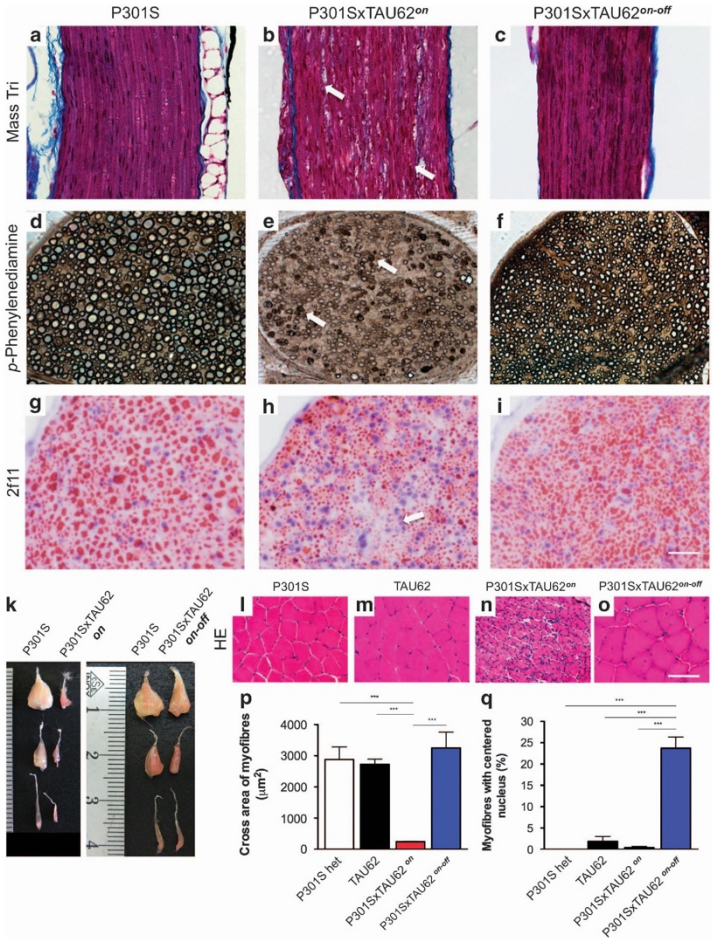


**Figure 3.** Co-expression of 4R P301S tau and Δtau (P301SxTAU62 mice) causes neuropathy and neurogenic muscle atrophy that are reversible upon cessation of Δtau expression. (**a–i**) Sciatic nerves stained using Masson's trichrom stain (**a–c**), *para*-phenylenediamine (**d–f**) and 2f11 immunohistochemistry (**g–i**). The scale bar in (**i**) corresponds to 50 µm in (**a–c**), 32 µm in (**d-f**) and 25 µm in (**g–i**). (**k**) Macroscopic view of hindlimb muscles. From the top: M. gastrocnemius and M. soleus; M. tibialis anterior; M. extensor digitorum longus. (**l–o**) M. gastrocnemius stained with hematoxylin and eosin (HE). The scale bar in (**o**) corresponds to 100 µm (for **l–o**). Quantification of myofiber area (**p**) and myofibers with internalized nucleus (**q**). P301S: heterozygous mice transgenic for human mutant P301S tau, aged 3 weeks; TAU62: heterozygous mice expressing 3R $tau_{151-421}$, aged 3 weeks; P301SxTAU62$^{on}$: paralyzed mice, aged 3 weeks; P301SxTAU62$^{on-off}$: recovered mice, 6 weeks after cessation of the expression of Δtau. ***$P < 0.001$.

soluble[52] or insoluble aggregated tau is required for the prion-like propagation of tau assemblies.[53] It will be interesting to see whether the soluble high-molecular-weight tau described here can seed tau assembly.

Similar to Alzheimer's disease,[54] axonal spheroids filled with small congested mitochondria and neurofilaments accumulated in the bigenic mouse lines, suggestive of axonal transport deficits. Microtubules were sparse in spinal cord axons, where neurofilaments accumulated, reminiscent of what has been described in Alzheimer's disease[55] and transgenic mouse models of human tauopathies.[56,57] Axonal transport defects have been reported in a broad spectrum of neurodegenerative diseases, including Alzheimer's disease, and the term 'dysferopathies' has been introduced for this group of disorders.[58,59] Paralyzed P301SxTAU62 mice exhibited dislocated and clustered mitochondria, similar to Alzheimer's disease and tauopathy models, where perinuclear mitochondrial clumping correlated with the accumulation of soluble tau species.[60] Dispersed and swollen Golgi networks, associated with the somatic accumulation of synaptophysin, suggested disrupted cellular transport mechanisms, similar to previous findings in mice transgenic for human mutant P301L tau.[61] In Alzheimer's disease, Golgi fragmentation has been

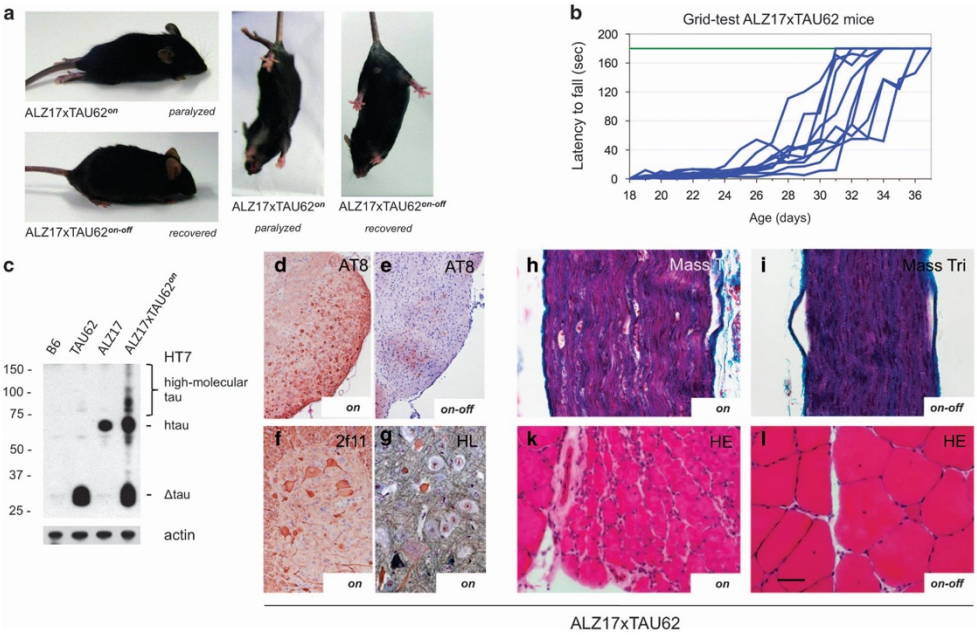


**Figure 4.** Co-expression of 4R wild-type tau and Δtau (ALZ17xTAU62) causes paralysis and neuropathy that are reversible upon cessation of Δtau expression. (**a**) Paralyzed (aged 3 weeks) and recovered (3 weeks after cessation of Δtau expression) ALZ17xTAU62 mice (see also Supplementary Videos S4 and S5). (**b**) Recovery of motor function as assessed by a grid test of ALZ17xTAU62 mice following the removal of doxycycline between 16 and 20 days of age (blue lines). Motor function of heterozygous ALZ17 littermates (green line) ($n = 6$). (**c**) Western blot with HT7 of brainstem tissue from nontransgenic (B6), TAU62, ALZ17 and ALZ17xTAU62 mice. Actin staining was used as the loading control. (**d–l**) Histological analysis of paralyzed ('*on*', **d**, **f**, **g**, **h** and **k**) and recovered ('*on-off*', **e**, **i** and **l**) ALZ17xTAU62 mice using anti-tau antibody AT8 (**d** and **e**), anti-neurofilament antibody 2f11 (**f**), Masson's trichrome (**h** and **i**), Holmes–Luxol (HL) (**g**) and hematoxylin–eosin (HE) (**k** and **l**). The scale bar in (**l**) corresponds to 50 μm in (**h**, **i**, **g**, **k** and **l**), 100 μm in (**f**) and 200 μm in (**d** and **e**).

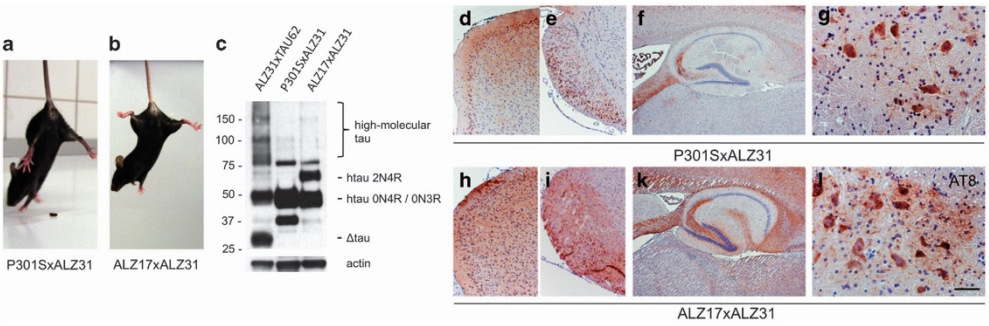


**Figure 5.** Co-expression of 4R mutant or wild-type tau and 3R wild-type (P301SxALZ31 or ALZ17xALZ31 mice) does not cause paralysis and results in pretangle pathology. (**a** and **b**) Unimpaired P301SxALZ31 and ALZ17xALZ31 mice aged 3 weeks (see also Supplementary Videos S7 and S8). (**c**) Western blot with HT7 of brainstem tissue from paralyzed ALZ31xTAU62 mice aged 3 weeks, unimpaired P301SxALZ31 aged 3 weeks and unimpaired ALZ17xALZ31 mice aged 4 months. Actin staining was used as the loading control. (**d–l**) Immunohistochemistry of 9-month-old P301SxALZ31 mouse and 4-month-old ALZ17xALZ31 mouse with AT8 ((**d** and **h**) cortex, (**e** and **i**) brainstem, (**f** and **k**) hippocampus and (**g** and **l**) spinal cord). The scale bar in (**l**) corresponds to 200 μm in (**d**, **e**, **h** and **i**), 500 μm in (**f** and **k**) and 50 μm in (**g** and **l**).

described in nontangle-bearing neurons,[62] consistent with the present findings. The neuronal dysfunction present in the absence of tau filaments in our bigenic mouse models may mirror an early stage of tauopathy in Alzheimer's disease.[63]

Although we observed partial nerve fiber loss in paralyzed mice, reflecting toxicity of the oligomeric tau species, the palsy appears mainly attributable to functional neuronal impairment. When Δtau expression was halted, the severe limb paralysis largely improved,

despite the continued expression of full-length wild-type 4R or mutant P301S 4R tau. After a lag phase of a few days, paralyzed mice rapidly regained full motor control within 2 days, pointing to a reversible impairment of axonal transport. Rapidly regained nerve fiber function then enables remodeling of atrophic muscle. Only when Δtau had been expressed together with full-length wild-type 3R tau, was paralysis not reversible following the cessation of the expression of truncated tau. Functional recovery thus appears to depend on the presence of mixed 3R/4R tau oligomers. Following cessation of Δtau expression and functional recovery, the high-molecular-weight tau bands disappeared. Co-expression of full-length and Δtau was required, because co-expression of full-length 3R and 4R tau did not cause paralysis.

While the C-terminal end of Δtau constitutes a main tau cleavage site in Alzheimer's disease, its N-terminal end has been set at the structural transition of the proline-rich region to the acidic N-terminal projection domain of tau. This limitation of our model has been unavoidable, as N-terminal tau cleavage sites are yet poorly characterized, and only few N-terminal cleavage sites, located at the beginning of the acidic region of tau, have been confirmed *in situ*.[18,64,65]

In conclusion, we show here that an interaction between full-length and Δtau can lead to the formation of neurotoxic tau species that interfere with axonal transport. The reversibility of paralysis upon cessation of truncated tau expression augurs well for the development of new therapies for Alzheimer's disease and other tauopathies.

## CONFLICT OF INTEREST

The authors declare no conflict of interest.

## ACKNOWLEDGMENTS

We thank Nicholas Gonatas, University of Pennsylvania Medical Center, Philadelphia, PA, for the MG160 antibody, the Microscopy Center of the University of Basel (M Dürrenberger and U Sauder) for experimental help and Professor Ludwig Kappos, University Hospital Basel, for helpful discussions and support of this work. MT and DTW are supported by the Swiss National Science Foundation (310030_135214 to MT and 32323B_123812 to DTW), the Velux Foundation, the Mach-Gaensslen Foundation, the Synapsis Foundation and the D&N Yde Foundation, Switzerland. GF and MG are supported by the UK Medical Research Council (U105184291).

## REFERENCES

1 Spillantini MG, Goedert M. Tau pathology and neurodegeneration. *Lancet Neurol* 2013; **12**: 609–622.
2 Spires-Jones TL, Hyman BT. The intersection of amyloid beta and tau at synapses in Alzheimer's disease. *Neuron* 2014; **82**: 756–771.
3 Frost B, Hemberg M, Lewis J, Feany MB. Tau promotes neurodegeneration through global chromatin relaxation. *Nat Neurosci* 2014; **17**: 357–366.
4 Rosenmann H. Asparagine endopeptidase cleaves tau and promotes neurodegeneration. *Nat Med* 2014; **20**: 1236–1238.
5 Eisenberg D, Jucker M. The amyloid state of proteins in human diseases. *Cell* 2012; **148**: 1188–1203.
6 Masters CL, Selkoe DJ. Biochemistry of amyloid beta-protein and amyloid deposits in Alzheimer disease. *Cold Spring Harb Perspect Med* 2012; **2**: a006262.
7 Vidal R, Frangione B, Rostagno A, Mead S, Revesz T, Plant G *et al.* A stop-codon mutation in the BRI gene associated with familial British dementia. *Nature* 1999; **399**: 776–781.
8 Baba M, Nakajo S, Tu PH, Tomita T, Nakaya K, Lee VM *et al.* Aggregation of alpha-synuclein in Lewy bodies of sporadic Parkinson's disease and dementia with Lewy bodies. *Am J Pathol* 1998; **152**: 879–884.
9 Goedert M, Spillantini MG, Del Tredici K, Braak H. 100 years of Lewy pathology. *Nat Rev Neurol* 2013; **9**: 13–24.
10 Neumann M, Sampathu DM, Kwong LK, Truax AC, Micsenyi MC, Chou TT *et al.* Ubiquitinated TDP-43 in frontotemporal lobar degeneration and amyotrophic lateral sclerosis. *Science* 2006; **314**: 130–133.
11 Arai T, Hasegawa M, Akiyama H, Ikeda K, Nonaka T, Mori H *et al.* TDP-43 is a component of ubiquitin-positive tau-negative inclusions in frontotemporal lobar degeneration and amyotrophic lateral sclerosis. *Biochem Biophys Res Commun* 2006; **351**: 602–611.
12 Nonaka T, Kametani F, Arai T, Akiyama H, Hasegawa M. Truncation and pathogenic mutations facilitate the formation of intracellular aggregates of TDP-43. *Hum Mol Genet* 2009; **18**: 3353–3364.
13 Brower CS, Piatkov KI, Varshavsky A. Neurodegeneration-associated protein fragments as short-lived substrates of the N-end rule pathway. *Mol Cell* 2013; **50**: 161–171.
14 Gamblin TC, Chen F, Zambrano A, Abraha A, Lagalwar S, Guillozet AL *et al.* Caspase cleavage of tau: linking amyloid and neurofibrillary tangles in Alzheimer's disease. *Proc Natl Acad Sci USA* 2003; **100**: 10032–10037.
15 Rissman RA, Poon WW, Blurton-Jones M, Oddo S, Torp R, Vitek MP *et al.* Caspase-cleavage of tau is an early event in Alzheimer disease tangle pathology. *J Clin Invest* 2004; **114**: 121–130.
16 de Calignon A, Fox LM, Pitstick R, Carlson GA, Bacskai BJ, Spires-Jones TL *et al.* Caspase activation precedes and leads to tangles. *Nature* 2010; **464**: 1201–1204.
17 Khurana V, Elson-Schwab I, Fulga TA, Sharp KA, Loewen CA, Mulkearns E *et al.* Lysosomal dysfunction promotes cleavage and neurotoxicity of tau in vivo. *PLoS Genet* 2010; **6**: e1001026.
18 Horowitz PM, Patterson KR, Guillozet-Bongaarts AL, Reynolds MR, Carroll CA, Weintraub ST *et al.* Early N-terminal changes and caspase-6 cleavage of tau in Alzheimer's disease. *J Neurosci* 2004; **24**: 7895–7902.
19 Matsumoto SE, Motoi Y, Ishiguro K, Tabira T, Kametani F, Hasegawa M *et al.* The twenty-four KDa C-terminal tau fragment increases with aging in tauopathy mice: implications of prion-like properties. *Hum Mol Genet* 2015; **24**: 6403–6416.
20 Henriksen K, Wang Y, Sorensen MG, Barascuk N, Suhy J, Pedersen JT *et al.* An enzyme-generated fragment of tau measured in serum shows an inverse correlation to cognitive function. *PLoS One* 2013; **8**: e64990.
21 Avila J. Alzheimer disease: caspases first. *Nat Rev Neurol* 2010; **6**: 587–588.
22 Zhang Z, Song M, Liu X, Kang SS, Kwon IS, Duong DM *et al.* Cleavage of tau by asparagine endopeptidase mediates the neurofibrillary pathology in Alzheimer's disease. *Nat Med* 2014; **20**: 1254–1262.
23 Delobel P, Lavenir I, Fraser G, Ingram E, Holzer M, Ghetti B *et al.* Analysis of tau phosphorylation and truncation in a mouse model of human tauopathy. *Am J Pathol* 2008; **172**: 123–131.
24 Lin WL, Dickson DW, Sahara N. Immunoelectron microscopic and biochemical studies of caspase-cleaved tau in a mouse model of tauopathy. *J Neuropathol Exp Neurol* 2011; **70**: 779–787.
25 Goedert M, Wischik CM, Crowther RA, Walker JE, Klug A. Cloning and sequencing of the cDNA encoding a core protein of the paired helical filament of Alzheimer disease: identification as the microtubule-associated protein tau. *Proc Natl Acad Sci USA* 1988; **85**: 4051–4055.
26 Wischik CM, Novak M, Thogersen HC, Edwards PC, Runswick MJ, Jakes R *et al.* Isolation of a fragment of tau derived from the core of the paired helical filament of Alzheimer disease. *Proc Natl Acad Sci USA* 1988; **85**: 4506–4510.
27 Goedert M, Spillantini MG, Cairns NJ, Crowther RA. Tau proteins of Alzheimer paired helical filaments: abnormal phosphorylation of all six brain isoforms. *Neuron* 1992; **8**: 159–168.
28 Abraha A, Ghoshal N, Gamblin TC, Cryns V, Berry RW, Kuret J *et al.* C-terminal inhibition of tau assembly in vitro and in Alzheimer's disease. *J Cell Sci* 2000; **113**: 3737–3745.
29 Spires-Jones TL, Kopeikina KJ, Koffie RM, de Calignon A, Hyman BT. Are tangles as toxic as they look? *J Mol Neurosci* 2011; **45**: 438–444.
30 Wang YP, Biernat J, Pickhardt M, Mandelkow E, Mandelkow EM. Stepwise proteolysis liberates tau fragments that nucleate the Alzheimer-like aggregation of full-length tau in a neuronal cell model. *Proc Natl Acad Sci USA* 2007; **104**: 10252–10257.
31 Probst A, Gotz J, Wiederhold KH, Tolnay M, Mistl C, Jaton AL *et al.* Axonopathy and amyotrophy in mice transgenic for human four-repeat tau protein. *Acta Neuropathol* 2000; **99**: 469–481.
32 Allen B, Ingram E, Takao M, Smith MJ, Jakes R, Virdee K *et al.* Abundant tau filaments and nonapoptotic neurodegeneration in transgenic mice expressing human P301S tau protein. *J Neurosci* 2002; **22**: 9340–9351.
33 Luthi A, Putten H, Botteri FM, Mansuy IM, Meins M, Frey U *et al.* Endogenous serine protease inhibitor modulates epileptic activity and hippocampal long-term potentiation. *J Neurosci* 1997; **17**: 4688–4699.
34 Huang C, Tong J, Bi F, Zhou H, Xia XG. Mutant TDP-43 in motor neurons promotes the onset and progression of ALS in rats. *J Clin Invest* 2012; **122**: 107–118.
35 Demonbreun AR, Fahrenbach JP, Deveaux K, Earley JU, Pytel P, McNally EM. Impaired muscle growth and response to insulin-like growth factor 1 in dysferlin-mediated muscular dystrophy. *Hum Mol Genet* 2011; **20**: 779–789.
36 Winkler DT, Biedermann L, Tolnay M, Allegrini PR, Staufenbiel M, Wiessner C *et al.* Thrombolysis induces cerebral hemorrhage in a mouse model of cerebral amyloid angiopathy. *Ann Neurol* 2002; **51**: 790–793.

37 Romeis B. *Mikroskopische Technik*. Urban u. Schwarzenberg: München, Wien, Baltimore, 1989.
38 Leger M, Quiedeville A, Bouet V, Haelewyn B, Boulouard M, Schumann-Bard P *et al.* Object recognition test in mice. *Nat Protoc* 2013; **8**: 2531–2537.
39 Filipcik P, Zilka N, Bugos O, Kucerak J, Koson P, Novak P *et al.* First transgenic rat model developing progressive cortical neurofibrillary tangles. *Neurobiol Aging* 2012; **33**: 1448–1456.
40 Lasagna-Reeves CA, Castillo-Carranza DL, Sengupta U, Sarmiento J, Troncoso J, Jackson GR *et al.* Identification of oligomers at early stages of tau aggregation in Alzheimer's disease. *FASEB J* 2012; **26**: 1946–1959.
41 Blair LJ, Nordhues BA, Hill SE, Scaglione KM, O'Leary JC 3rd, Fontaine SN *et al.* Accelerated neurodegeneration through chaperone-mediated oligomerization of tau. *J Clin Invest* 2013; **123**: 4158–4169.
42 Gerson JE, Kayed R. Formation and propagation of tau oligomeric seeds. *Front Neurol* 2013; **4**: 93.
43 Maeda S, Sahara N, Saito Y, Murayama S, Ikai A, Takashima A. Increased levels of granular tau oligomers: an early sign of brain aging and Alzheimer's disease. *Neurosci Res* 2006; **54**: 197–201.
44 Patterson KR, Remmers C, Fu Y, Brooker S, Kanaan NM, Vana L *et al.* Characterization of prefibrillar Tau oligomers in vitro and in Alzheimer disease. *J Biol Chem* 2011; **286**: 23063–23076.
45 Gerson JE, Sengupta U, Lasagna-Reeves CA, Guerrero-Munoz MJ, Troncoso J, Kayed R. Characterization of tau oligomeric seeds in progressive supranuclear palsy. *Acta Neuropathol Commun* 2014; **2**: 73.
46 Oddo S, Caccamo A, Shepherd JD, Murphy MP, Golde TE, Kayed R *et al.* Triple-transgenic model of Alzheimer's disease with plaques and tangles: intracellular Abeta and synaptic dysfunction. *Neuron* 2003; **39**: 409–421.
47 Spires TL, Orne JD, SantaCruz K, Pitstick R, Carlson GA, Ashe KH *et al.* Region-specific dissociation of neuronal loss and neurofibrillary pathology in a mouse model of tauopathy. *Am J Pathol* 2006; **168**: 1598–1607.
48 Berger Z, Roder H, Hanna A, Carlson A, Rangachari V, Yue M *et al.* Accumulation of pathological tau species and memory loss in a conditional model of tauopathy. *J Neurosci* 2007; **27**: 3650–3662.
49 Wittmann CW, Wszolek MF, Shulman JM, Salvaterra PM, Lewis J, Hutton M *et al.* Tauopathy in Drosophila: neurodegeneration without neurofibrillary tangles. *Science* 2001; **293**: 711–714.
50 Santacruz K, Lewis J, Spires T, Paulson J, Kotilinek L, Ingelsson M *et al.* Tau suppression in a neurodegenerative mouse model improves memory function. *Science* 2005; **309**: 476–481.
51 Clavaguera F, Hench J, Lavenir I, Schweighauser G, Frank S, Goedert M *et al.* Peripheral administration of tau aggregates triggers intracerebral tauopathy in transgenic mice. *Acta Neuropathol* 2014; **127**: 299–301.
52 Lasagna-Reeves CA, Castillo-Carranza DL, Sengupta U, Guerrero-Munoz MJ, Kiritoshi T, Neugebauer V *et al.* Alzheimer brain-derived tau oligomers propagate pathology from endogenous tau. *Sci Rep* 2012; **2**: 700.
53 Clavaguera F, Bolmont T, Crowther RA, Abramowski D, Frank S, Probst A *et al.* Transmission and spreading of tauopathy in transgenic mouse brain. *Nat Cell Biol* 2009; **11**: 909–913.
54 Schmidt ML, Lee VM, Trojanowski JQ. Relative abundance of tau and neurofilament epitopes in hippocampal neurofibrillary tangles. *Am J Pathol* 1990; **136**: 1069–1075.
55 Cash AD, Aliev G, Siedlak SL, Nunomura A, Fujioka H, Zhu X *et al.* Microtubule reduction in Alzheimer's disease and aging is independent of tau filament formation. *Am J Pathol* 2003; **162**: 1623–1627.
56 Yoshiyama Y, Zhang B, Bruce J, Trojanowski JQ, Lee VM. Reduction of detyrosinated microtubules and Golgi fragmentation are linked to tau-induced degeneration in astrocytes. *J Neurosci* 2003; **23**: 10662–10671.
57 Zhang B, Carroll J, Trojanowski JQ, Yao Y, Iba M, Potuzak JS *et al.* The microtubule-stabilizing agent, epothilone D, reduces axonal dysfunction, neurotoxicity, cognitive deficits, and Alzheimer-like pathology in an interventional study with aged tau transgenic mice. *J Neurosci* 2012; **32**: 3601–3611.
58 Morfini GA, Burns M, Binder LI, Kanaan NM, LaPointe N, Bosco DA *et al.* Axonal transport defects in neurodegenerative diseases. *J Neurosci* 2009; **29**: 12776–12786.
59 Vossel KA, Zhang K, Brodbeck J, Daub AC, Sharma P, Finkbeiner S *et al.* Tau reduction prevents Abeta-induced defects in axonal transport. *Science* 2010; **330**: 198.
60 Kopeikina KJ, Carlson GA, Pitstick R, Ludvigson AE, Peters A, Luebke JI *et al.* Tau accumulation causes mitochondrial distribution deficits in neurons in a mouse model of tauopathy and in human Alzheimer's disease brain. *Am J Pathol* 2011; **179**: 2071–2082.
61 Liazoghli D, Perreault S, Micheva KD, Desjardins M, Leclerc N. Fragmentation of the Golgi apparatus induced by the overexpression of wild-type and mutant human tau forms in neurons. *Am J Pathol* 2005; **166**: 1499–1514.
62 Stieber A, Mourelatos Z, Gonatas NK. In Alzheimer's disease the Golgi apparatus of a population of neurons without neurofibrillary tangles is fragmented and atrophic. *Am J Pathol* 1996; **148**: 415–426.
63 Khan UA, Liu L, Provenzano FA, Berman DE, Profaci CP, Sloan R *et al.* Molecular drivers and cortical spread of lateral entorhinal cortex dysfunction in preclinical Alzheimer's disease. *Nat Neurosci* 2013; **17**: 304–311.
64 Derisbourg M, Leghay C, Chiappetta G, Fernandez-Gomez FJ, Laurent C, Demeyer D *et al.* Role of the Tau N-terminal region in microtubule stabilization revealed by new endogenous truncated forms. *Sci Rep* 2015; **5**: 9659.
65 Rohn TT, Rissman RA, Davis MC, Kim YE, Cotman CW, Head E. Caspase-9 activation and caspase cleavage of tau in the Alzheimer's disease brain. *Neurobiol Dis* 2002; **11**: 341–354.



Supplementary Information accompanies the paper on the Molecular Psychiatry website (http://www.nature.com/mp)

## Supplemental Information

Supplementary Information accompanies the paper on the Molecular Psychiatry website (http://www.nature.com/mp)

***Supplementary Videos:***

**Video S1**

A 3-week-old P301SxTAU62$^{on}$ double transgenic mouse is shown. Note the paralysis of the hindlimbs, while the mouse is still capable of moving by using the forelimbs.

**Video S2**

Video of a 5-month-old homozygous P301S mouse. Homozygous P301S mice develop overt motor impairments starting at ages of 3-4 months. This mouse is walking slowly, however, there is no severe hindlimb palsy occurring in P301S mice up to ages of 5 months.

**Video S3**

The same P301SxTAU62$^{on\text{-}off}$ mouse seen in Video S1 is shown, but now 38 days after $\Delta$tau expression has been stopped by withdrawal of doxycycline. The hindlimb palsy is significantly improved and the mouse is again walking almost normally.

**Video S4**

A 3-week-old ALZ17xTAU62$^{on}$ double transgenic mouse is shown. Note the paralysis of the hind limbs, while the mouse is still capable of moving by using the forelimbs.

**Video S5**

A recovered ALZ17xTAU62$^{on\text{-}off}$ mouse is shown one month after $\Delta$tau expression has been stopped by withdrawal of doxycycline.

**Video S6**

Paralyzed ALZ31xTAU62$^{on}$ mouse aged three weeks.

**Video S7**

12-month-old P301SxALZ31 mouse. Note the normal grid climbing capability of this double transgenic mouse.

**Video S8**

4-month-old ALZ17SxALZ31 mouse. Note the normal grid climbing capability of this double transgenic mouse.

## *Supplementary Table and Figures:*

## Table S1

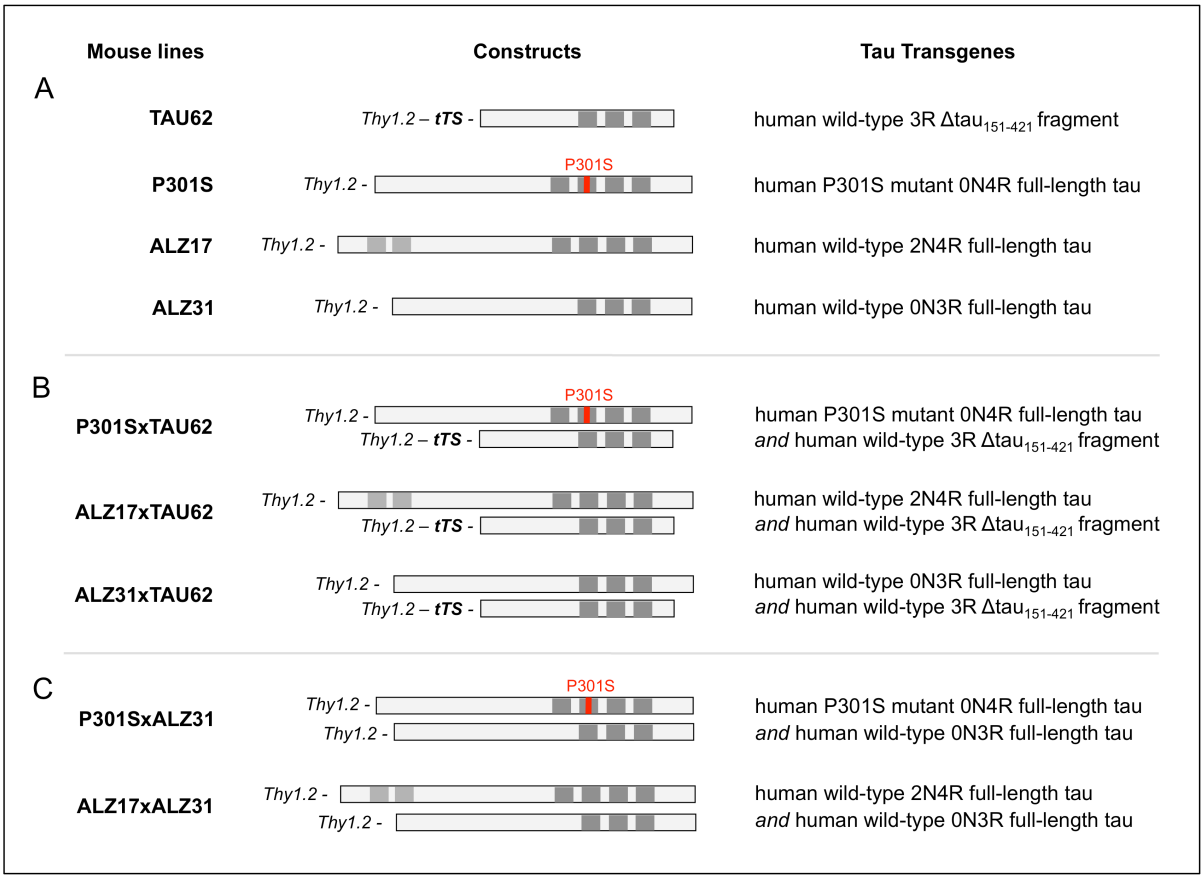


(**a-c**) Overview on the transgenic and co-transgenic mouse lines used for the present studies. Tau isoforms expressed are shown. Dark grey boxes indicate the tau repeat domains (3R or 4R isoforms), and light grey boxes N-terminal inserts (e.g. ALZ17 ≙ 2N4R).
The tau cDNA constructs are either driven by a standard Thy1.2 minigene (Thy1.2) or by a modified Thy1.2 minigene that contains a tetracycline controlled transcriptional silencer element (Thy1.2-tTS) in case of the TAU62 mouse. (**a**) shows the tau isoforms expressed in single-transgenic lines. (**b**) shows the tau forms of 3 mouse lines co-expressing full-length tau with Δtau. (**c**) depicts 2 mouse lines co-expressing different full-length tau isoforms.

**Figure S1**

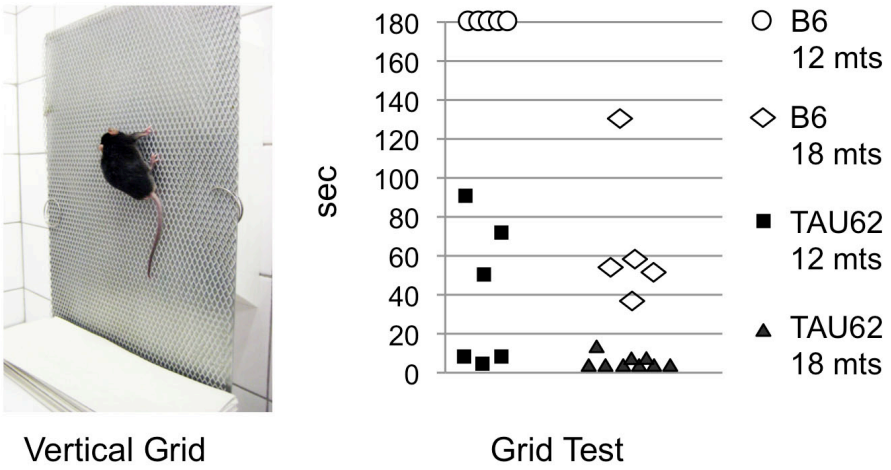


*TAU62 mice develop a slowly progressive motor phenotype.*
Motor fitness was assessed on a vertical mesh grid. Time spent on the grid progressively declined in TAU62 mice, while B6 controls were unimpaired at 12 months and showed a mild decline at 18 months of age.

## Figure S2

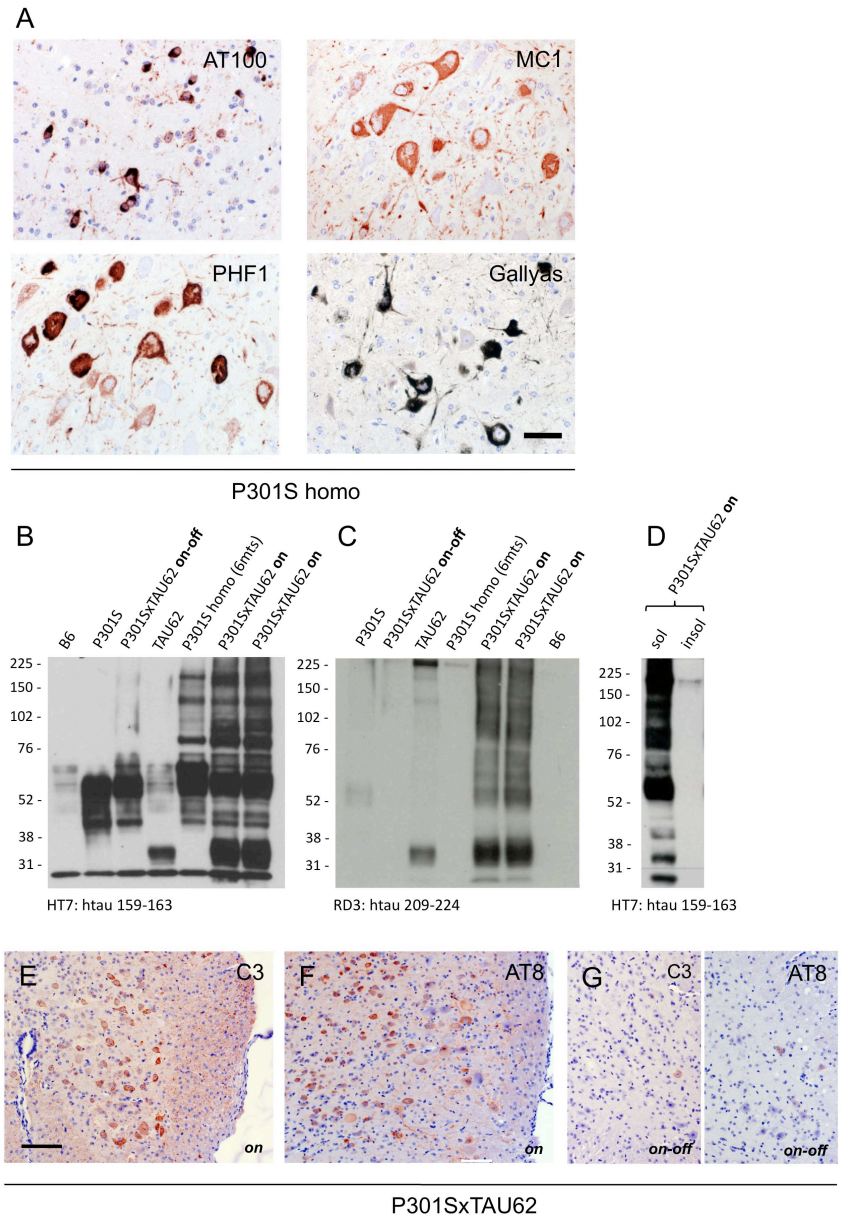


(**a**) Extensive hyperphosphorylation of tau was seen in the brainstem of old homozygous P301S mice by staining with antibodies targeting late phospho-epitopes. Multiple tau tangles and granular aggregates were detectable in these mice by Gallyas silver stain. The scale bar in **a** corresponds to 50 μm. (**b**) Western blotting under non-reducing conditions revealed high-molecular tau species in paralyzed P301SxTAU62$^{on}$ mice (lanes 6&7); similar tau species were seen in aged tangle bearing homozygous P301S mice (lane 5). When tau expression was halted, no more high-molecular tau forms were detectable in P301SxTAU62$^{on\text{-}off}$ mice (lane 3; Western blot performed with anti-tau antibody HT7). (**c**) Staining with the RD3 antibody targeting Asp421 shows the presence of Δtau in the high molecular weight tau species. (**d**) Sarkosyl-extraction detects only soluble tau species in paralyzed P301SxTAU62$^{on}$ mice ("sol": sarkosyl-soluble tau; "insol": sarkosyl-insoluble fraction). (**e-g**) Δtau was widely expressed in the spinal cord of P301SxTAU62$^{on}$ mice (**e**) and phosphorylated at the AT8 epitope **(f)**. Upon cessation of Δtau expression, Δtau- and AT8-positive tau was no longer detectable **(g)**. The scale bar in **e** corresponds to 100 μm in **e-g**.

**Figure S3**

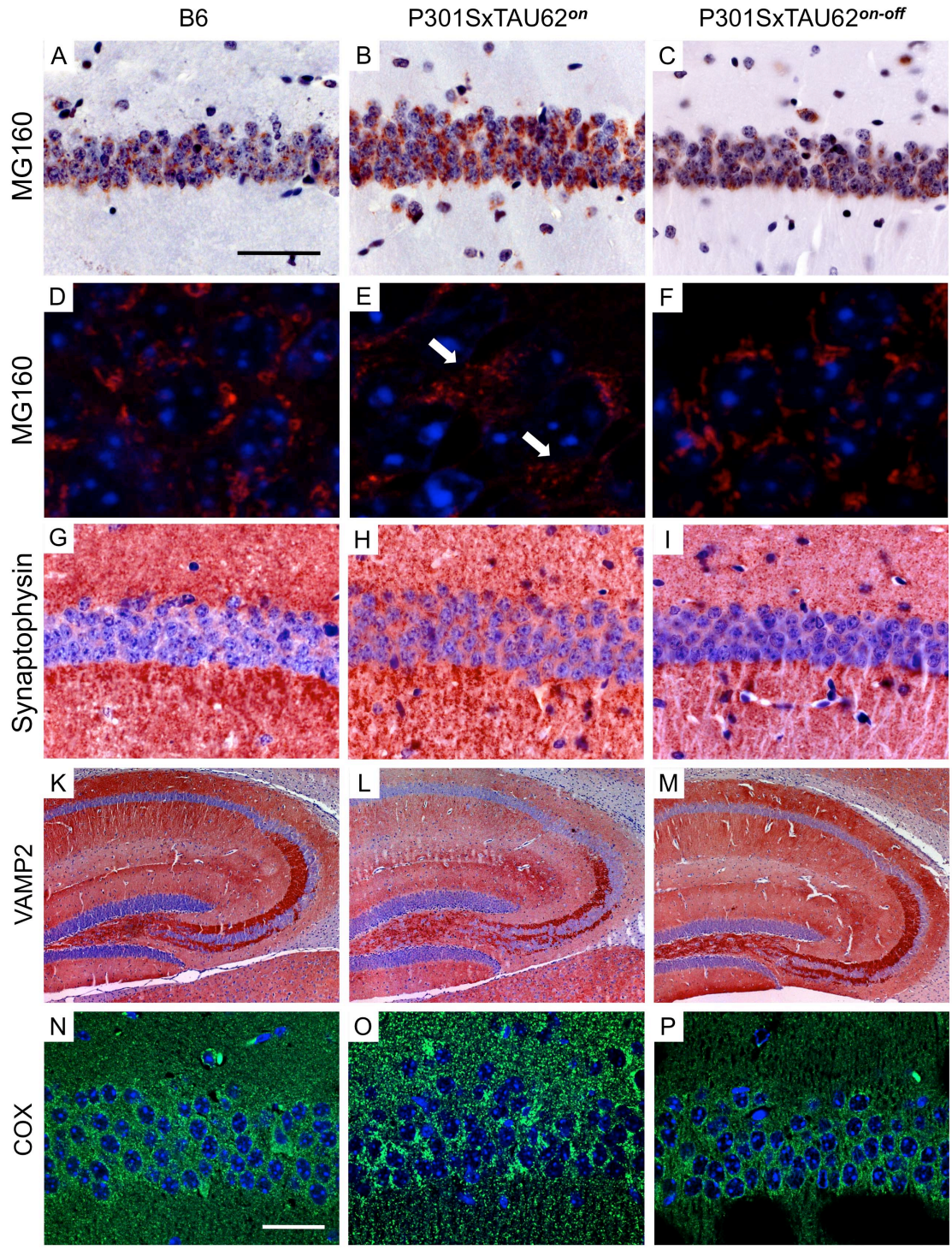


(**a-m**) P301SxTAU62 mice exhibit signs of Golgi disruption, protein missorting and mitochondrial clustering. These signs are reversible upon cessation of Δtau expression. Immunohistochemistry using antibodies against MG160 (**a-f**), synaptophysin (**g-i**), VAMP2 (**k-m**), and cytochrome C oxidase (COX) (**n-p**), in the hippocampus of non-transgenic mice (B6)**,** 3-week-old paralyzed mice (P301SxTAU62$^{on}$) and recovered mice 6 weeks after cessation of Δtau expression (P301SxTAU62$^{on\text{-}off}$). The scale bar in **a** corresponds to 19 μm in **d-f**, 63 μm in **a-c** and **g-i,** and 400 μm in **k-m**. The scale bar in **n** corresponds to 30 μm for **n-p**. Arrows in (**e**) indicate fragmented Golgi structures.

## Figure S4

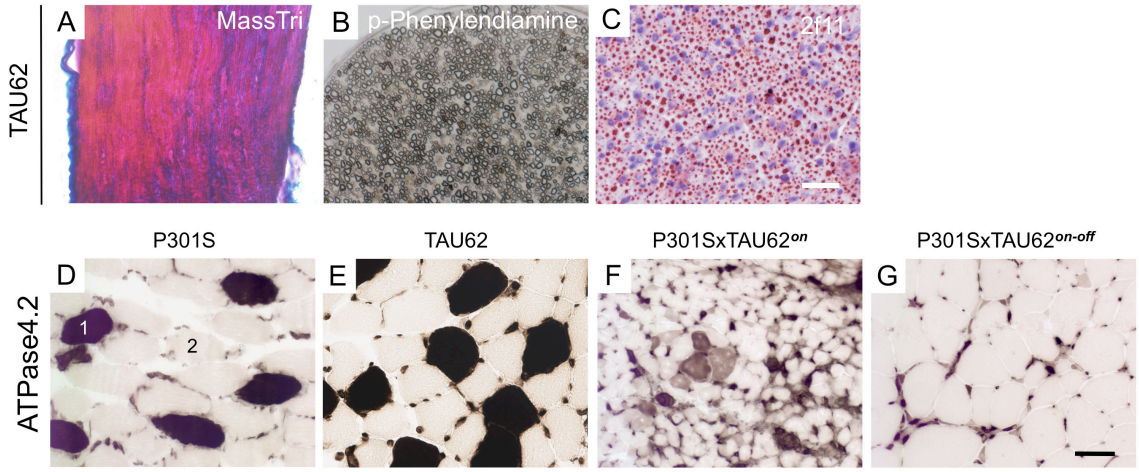


(**a-c**) Young TAU62 mice exhibit normal sciatic nerves (Masson's trichrom stain (**a**); para-Phenylenediamine (**b**); immunohistochemistry using 2f11 antibody (**c**). The scale bar in **c** corresponds to 30 μm in **a-c.** (**d-g**) M. gastrocnemius stained for ATPase (pH 4.2). Dark type 1 fibres (1) and light type 2 fibres (2). The scale bar in **g** corresponds to 50 μm (for **d-g**). P301S: heterozygous mice transgenic for human mutant P301S tau, aged 3 weeks; TAU62: heterozygous mice expressing 3R $tau_{151-421}$, aged 3 weeks; P301SxTAU62$^{on}$: paralyzed mice, aged 3 weeks; P301SxTAU62$^{on-off}$: recovered mice, 6 weeks after cessation of the expression of Δtau.

## Figure S5

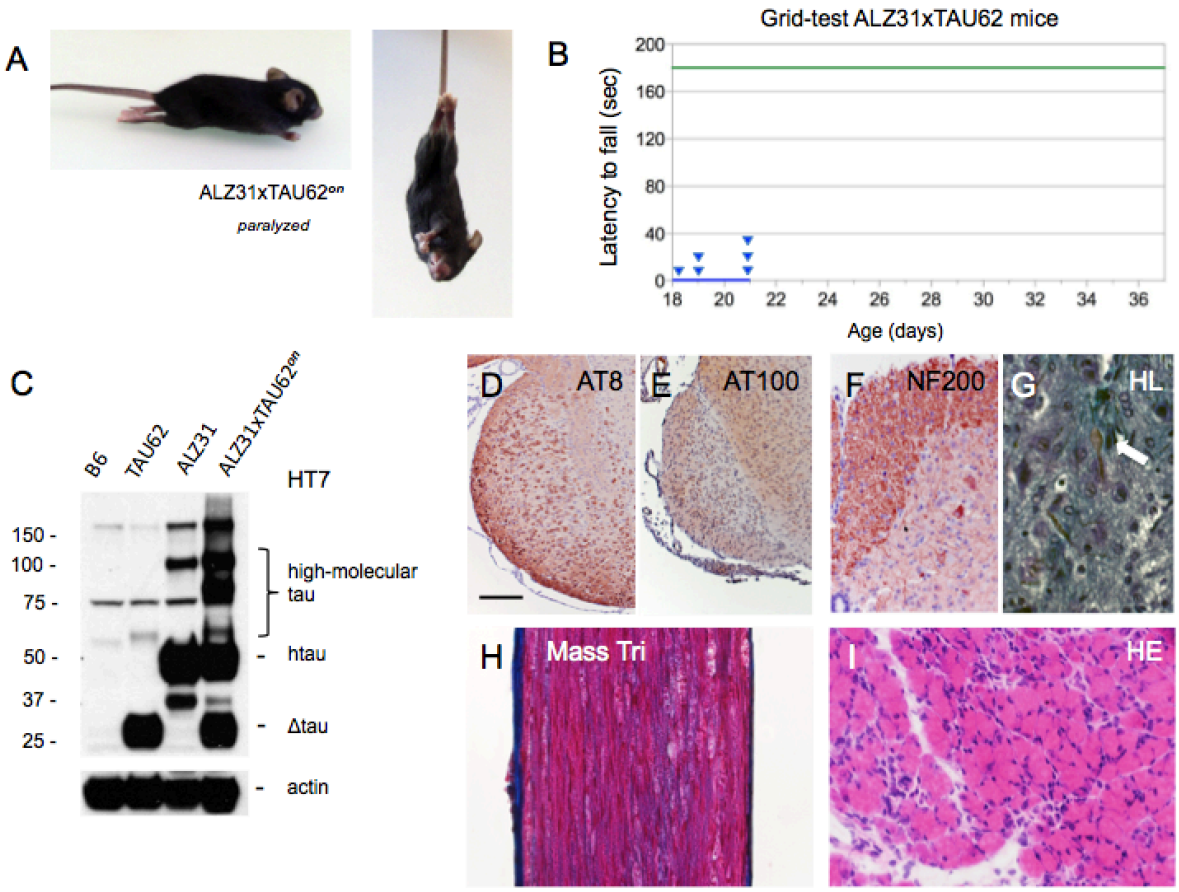


**(a-i)** Co-expression of 3R wild-type tau and Δtau (ALZ31xTAU62 mice) causes paralysis and neuropathy, which are not reversed upon cessation of Δtau expression. (**a**) Paralyzed (aged 3 weeks) and non-recovered (3 weeks after cessation of Δtau expression) ALZ31xTAU62 mice (see also video S6). (**b**) Absence of recovery of motor function as assessed by a grid-test of ALZ31xTAU62 mice following the removal of doxycycline between 14 and 16 days (blue line; triangles indicate the times of euthanasia, n=6). Motor function of heterozygous ALZ31 mice (green line, n=7). (**c**) Western blot with HT7 of brainstem tissue from non-transgenic mice (B6), TAU62 mice, ALZ31 mice and ALZ31xTAU62 mice. Actin staining was used as the loading control. (**d-i**) Histological analysis of paralyzed ALZ31xTAU62 mice aged 3 weeks, using AT8 (**d**), AT100 (**e**), NF200 (**f**), Holmes-Luxol (HL) (**g**), Masson's trichrome (**h**), and Hematoxylin-eosin (HE) staining (**i**). The arrow in (**g**) points to a spheroid. The scale bar in **d** corresponds to 200 μm in **d** and **e**; 100 μm in **f**; 33 μm in **g**; 50 μm in **h, i**.

## Figure S6

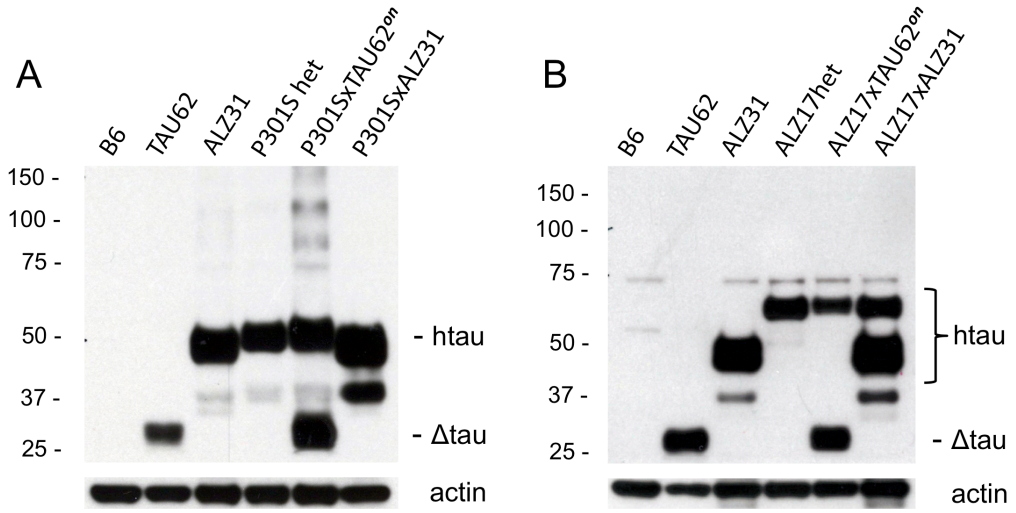


(**a,b**) Robust expression of the two full-length tau isoforms in P301SxALZ31 (**a**) and ALZ17xALZ31 (**b**) co-transgenic mice. For comparison, expression of mice co-transgenic for Δtau with full-length tau, as well as the respective single transgenic mice is shown. Western blots run under reducing conditions using HT7 antibody.

## Supplemental Experimental Procedures

*Antibodies used for immunohistochemistry (IHC) and Western blotting (WB)*
(species is mouse, unless indicated otherwise):

| Antibody | Target | Dilution | Source |
|---|---|---|---|
| HT7 | human tau<br>aa 159-163 | WB 1:4000<br>IHC 1:800 | Pierce, Rockford, IL<br>#MN1000 |
| BR134 | human tau | WB 1:1000 | (Goedert et al., 1989) |
| Tau-C3 | Tau cleaved at residue Asp421 | WB 1:1000<br>IHC 1:1000 | Santa Cruz Biotechnology, Inc, Dallas, TX<br>#sc-32240 |
| AT8 | Tau<br>pSer202/Thr205 | WB 1:1000<br>IHC 1:800 | Pierce, Rockford, IL #MN1020 |
| AT100 | Tau<br>pThr212/Ser214 | WB 1:1000<br>IHC 1:500 | Pierce, Rockford, IL #MN1060 |
| PHF-1 | Tau<br>pSer396/404 | WB 1:2000<br>IHC 1:1000 | Peter Davies, Albert Einstein College of Medecine, Bronx, NY |
| MC1 | Tau<br>aa 5-15, 312-322 | IHC 1:100 | Peter Davies, Albert Einstein College of Medecine, Bronx, NY |
| 2F11 | neurofilament (NF)<br>NF-L, NF-H (70kD) | IHC 1:800 | Dako, Glostrup, DK<br>#M0762 |
| NF200 | neurofilament (200kD) | IHC 1:100 | (Probst et al., 2000) |
| GFAP | glial fibrillary acidic protein | IHC 1:500 | Thermo Fisher Scientific Inc., Kalamazoo, MI<br>#MS-1407-R7 |
| Synaptophysin | synaptophysin | IHC 1:1000 | Millipore Corporation, Billerica, MA<br>#MAB5258 |
| MG160 (rabbit) | Golgi apparatus | IHC 1:1000 | Nicholas Gonatas, Pathology and Laboratory Medicine, University of Pennsylvania, PA |
| VAMP2/Synaptobrevin 2 (rabbit) | transport vesicles | IHC 1:1000 | Synaptic system, Goettingen, Germany<br># 104 202 |
| GAPDH (6C5) | GAPDH | WB 1:1000 | Santa Cruz Biotechnology, Santa Cruz, CA,<br>#32233 |
| ß-actin | actin | WB 1:5000 | Sigma-Aldrich, Saint Louis, MO #A5316 |
| Cox subunit 1a | mitochondrial staining | IHC 1:200 | Abcam plc, Cambridge, UK<br>#ab14705 |

## 3.2 Preliminary data

### Protective effect of early tau burden on late neurotoxic distress level – Mechanisms underlying tauopathy and consequences for future therapies

## Protective effect of early tau burden on late neurotoxic distress level – Mechanisms underlying delayed tauopathy and consequences for future therapies

Preliminary results

We have recently provided evidence that assembly of filamentous tau aggregates is not solely responsible for the characteristic tau toxicity in neurodegenerative disorders. We could show that both, co-expression of full-length P301S mutant, as well as full-length wildtype tau with $\Delta tau_{151\text{-}421}$ results in a high *in vivo* neurotoxicity associated with the formation of soluble high molecular weight tau oligomers, extensive nerve cell dysfunction and severe motor palsy albeit in absence of insoluble tau aggregates or tangles (Ozcelik et al., 2016).
Given that our P301SxTAU62$^{on\text{-}off}$ mice were exposed to drastic neurotoxic stress during early postnatal life, we asked whether this event has any possible impact on tau pathology later in life, even after the expression of truncated tau is halted. Initially, we hypothesized that the observed prevalent oligomeric tau species might act as a form of toxic seed for more drastic tau pathology in later stages, ultimately manifesting in earlier tau tangle formation. Interestingly, compared to their heterozygous P301S tau transgenic littermates that have never been paralyzed, recovered P301SxTAU62$^{on\text{-}off}$ mice that, in contrast, experienced early neurotoxicity tau burden however exhibit a better motor phenotype associated with considerably less tau protein levels and an overall attenuated tau pathology.

### 3.2.1 Delayed motor phenotype in aged P301SxTAU62$^{on\text{-}off}$ mice after recovery of severe neurotoxicity

To monitor the behavioural phenotype in P301SxTAU62$^{on\text{-}off}$ mice after cessation of $\Delta tau_{151\text{-}421}$ but continuous full-length P301S tau expression, we performed a battery of motor function tests at ages of 12 to 16 months. Given that the pathological hind limb posture is normalized in recovered P301SxTAU62$^{on\text{-}off}$ mice (Ozcelik et al, 2016, Figure 3.1 a), we chose to repeat the tail suspension test: 14-month-old heterozygous P301S transgenic littermates showed already first signs of hind limb clasping that aggravated at 16 months of age, while the hind limb spreading of P301SxTAU62$^{on\text{-}off}$ mice stayed almost normal up to 16 months of age (Figure 3.1

b and c). Indeed, compared to their heterozygous P301S littermates, P301SxTAU62$^{on\text{-}off}$ mice maintain a significantly better motor strength, coordination and balance at 14 months of age that is still pronounced, but non-significant at the age of 16 months (Figure 3.1 d and e). Of note, both transgenic lines showed comparable performances on the grid and rotarod at the age of 12 months, as well as no differences in sex-specific bodyweight were found at 16 months of age (Figure 3.1 d, e and f).

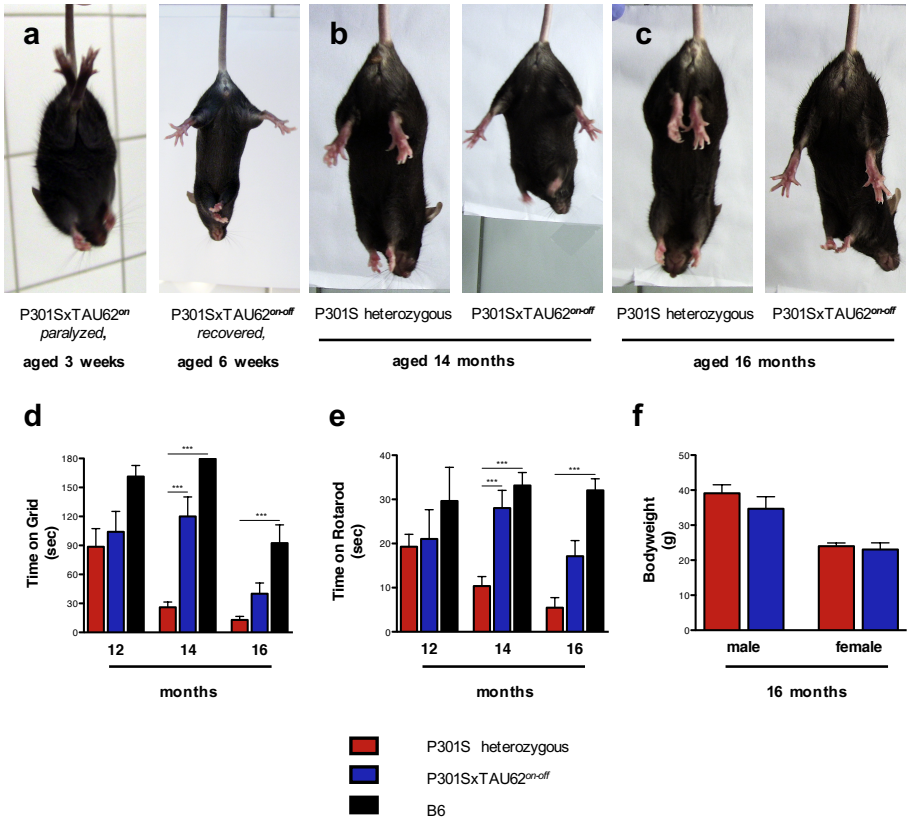


**Figure 3.1. Formerly paralyzed P301SxTAU62$^{on\text{-}off}$ mice develop a significant delayed motor phenotype**. In contrast to their heterozygous P301S transgenic littermates, P301SxTAU62$^{on\text{-}off}$ mice exhibit a better grid reflex, motor strength and motor coordination at ages of 12, 14, and 16 months. (**a-c**) Pathological hind limb spreading was assessed by a tail suspension test. (**a**) Paralyzed P301SxTAU62$^{on}$ mice at age of 3 weeks exhibit pathological hind limb posture. 3 weeks after cessation of $\Delta tau_{151\text{-}421}$ expression, P301SxTAU62$^{on\text{-}off}$ mice recover from their palsy, albeit continuative expression of P301S mutant tau (for details see Ozcelik et al 2016). (**b** and **c**) Less visible upon P301SxTAU62$^{on\text{-}off}$ mice, pathological hind limb spreading manifested predominantly in heterozygous P301S transgenic littermates at 14 to 16 months of age. (**d-f**) Based on the grid (**d,** P301S heterozygous: 12 months, *n*=15; 14 months, *n*=21; 16 months, *n*=21; P301SxTAU62$^{on\text{-}off}$: 12 months, *n*=5; 14 months, *n*=11; 16 months, *n*=13; non-transgenic B6: 12 months, *n*=5; 14 months, *n*=13; 16 months, *n*=12 ) and rotarod (**e,** P301S heterozygous: 12 months, *n*=15; 14 months, *n*=25; 16 months, *n*=21; P301SxTAU62$^{on\text{-}off}$: 12 months, *n*=5; 14 months, *n*=14; 16 months, *n*=13; non-transgenic B6: 12 months, *n*=5; 14 months, *n*=13; 16 months, *n*=12 ) performance test, P301SxTAU62$^{on\text{-}off}$ mice exhibit significantly better motor fitness at ages of 14 to 16 months, compared to heterozygous P301S transgenic littermates. (**f**) Sex-sorted body weight monitoring at 16 months of age (P301S heterozygous: male, *n*=6; female, *n*=17; P301SxTAU62$^{on\text{-}off}$: male, *n*=5; female, *n*=6). Data represents the mean and s.d. of indicated animals per group. ***$P$<0.001.

### 3.2.2 Reduced tau pathology in aged P301SxTAU62$^{on\text{-}off}$ mice after recovery of severe neurotoxicity

In order to elucidate whether the considerably delayed motor phenotype in P301SxTAU62$^{on\text{-}off}$ mice was associated with a varying degree of severity of tau pathology, we screened brain sections of both, 16-months-old P301SxTAU62$^{on\text{-}off}$ mice and their heterozygous P301S littermates, for the presence of certain tau species. Indeed, we could show that neurofibrillary tangles paralleled the previously observed impaired motor phenotype in heterozygous P301S littermates; specifically, Gallyas Braak Silver staining showed massive tau tangle formation in the brainstem of heterozygous P301S mutant littermates, whereas formerly paralyzed P301SxTAU62$^{on\text{-}off}$ mice remained almost devoid of fibrillary tau inclusions (Figure 3.2 a, b and e).

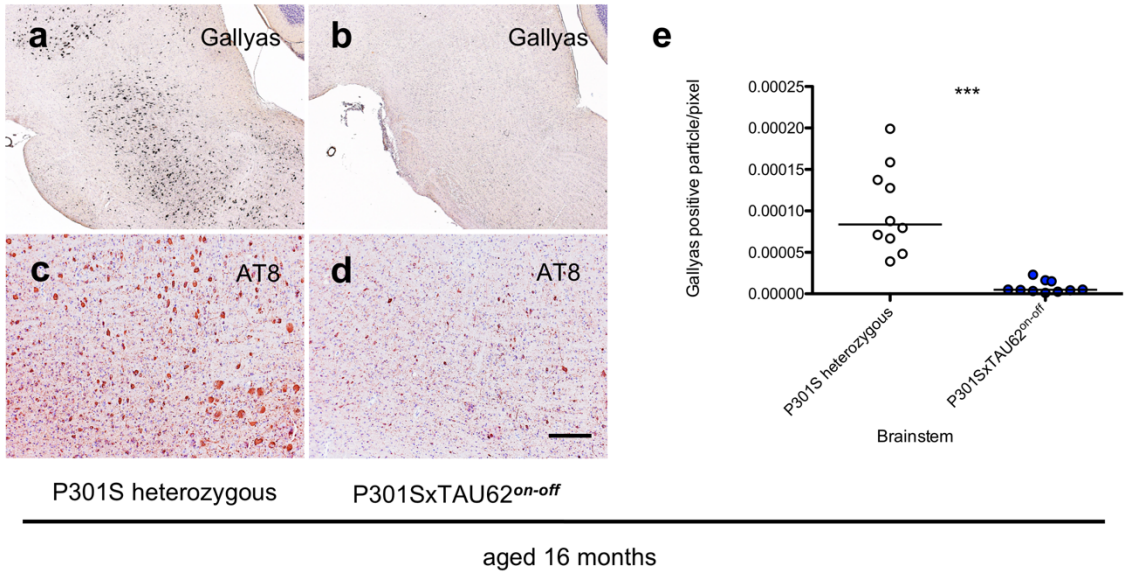


**Figure 3.2**. **Formerly paralyzed P301SxTAU62$^{on\text{-}off}$ mice reveal significant less tau pathology.** Compared to their heterozygous P301S littermates, P301SxTAU62$^{on\text{-}off}$ mice that underwent severe, early tau stress remain almost devoid of tau tangle pathology in the brainstem and exhibit attenuated tau hyperphosphorylation. (**a** - **d**) Histological analysis of 16-month-old P301SxTAU62$^{on\text{-}off}$ mice (**b** and **d**) and heterozygous P301S transgenic littermates (**a** and **c**) using Gallyas–Braak silver (**a** and **b**) and anti-tau antibody AT8 (**c** and **d**). The scale bar in **(d)** corresponds to 500 µm in (a and b) and 200 µm in (c and d)**.** Quantification of Gallyas positive tau tangles in the brainstem of P301S heterozygous (*n*=10) and P301SxTAU62$^{on\text{-}off}$ (*n*=10) mice. ***$P$<0.001.

Furthermore, in line with these histopathological findings, anti-tau antibody AT8 revealed attenuated tau hyperphosphorylation in P301SxTAU62$^{on\text{-}off}$ mice when compared to their

heterozygous P301S littermates (Figure 3.2 c and d). Though, tau protein is most expressed in the brainstem area under the control of neuron-specific Thy1.2-promoter element, we also found significant less tau pathology in the cervical spinal cord (Supplemental Figure S3.1 c-d) and the forebrain area (Supplemental Figure S3.1 d-f) of P301SxTAU62$^{on\text{-}off}$; as opposed to this, no significant difference in filamentous tau formation could be detected in the hippocampal area (Supplemental Figure S3.1 g-i).

Further, only heterozygous P301S littermates showed hyperphosphorylation of late epitopes in the brainstem, visualized by anti-tau AT100 antibody, consistent with the presence of tau filaments (Supplemental Figure S3.2 a and c); of note, $\Delta tau_{151\text{-}421}$ was not expressed in the brainstem of either the transgenic mouse lines (Supplemental Figure S3.2 b and d).

### 3.2.3 Reduced tau protein levels in aged P301SxTAU62$^{on\text{-}off}$ mice after recovery of severe neurotoxicity

Given the obtained data so far available we considered that changes in tau protein expression levels correspond to the present histopathological phenotypes in formerly paralyzed P301SxTAU62$^{on\text{-}off}$ mice and their heterozygous P301S mutant littermates. Through Western Blot analysis, we confirmed, as expected, a significant reduction in both the total tau and sarkosyl-soluble tau expression level in P301SxTAU62$^{on\text{-}off}$ mice (Figure 3.3 a-d); notably, in heterozygous P301S littermates, the marked histopathological tau tangle pathology is reflected in a significant increase of the sarkosyl-insoluble tau fraction expression levels (Figure 3.3 a and b, stars).

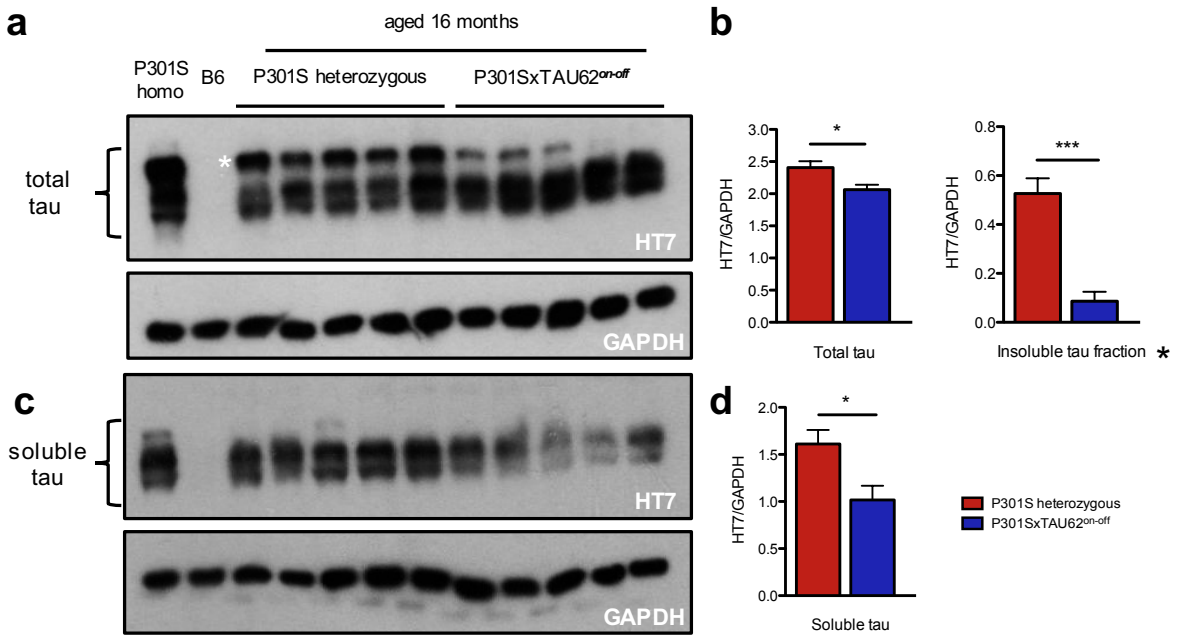


**Figure 3.3. Formerly paralyzed P301SxTAU62$^{on\text{-}off}$ mice reveal significant less total, insoluble and soluble tau protein levels.** (**a**-**d**) Western blotting with human-specific anti-tau antibody HT7 of brainstem tissue from P301S homozygous (lane 1), non-transgenic B6 (lane 2), P301S heterozygous (lanes 3-7) and P301SxTAU62$^{on\text{-}off}$ (lanes 8-12) mice (**a** and **c**); GAPDH staining was used for protein normalization (**b** and **d**). At the age of 16 months, significantly increased total tau protein levels were detected in heterozygous P301S transgenic littermates; associated with elevated insoluble tau fraction levels (**a** and **b,** stars). (**c** and **d**) Sarkosyl-extraction detects only soluble tau species that were found to be significantly attenuated in P301SxTAU62$^{on\text{-}off}$ mice. Data represents the mean and s.d. of 5 animals per group. *$P$<0.05 and ***$P$<0.001.

### 3.2.4 Supplemental material

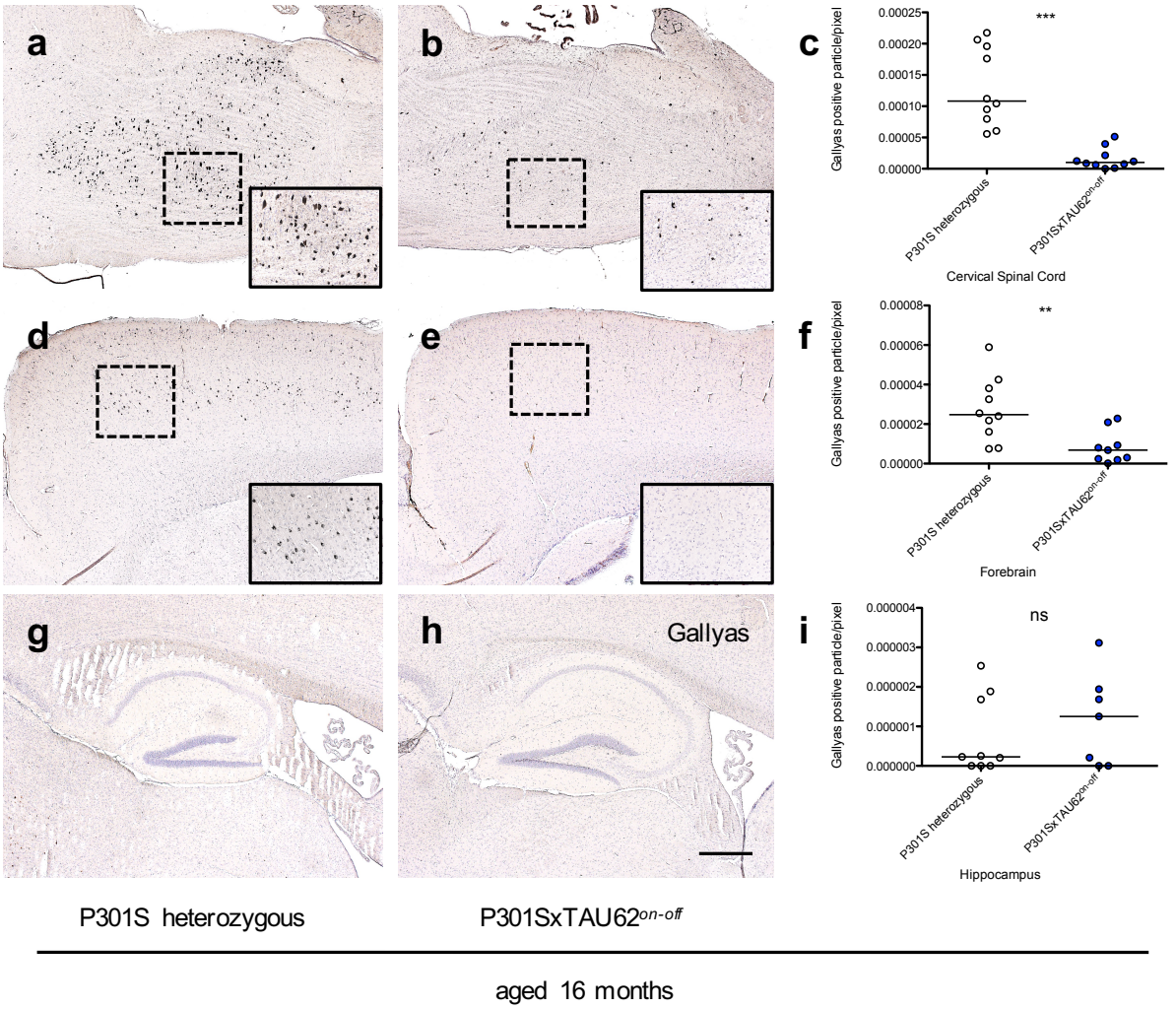


**Figure S 3.1**. **Formerly paralyzed P301SxTAU62$^{on\text{-}off}$ mice reveal significant less tau pathology in the cervical spinal cord and forebrain area.** (**a**-**i**) Histological analysis of 16-month-old P301SxTAU62$^{on\text{-}off}$ mice (**b**, **e**, and **h**) and heterozygous P301S transgenic littermates (**a**, **d** and **c**) using Gallyas–Braak silver stain of the cervical spinal cord (**a**-**c**), forebrain (**d**-**f**) and hippocampal area (**g**-**i**). Dotted squares indicate area of magnification in the lower-right corner (**a**, **b**, **d** and **e**). The scale bar in **(h)** corresponds to 500 µm in **(a, b, d, e, g** and **h)**. (**c**, **f** and **i**) Quantification of Gallyas positive tau tangles in the cervical spinal cord (**c**), forebrain (**f**) and hippocampus (**i)** of P301S heterozygous (*n*=10) and P301SxTAU62$^{on\text{-}off}$ (*n*=10) mice. ns=non-significant, ***P*<0.01 and ****P*<0.001.

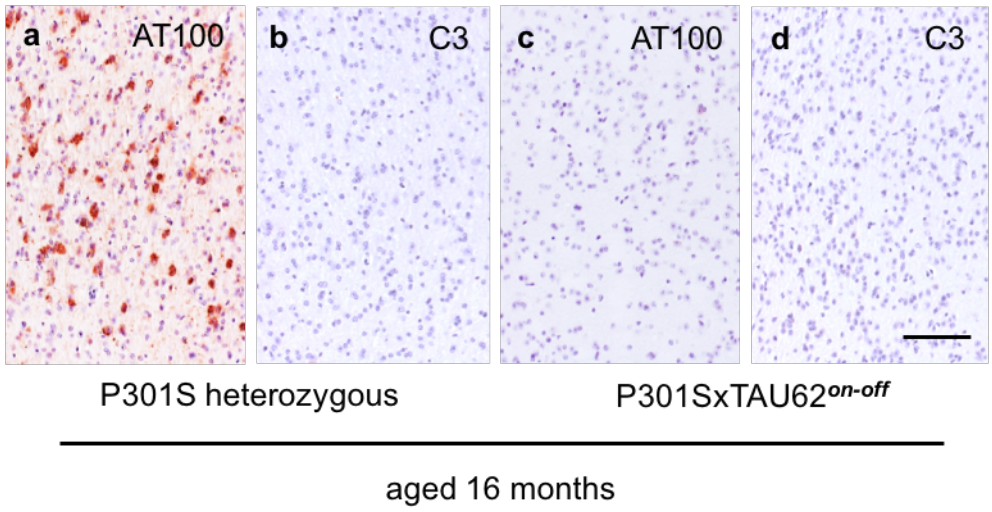


Figure S **3.2**. **(a** and **b)** Immunohistochemistry with anti-tau antibodies targeting late phospho-epitopes and Δtau. After cessation of Δtau expression, extensive hyperphosphorylation of AT100-positive tau was only seen in the brainstem of heterozygous P301S littermates (**a**), but not in P301SxTAU62$^{on\text{-}off}$ mice (**b**). In the brainstem of both transgenic lines, no C3-positive Δtau could be detected at the age of 16 months (**a** and **b**). The scale bar in **(d)** corresponds to 100 µm in **(a and d)**.

## 3.3 Publication No. 2

### Amyloid-beta in the cerebrospinal fluid of APP transgenic mice does not show prion-like properties

Skachokova Z, **Sprenger F**, Breu K, Abramowski D, Clavaguera F, Hench J, Staufenbiel M, Tolnay M, Winkler DT.

*Curr Alzheimer Res. 2015*

*Send Orders for Reprints to reprints@benthamscience.ae*

886 *Current Alzheimer Research*, 2015, *12*, 886-891

# Amyloid-β in the Cerebrospinal Fluid of APP Transgenic Mice Does not Show Prion-like Properties

Zhiva Skachokova[1,2], Frederik Sprenger[1,2], Karin Breu[1,2], Dorothee Abramowski[3], Florence Clavaguera[1], Jürgen Hench[1], Matthias Staufenbiel[3,4], Markus Tolnay[1] and David T. Winkler[1,2,*]

[1]*Institute of Pathology, University Hospital Basel, Basel, Switzerland;* [2]*Department of Neurology, University Hospital Basel, Basel, Switzerland;* [3]*Institute of Biomedical Research, Novartis Pharma AG, Basel, Switzerland;* [4]*Department of Cellular Neurology, Hertie Institute for Clinical Brain Research, University of Tübingen, Tübingen, Germany*

**Abstract:** Early diagnosis of Alzheimer`s disease (AD) is currently difficult and involves a complex approach including clinical assessment, neuroimaging, and measurement of amyloid-β (Aβ) and tau levels in cerebrospinal fluid (CSF). A better mechanistic understanding is needed to develop more accurate and even presymptomatic diagnostic tools. It has been shown that Aβ derived from amyloid-containing brain tissue has prion-like properties: it induces misfolding and aggregation of Aβ when injected into human amyloid precursor protein (APP) transgenic mice. In contrast, Aβ in the CSF has been less studied, and it is not clear whether it also exhibits prion-like characteristics, which might provide a sensitive diagnostic tool. Therefore, we collected CSF from APP transgenic mice carrying the Swedish mutation (APP23 mice), and injected it intracerebrally into young mice from the same transgenic line. We found that CSF derived Aβ did not induce increased β-amyloidosis, even after long incubation periods and additional concentration. This suggests that Aβ present in the CSF does not have the same prion-like properties as the Aβ species in the brain.

**Keywords:** Alzheimer's disease, amyloid-beta, Aβ, prion, cerebrospinal fluid, diagnostics, transgenic mouse models.

## 1. INTRODUCTION

Alzheimer's disease (AD) is the most common neurodegenerative disorder, and while its prevalence is increasing [1], curative treatment options are still lacking. In the course of AD, amyloid-β (Aβ) aggregates to form extracellular plaques, while hyperphosphorylated tau protein constitutes intracellular neurofibrillary tangles. The aggregation of Aβ is thought to be an early event that drives AD pathogenesis and begins at least a decade before clinical symptoms emerge [2-5].

In routine clinical practice, diagnosis of AD is often late and of limited accuracy [6]. At present, levels of Aβ and tau in the cerebrospinal fluid (CSF) are used as biomarkers of AD within a multimodal diagnostic approach [7, 8]. However, the validity of CSF biomarkers and their use for early or even presymptomatic diagnosis of AD is still a matter of debate. At the same time, an increasing number of experimental studies suggest that the aggregation of the proteins involved in AD pathogenesis occurs by a self-propagating process during which misfolded proteins act as templates, inducing misfolding and aggregation of native molecules [9-12]. As this self-propagating propensity is shared with prions, these proteins have been termed prion-like [13], even though they substantially differ from prions in their pathomechanisms [14, 15]. Aβ present in brain homogenates derived from AD patients or plaque-bearing amyloid precursor protein (APP) transgenic mice induces and/or accelerates Aβ deposition when injected into susceptible mouse models, in a prion-like manner [16-20]. This suggests that the pathological protein conformation can be transmitted and locally propagated a process we refer to here as 'seeding'.

Transgenic mice overexpressing human APP are widely used to model aspects of AD *in vivo*, since they develop Aβ plaques progressively with the age and have been established as a seeding model [16-18]. At the same time, little is known about the presence of pathological Aβ variants in their CSF. Such molecules could serve as sensitive early AD diagnostic markers. In a recent study, Fritschi *et al.* [21] demonstrated that CSF from both AD patients and APP transgenic mice lack *in vivo* seeding activity. Here we investigate this question further by injecting murine CSF into young APP mice and analyzing them after very long seeding times and inoculation of highly concentrated CSF. Even under these conditions, we didn't observe a significant increase in Aβ aggregation, neither at the injection site nor within the injected hippocampus, suggesting a low to absent prion-like activity of the Aβ forms present in the CSF.

*Address correspondence to this author at the Institute of Pathology, University Hospital Basel, Basel, Switzerland; Tel: 0041 61 265 25 25; Fax: 0041 61 265 41 00; E-mail: david.winkler@usb.ch

1875-5828/15 $58.00+.00 

## 2. METHODS

### 2.1. Mice

We used heterozygous APP23 transgenic mice [22], expressing human APP (751-aa isoform) containing the Swedish mutation under the control of the Thy-1.2 promoter. All experiments were approved by the University of Basel Ethics and Animal Care and Use Committees. Initial qualitative data of a subset of the mice used for the present analysis has been included in a previous study [21]. An overview of all the mice included in the study is provided in Table **S1**.

### 2.2. Stereotaxic Injections

Three months old APP23 mice (n=20) and non-transgenic C57BL6 (n=10) control mice were anaesthetized with a mixture of ketamine (10 mg/kg) and xylazine (20 mg/kg) and placed on a heating pad to maintain body temperature during surgery. Mice were injected in the right hippocampus (A/P, −2.5 mm from bregma; L, − 2.0 mm; D/V, −1.8 mm) using a Hamilton syringe, as previously reported [23]. Each received a unilateral stereotaxic injection of 5 µl at a speed of 1.25 µl/min. Mice were monitored until recovery from anesthesia and checked regularly following surgery.

### 2.3. CSF Sampling

For CSF sampling we used 3, 18 and 24 months old APP23 and C57BL6 mice (n=45). CSF was collected by puncturing the cisterna magna after deeply anesthetizing the animals, as previously described [24]. Next it was spun down at 2500 rpm for 2 min and the supernatant was collected and immediately frozen. Visibly blood contaminated CSF was discarded. For injections, CSF from 3 mice at the same age was pooled. For concentration, pooled CSF from 5-7 mice was lyophilized and later resuspended with a reduced volume of sterile $H_2O$.

### 2.4. Immunohistochemistry

Following 11 to 21 months from the date of injection, mice were deeply anaesthetized with pentobarbital (100 mg/kg) and killed by transcardial perfusion with cold PBS, followed by 4% paraformaldehyde in PBS. The brains were dissected and post-fixed overnight. 4 µm coronal sections were prepared following paraffin embedding. For immunohistochemical analysis, sections were deparaffinized, pretreated with 100% formic acid for 5 min, blocked with 10% normal horse serum and incubated overnight with an anti-Aβ 82E1 antibody (human N-terminal specific, 1:1000, *Demeditec Diagnostics GmbH*). For detection we used the Vectastain ABC Peroxidase kit (*Vector Laboratories*). Slides were counterstained with hematoxylin and eosine, and pictures were taken using Olympus DP73 microscope.

### 2.5. Quantification and Statistical Analysis

For quantification, we used 8 to 10 82E1 stained brain sections, depending on the tissue quality. Sections were selected for each animal from the injected right (R) and lateral left (L) hemisphere at corresponding Bregma levels, spanning the hippocampus (starting anterior to the injection site at -1.8 mm and extending to -3.1 mm posterior), with at least 50 µm distance in between. The hippocampal Aβ-plaque burden (the area occupied by all plaques as percent of the total area) was estimated for each section using ImageJ software [25]. In order to analyze the effect of CSF inoculation on Aβ-plaque-burden, linear mixed-effects models were used. We thereby compared the injected to the non-injected hippocampal side. Aβ-plaque burden served as dependent variables, independent variables were hippocampal sides (injected vs. non-injected). Subject was treated as a random factor. Side was nested within time point and group. To achieve approximately normal distribution, Aβ-plaque burden values were log-transformed (zeros were replaced by half the smallest value). Results were expressed as geometric mean ratios (GMR) with corresponding 95% confidence intervals and p-values. A p-value $<0.05$ was considered as significant. All analyses were done using R version 3.0.1 (R Foundation for Statistical Computing, Vienna, Austria).

## 3. RESULTS

### 3.1. Prolonged Seeding with APP23 CSF Did not Induce Increased Aβ Pathology

To test the prion-like properties of CSF derived amyloid-β, we inoculated CSF from aged APP23 or C57BL6 mice into the hippocampus of young APP23 mice. APP23 mice show robust plaque development starting at the age of 8-9 months [22], and seeding studies are mostly terminated close to this stage. To allow longer inoculation periods, we analyzed the seeding effect of CSF from aged APP23 mice 14 or 21 months post inoculation. In order to control for the endogenous pathology present at this age, we compared Aβ plaque densities of the injected with the non-injected hippocampus for each mouse. However, we did not observe a significant difference in hippocampal Aβ pathology in mice injected with transgenic CSF (Fig. **1A, B**, Fig. **2A, B**), showing that additional inoculation time did not contribute to a possible local increase of the pathology. As expected, Aβ plaque burden was unchanged after inoculation of wild type CSF (Fig. **1C**, Fig. **2C**). Seeding with APP23 brain homogenates resulted in a significant enhancement of the endogenous Aβ pathology in the right hippocampus and visible focal aggregation around the injection site, similar to previous reports (Fig. **1D**, Fig. **2D**) [17, 18]. No Aβ pathology was induced up to 21 months post inoculation of APP23 CSF into C57BL6 host mice (Fig. **1E**, Table **S3**).

### 3.2. Seeding with Concentrated APP23 CSF Did not Induce Increased Aβ Pathology

In order to test the hypothesis that Aβ concentration in the CSF might be too low to induce a seeding effect, we injected APP23 mice with concentrated APP23 CSF comprising a 22 fold higher amount of $A\beta_{40}$ (Table **S2**). This highly concentrated CSF did not cause tissue necrosis at or in proximity to the injection site. Because of the high number of donor mice required for the collection of a sufficient amount of mouse CSF for concentration, we were able to inject only a very limited number of mice. A quantitative analysis of the Aβ plaque load, comparing the injected versus non-injected hippocampus did not show a significant seeding effect after 11 (Fig. **3A**, Table **S3**) or 20 months (Fig. **3B**, Table **S3**). No focal Aβ aggregation was visible at or close to the injection

site. In addition, inoculation of concentrated C57BL6 CSF did not result in any seeding effect after 11 months, as expected (Fig. **3C**, Table **S3**).

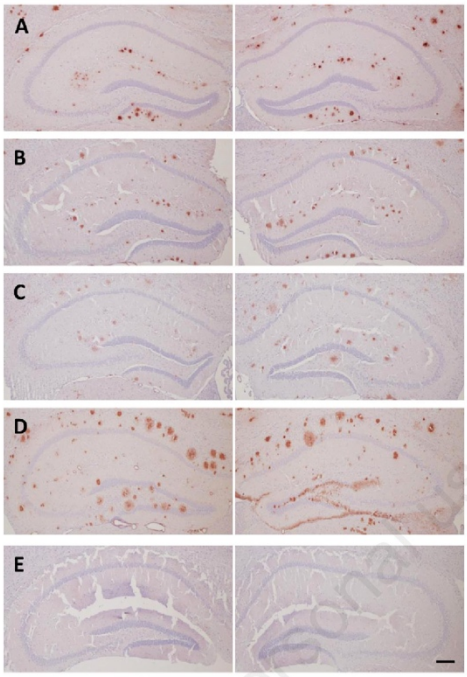


**Fig. (1). Immunohistochemical anaylsis of injected mice using 82E1 antibody.** APP23 mice analyzed 14 (**A**) or 21 months (**B**) after inoculation with CSF derived from aged APP23 mice (18 and 24 months old, respectively) did not show an increase in Aβ plaque burden in the injected hippocampus (right images), compared to the non-injected side (left images). Inoculation of wild-type mouse CSF did not provoke any seeding effect (**C**), while mice seeded with forebrain homogenate derived from aged APP23 mice exhibited enhanced Aβ deposition in the injected hippocampus (**D**). C57BL6 mice injected with APP23 CSF did not demonstrate any pathology (**E**). Scale bar equals 200 μm.

## DISCUSSION/CONCLUSION

This study extends the findings recently reported on CSF Aβ seeding [21]. Our analysis includes mice injected with concentrated CSF for very long incubation time, and confirms the absence of relevant *in vivo* seeding effect of CSF derived Aβ.

In the present study, we used APP23 mice as a seeding model to test whether CSF Aβ exhibits prion-like properties. APP23 mice were inoculated unilaterally into the hippocampus with forebrain homogenate or CSF. This allowed an intra-individual comparison of the pathology between the injected and non-injected hippocampus. APP23 mice seeded with forebrain homogenate for 20 months exhibited a significantly higher Aβ plaque load and focal seeding effects in the injected hippocampus, confirming previous reports [16-20]. In contrast, APP23 mice injected with CSF derived from plaque-bearing APP23 mice for a period of up to 21 months did not show any increase in Aβ load at or close to the injection site. This suggests a lower seeding effect of the Aβ in the CSF, as compared to the one in the brain.

The lack of seeding activity of Aβ containing CSF could be attributed to different factors. Previously, it has been reported that seed-induced Aβ deposition increases significantly with time [16]. For this reason, we have extended our seeding time to the maximum possible with regard to the mouse life span. Our seeding periods by far exceed those reported previously (6-9 months) in studies using brain homogenates [16-20]. The time factor is thus not very likely to be responsible for the observed lack of seeding by CSF compared to brain extract.

Induction of Aβ seeding is furthermore dependent on the amount of Aβ present in the injected extract [17]. Indeed, the Aβ concentration is much lower in the CSF compared to that in standard diluted brain homogenates from plaque-bearing mice. However, only minimal amounts of brain-derived Aβ are required to induce seeding. Langer and co-workers have previously demonstrated that Aβ within the soluble fraction of ultracentrifugated brain homogenates harbors a very high seeding potential even at low concentrations [26]. In this light, concentrated AD patients' CSF was intra hippocampally injected into APP transgenic mice in a recent study, but also failed to demonstrate any Aβ seeding activity after 6-8 months [21]. In contrast, diluted brain extracts containing comparable amounts of Aβ did increase amyloid deposition [21]. We here used concentrated CSF comprising a much higher Aβ concentration than the one used in the aforementioned study (0.46 vs 0.008 ng/μl), and extended the seeding time up to 20 months. The absence of quantitative and qualitative seeding effects even under these conditions suggests that seeding competent Aβ species are absent in CSF, or their fraction is much smaller in the CSF than in the brain, and thus not detectable in a standard *in vivo* seeding model as the APP23 mice. As a limitation, we can not exclude a reduction of the seeding competence of the concentrated CSF due to freeze-thawing and/or lyophilization [27].

Small and soluble Aβ containing assemblies constitute the most potent Aβ seeds in brain extracts derived from APP23 transgenic mice [26]. Such small aggregates may be almost absent in the CSF, even if oligomeric Aβ forms have recently been detected in human CSF [28-31]. The lower level of Aβ seeds in CSF compared to brain tissue could be attributed to a reduced transport rate to the CSF compartment, possibly caused by their binding to cerebral amyloid-plaques, or an increased degradation within the CSF compartment. Additionally, the rapid turn-over of CSF might in parallel prevent a de novo assembly of prion-like Aβ strains within the CSF compartment. Aβ species present in brain homogenates or CSF may differ in their seeding potential due to structural varieties. As an example, N-truncated Aβ have been detected in the brain, but found largely absent in the CSF of AD patients [21]. Although it remains difficult to study the conformational state of Aβ *in vivo*, studies so far suggest the occurrence of conformationally distinct Aβ

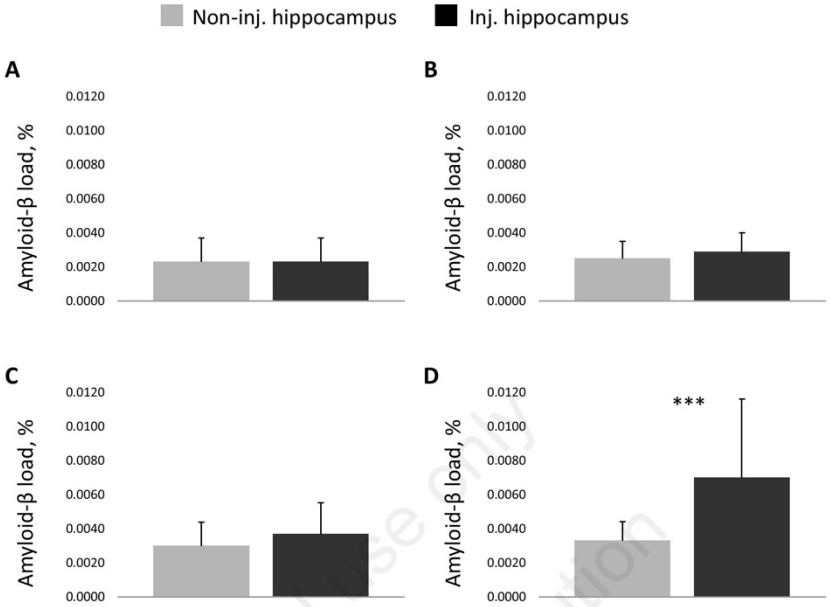


**Fig. (2). Quantitative analysis of seeded mice.** To assess a possible seeding effect we compared Aβ plaque burden between the non-injected (non-inj.) and injected (inj.) hippocampus in a mixed effect model for APP23 mice injected with transgenic CSF for 14 (**A**, n=4) or 21 months (**B**, n=5). In addition, we analysed APP23 mice seeded with wild type CSF (**C**, n=3) and with transgenic forebrain homogenates (**D**, n=2), as only in the last group there was a seeding effect present. Aβ plaque burden was calculated as a mean from all assessed hippocampal sections of mice in a group; error bars represent SD; *** indicates $p<0.001$. All p-values are listed in Table **S3**.

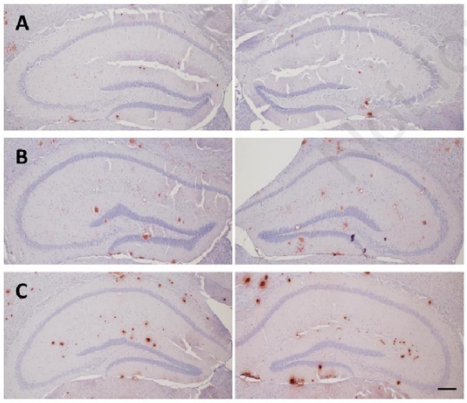


**Fig. (3). Immunohistochemical analysis of mice injected with concentrated mouse CSF using 82E1 antibody.** APP23 mice injected with concentrated APP23 CSF and analyzed 11 (**A**) or 20 (**B**) months later did not show an increased Aβ deposition in the inoculated hippocampus (right images), as compared to their non-injected sides (left images). The same was observed for littermates seeded with concentrated C57BL6 CSF (**C**). Scale bar equals 200 µm.

deposits in the brain [32, 33]. Different Aβ morphotypes may indicate that local factors may influence Aβ aggregation [34, 35]. Given its very low concentration in CSF, the structure of Aβ present there has still remained undescribed. This precludes us from drawing specific conclusions on the Aβ structure required for its seeding competence.

In addition, Aβ seeding may be dependent on brain components that are absent in the CSF compartment. For instance, the synaptic variant of acetylcholinesterase (AChE) has been shown to facilitate Aβ fibril formation [36]. In return, inhibitory cofactors may preferentially reach the CSF, such as the monomeric read through variant of AChE, which has been shown to delay aggregation [37].

Toxicity and seeding competence of Aβ may furthermore be influenced by RNA metabolism. miRNAs may be transmitted from one cell to another via exosomes, and RNA binding proteins have furthermore been shown to promote fibril formation [38-40]. This may contribute to the observed difference in seeding competence of brain-derived material versus CSF.

Further analysis of the potentially selective transport of particular Aβ species to the CSF and the possible co-factors involved might help to explain the apparent lack of *in vivo* active Aβ seeds in AD CSF. This knowledge could also help the development of sensitive early AD diagnostic tools.

## CONFLICT OF INTEREST

The authors confirm that this article content has no conflict of interest.


## ACKNOWLEDGEMENTS

We thank Andreas Schötzau (www.eudox.ch) for expert statistical advice. This work has been supported by the Swiss National Science Foundation (32323B_123812 to D.T.W.), the Mach-Gaensslen Foundation, the D&N Yde Foundation, the Velux Foundation, and the Synapsis Foundation, Switzerland.

DTW designed the study, KB, FC, JC, DA, and DTW developed the methodology, ZS, KB, FS and DTW collected the data and performed the analysis, and ZS, MS, MT, and DTW wrote the manuscript.


## SUPPLEMENTARY MATERIAL

Supplementary materials are available on the publishers website along with the published article.

## REFERENCES


[1] Thies W, Bleiler L. Alzheimer's disease facts and figures. Alzheimer's Dement 7: 208-244 (2011).

[2] Bateman RJ, Xiong C, Benzinger TLS, Fagan AM, Goate A, Fox NC, *et al.* Clinical and biomarker changes in dominantly inherited Alzheimer's disease. N Engl J Med 367(9): 795-804 (2012).

[3] Holtzman DM, Morris JC, Goate AM. Alzheimer's disease: the challenge of the second century. Sci Trans Med 3: 77sr1 (2011).

[4] Villemagne VL, Burnham S, Bourgeat P, Brown B, Ellis KA, Salvado O, *et al.* Amyloid β deposition, neurodegeneration, and cognitive decline in sporadic Alzheimer's disease: a prospective cohort study. Lancet Neurol 12: 357-367 (2013).

[5] Skoog I, Davidsson P, Aevarsson O, Vanderstichele H, Vanmechelen E, Blennow K. Cerebrospinal fluid beta-amyloid 42 is reduced before the onset of sporadic dementia: a population based study in 85-year-olds. Dement Geriatr Cogn Disord 15: 169-176 (2003).

[6] Blennow K, Dubois B, Fagan AM, Lewczuk P, de Leon MJ, Hampel H. Clinical utility of cerebrospinal fluid biomarkers in the diagnosis of early Alzheimer's disease. Alzheimers Dement 11(1): 58-69 (2015).

[7] Blennow K, Hampel H, Weiner M, Zetterberg H. Cerebrospinal fluid and plasma biomarkers in Alzheimer disease. Nat Rev Neurol 6: 131-144 (2010).

[8] Fagan AM, Holtzman DM. Cerebrospinal fluid biomarkers of Alzheimer's disease. Biomark Med 4: 51-63 (2010).

[9] Braak H, Braak E. Neuropathological stageing of Alzheimer-related changes. Acta Neuropathol 82: 239-259 (1991).

[10] Harper JD, Lansbury PT. Models of amyloid seeding in Alzheimer's disease and scrapie: mechanistic truths and physiological consequences of the time-dependent solubility of amyloid proteins. Annu Rev Biochem 66: 385-407 (1997).

[11] Jucker M, Walker LC. Self-propagation of pathogenic protein aggregates in neurodegenerative diseases. Nature 501: 45-51 (2013).

[12] Thal DR, Rüb U, Orantes M, Braak H. Phases of Aβ-deposition in the humanbrain and its relevance for the development of AD. Neurology 58: 1791-1800 (2002).

[13] Ashe KH, Aguzzi A. Prions, prionoids and pathogenic proteins in Alzheimer disease. Prion 7: 55-59 (2013).

[14] Lahiri DK, Maloney B, Zawia NH. The LEARn model: an epigenetic explanation for idiopathic neurobiological diseases. Mol Psychiatry 11: 992-1003 (2009).

[15] Lahiri DK. Prions: a piece of the puzzle? Science 337: 1172 (2012).

[16] Kane MD, Lipinski WJ, Callahan MJ, Bian F, Durham RA, Schwarz RD, *et al.* Evidence for seeding of beta-amyloid by intracerebral infusion of Alzheimer brain extracts in beta-amyloid precursor protein-transgenic mice. J Neurosci 20: 3606-3611 (2000).

[17] Meyer-Luehmann M, Coomaraswamy J, Bolmont T, Kaeser S, Schaefer C, Kilger E, *et al.* Exogenous induction of cerebral beta-amyloidogenesis is governed by agent and host. Science 313: 1781-1784 (2006).

[18] Eisele YS, Obermüller U, Heilbronner G, Baumann F, Kaeser SA, Wolburg H, *et al.* Peripherally applied Abeta-containing inoculates induce cerebral beta-amyloidosis. Science 330: 980-982 (2010).

[19] Morales R, Duran-Aniotz C, Castilla J, Estrada LD, Soto C. De novo induction of amyloid-β deposition *in vivo*. Mol Psychiatry 17: 1347-1353 (2012).

[20] Watts JC, Condello C, Stöhr J, Oehler A, Lee J, DeArmond SJ, *et al.* Serial propagation of distinct strains of Aβ prions from Alzheimer`s disease patients. Proc Natl Acad Sci USA 111: 10323-10328 (2014).

[21] Fritschi S, Langer F, Kaeser S, Maia L, Portelius E, Pinotsi D, *et al.* Highly potent soluble Aβ seeds in human Alzheimer brain but not cerebrospinal fluid. Brain 137: 2909-2915 (2014).

[22] Sturchler-Pierrat C, Abramowski D, Duke M, Wiederhold KH, Mistl C, Rothacher S, *et al.* Two amyloid precursor protein transgenic mouse models with Alzheimer disease-like pathology. Proc Natl Acad Sci USA 94: 13287-13292 (1997).

[23] Clavaguera F, Bolmont T, Crowther RA, Abramowski D, Frank S, Probst A, *et al.* Transmission and spreading of tauopathy in transgenic mouse brain. Nat Cell Biol 11: 909-913 (2009).

[24] Winkler DT, Abramowski D, Danner S, Zurini M, Paganetti P, Tolnay M, *et al.* Rapid cerebral amyloid binding by Aβ antibodies infused into β-amyloid precursor protein transgenic mice. Biol Psychiatry 68: 971-974 (2010).

[25] Griciuc A, Serrano-Pozo A, Parrado AR, Lesinski AN, Asselin CN, Mullin K, *et al.* Alzheimer's disease risk gene CD33 inhibits microglial uptake of amyloid beta. Neuron 78: 631-643 (2013).

[26] Langer F, Eisele YS, Fritschi SK, Staufenbiel M, Walker LC, Jucker M. Soluble Aβ seeds are potent inducers of cerebral β-amyloid deposition. J Neurosci 31: 14488-14495 (2011).

[27] Schoonenboom NS, Mulder C, Vanderstichele H, Van Elk EJ, Kok A, Van Kamp GJ, *et al.* Effects of processing and storage conditions on amyloid beta (1-42) and tau concentrations in cerebrospinal fluid: implications for use in clinical practice. Clin Chem 51: 189-95 (2005).

[28] Gao CM, Yam AY, Wang X, Magdangal E, Salisbury C, Peretz D, *et al.* Aβ40 oligomers identified as a potential biomarker for the diagnosis of Alzheimer's disease. PLoS One 5: e15725 (2010).

[29] Klyubin I, Betts V, Welzel AT, Blennow K, Zetterberg H, Wallin A, *et al.* Amyloid beta protein dimer-containing CSF disrupts synaptic plasticity: prevention by systemic passive immunization. J Neurosci 28: 4231-4237 (2008).

[30] Santos AN, Ewers M, Minthon L, Simm A, Silber RE, Blennow K, *et al.* Amyloid-β oligomers in cerebrospinal fluid are associated with cognitive decline in patients with Alzheimets disease. J Alzheimers Dis 29: 171-176 (2012).

[31] Salvadores N, Shahnawaz M, Scarpini E, Tagliavini F, Soto C. Detection of misfolded Aβ oligomers for sensitive biochemical diagnosis of Alzheimers disease. Cell Rep 10: 261-268 (2014).

[32] Nilsson KP, Aslund A, Berg I, Nyström S, Konradsson P, Herland A, *et al.* Imaging distinct conformational states of amyloid-beta fibrils in Alzheimer's disease using novel luminescent probes. ACS Chem Biol 2: 553-60 (2007).

[33] Meier BH, Böckmann A. The structure of fibrils from 'misfolded' proteins. Curr Opin Struct Biol 30C: 43-4 (2014).

[34] Jucker M, Walker LC. Self-propagation of pathogenic protein aggregates in neurodegenerative diseases. Nature 501: 45-51 (2013).

[35] Eisenberg D, Jucker M. The amyloid state of proteins in human diseases. Cell 148: 1188-203 (2012).

[36] Inestrosa NC, Alvarez A, Pérez CA, Moreno RD, Vicente M, Linker C, *et al.* Acetylcholinesterase accelerates assembly of amyloid-beta-peptides into Alzheimer's fibrils: possible role of the peripheral site of the enzyme. Neuron 16: 881-91 (1996).

[37] Berson A, Knobloch M, Hanan M, Diamant S, Sharoni M, Schuppli D, *et al.* Changes in readthrough acetylcholinesterase expression modulate amyloid-beta pathology. Brain 131: 109-19 (2008).

[38] Barbash S, Soreq H. Threshold-independent meta-analysis of Alzheimer's disease transcriptomes shows progressive changes in hippocampal functions, epigenetics and microRNA regulation. Curr Alzheimer Res 9: 425-35 (2012).

[39] Lau P, Bossers K, Janky R, Salta E, Frigerio CS, Barbash S, *et al.* Alteration of the microRNA network during the progression of Alzheimer's disease. EMBO Mol Med 5: 1613-34 (2013).

[40] Kim HJ, Kim NC, Wang YD, Scarborough EA, Moore J, Diaz Z, *et al.* Mutations in prion-like domains in hnRNPA2B1 and hnRNPA1 cause multisystem proteinopathy and ALS. Nature 495: 467-73 (2013).

**Received: February 10, 2015** **Revised: April 13, 2015** **Accepted: June 17, 2015**

## Supplementary Information

### 1.1. ELISA

**Abeta 40 and sAPP levels were measured using Human 6E10 and APPalpha/sAPPbeta Kits respectively, both from Meso Scale Discovery, according to the manufacturer's instructions.**

### 1.2. Mice

| Genotype | Seed | Seed donor age, *mo* | Seeding time, *mo* |
|---|---|---|---|
| App23 | tg CSF | 18 | 14 |
| App23 | tg CSF | 24 | 14 |
| App23 | tg CSF | 24 | 14 |
| App23 | tg CSF | 24 | 14 |
| App23 | tg CSF | 18 | 21 |
| App23 | tg CSF | 18 | 21 |
| App23 | tg CSF | 24 | 21 |
| App23 | tg CSF | 24 | 21 |
| App23 | tg CSF | 24 | 21 |
| App23 | wt CSF | 3 | 21 |
| App23 | wt CSF | 24 | 21 |
| App23 | wt CSF | 24 | 21 |
| App23 | FB | 24 | 20 |
| App23 | FB | 24 | 20 |
| C57BL6 | tg CSF | 24 | 21 |
| C57BL6 | tg CSF | 18 | 21 |
| C57BL6 | tg CSF | 18 | 21 |
| App23 | conc. tg CSF | 24 | 11 |
| App23 | conc. wt CSF | 24 | 11 |
| App23 | conc. tg CSF | 24 | 20 |

**Table S1. Table of all mice used for quantitative analysis in the study.** Abbreviations used: tg=transgenic, wt=wild type, FB=forebrain homogenate, conc.=concentrated.

## Supplementary results

### 1.1. ELISA

| **Sample** | **Aβ40**, *pg/µl CSF* | **sAPPα**, *pg/µl CSF* | **sAPPβ**, *pg/µl CSF* |
|---|---|---|---|
| APP23 CSF | 4.2 | 92 | 121 |
| Concentrated APP23 CSF | 92.6 | 2594 | 3659 |

**Table S2. ELISA table of results.**

### 1.2. Quantification of Aβ pathology comparing injected vs non-injected hippocampus

| **Genotype** | **Treatment group** | **Seeding time, mo** | **N** | **Lower ratio** | **GMR** | **Upper ratio** | **P value** |
|---|---|---|---|---|---|---|---|
| APP23 | tg CSF | 14 | 4 | 0.77 | 0.94 | 1.15 | 0.56 |
| APP23 | tg CSF | 21 | 5 | 0.79 | 0.91 | 1.05 | 0.19 |
| APP23 | wt CSF | 21 | 3 | 0.65 | 0.81 | 1.01 | 0.06 |
| APP23 | FB | 20 | 2 | 0.41 | 0.54 | 0.70 | 0.00*** |
| C57BL6 | tg CSF | 21 | 3 | 0.00 | 0.00 | 0.00 | NA |
| APP23 | conc. tg CSF | 11 | 1 | 0.59 | 0.88 | 1.30 | 0.52 |
| APP23 | conc. wt CSF | 11 | 1 | 0.72 | 1.10 | 1.67 | 0.66 |
| APP23 | conc. tg CSF | 20 | 1 | 0.61 | 0.92 | 1.40 | 0.70 |

**Table S3. Geometric mean ratios (GMR) of amyloid-β ratios comparing non-injected vs injected hippocampus.** N indicates the number of mice used; tg=transgenic, wt=wild type, FB=forebrain homogenate, conc.=concentrated; *** indicates $p<0.001$.

# 4 Discussion

Alzheimer's disease represents the most prevalent form of a major subclass of various neurodegenerative diseases: the tauopathies. In Switzerland alone, over 100'000 people are estimated to suffer from dementia including AD; and this number is expected to triple by 2050 (Blankman et.al, 2012). To date, the lack of therapeutic treatments limits pharmacological therapies to symptomatic interventions and given that millions of people have been diagnosed worldwide, AD constitutes a crucial source of social and economic problems (Scheltens et al., 2016).

The disease spectrum in patients with neurodegenerative disorders including AD extends from genetic alterations to protein modifications and altered inner life of a cell in affected anatomical regions through to clinical manifestations. Years of research has led to the discovery of a plethora of proteins being crucial in the course of neurodegenerative syndromes; but ever since researchers are puzzled by pieces of the big picture. The cleavage of larger, neurodegeneration-associated proteins into smaller, potentially neurotoxic fragments has been subject of numerous studies; indeed, academic research suggests that fragmentation and other substantial events leading to neuronal dysfunction at the same time have led many people to suffer from variety of neurodegenerative diseases such as AD and other tauopathies, PD, HD, or CjD. However, the relevance of protein fragmentation in neurodegeneration is still under debate.

In human tauopathies, the distinct molecular and cellular mechanisms contributing to the pathogenesis and progression of tauopathies remain still opaque. Precisely, the initiator of neurotoxic events and how neurotoxicity is mediated is not known in detail. Aside the Aβ peptide and its pathological role in AD, the closer correlation between tau and disease progression arouse attention and promoted tau-focused research. Thus, the development of transgenic mouse models allowed to investigate core aspects of the pathogenesis of tauopathies by modeling particular disease steps *in vivo*; ultimately aiming for a better understanding of the neuropathological mechanisms behind the complex nature of neurodegenerative processes.

## The pursuit of neurotoxic tau species

The neuropathological identity of AD falls into two broad categories: extracellular senile plaques composed of the APP cleavage product Aβ and filamentous tau inclusions derived from accumulation of modified tau species.

Tau plays a central role in multiple neurodegenerative disorders; however, its contribution to the onset and progression of AD is still a matter of debate. But as tau gene mutation in FTDP-17T (Hutton et al., 1998; Poorkaj et al., 1998; Spillantini et al., 1998) paved the way for *in vivo* expression of mutant human tau protein, transgenic mouse models were generated that exhibit distinct aspects of tau pathology such as age-related filamentous tau deposits, neuronal degeneration and axonal transport dysfunction (Gotz et al., 2004).

The formation of tau aggregates is depending on the conformational switch to β-sheet structure; indeed, point mutations but also various post-translational modifications including phosphorylation, acetylation, glycosylation, ubiquitination, and truncation structurally alter tau and thus favour its accumulation. While aberrant aggregation and hyperphosphorylation of tau are proposed to be the pivotal neurotoxic elements in human tauopathies, the most toxic species and how toxicity is mediated is of ongoing debate (Braak and Del Tredici, 2011; Coleman and Yao, 2003; Goedert, 2015; Terry et al., 1991).

Notably, proteolytic cleavage of tau has been shown to be an early event in the pathological cascade with considerable impact on tau toxicity; indeed, fragmentation of tau occurs before

toxic tangle formation and facilitate and promote tau aggregation compared to full-length tau species (Abraha et al., 2000; Berger et al., 2007; Cowan et al., 2010). Various proteases including caspase 3, caspase 6 and calpains have been identified to cleave full-length tau into fragments which accumulation correlates with the progression of AD; notably, D421 constitutes the most prominent caspase cleavage site in all forms of tauopathies (Basurto-Islas et al., 2008; Fasulo et al., 2005; Guillozet-Bongaarts et al., 2005; Guo et al., 2004).

Within this framework, we have established an inducible mouse line (TAU62) overexpressing a short, human 3R $tau_{151–421}$ fragment (Δtau) that develop a mildly progressive motor phenotype with ataxia at about 18 months of age. Interestingly, TAU62 mice did not develop filamentous tau inclusions but exhibited neuron specific pretangle pathology in form of abnormally phosphorylated tau; this is in line with findings in other tau fragment expressing mouse models (McMillan et al., 2011), but contradicts the predominant neuropathological phenotype defined by cortical insoluble tau filaments in rat models overexpressing truncated tau (Filipcik et al., 2012). However, the observed mild neurotoxicity was comparable to that seen in mice expressing full-length wild-type forms of tau (Probst et al., 2000, 2N4R tau transgenic ALZ17 mice; 0N3R tau transgenic ALZ31).

In the course of the present work, I have focused on the drastic, but reversible neurotoxicity in our own novel mouse model co-expressing truncated and full-length tau (Ozcelik et al., 2016). In line with this, we set out to complete the neuropathological characterization of several transgenic mouse models that recapitulate different aspects of AD to study the neurodegenerative relevance of tau fragmentation and oligomerization *in vivo*.

## Truncated tau induces severe neurotoxicity in presence of full-length forms of tau

In AD, PHFs are composed of not only full-length tau species but also truncated forms of tau (Gamblin et al., 2003; Goedert et al., 1992; Mena et al., 1996; Rissman et al., 2004; Wischik et al., 1988b). We have approached this neuropathological condition with co-expression of Δtau and different full-length forms of tau *in vivo*.

First, we generated double transgenic P301SxTAU62$^{on}$ mice co-expressing Δtau and P301S mutant 0N4R tau. Aside, full-length tau expressing human mutant P301S heterozygous transgenic mice develop insoluble tau filaments and paralysis around 12 months of age (Allen et al., 2002). Strikingly, our P301SxTAU62$^{on}$ exhibited extensive nerve cell dysfunction and severe motor palsy already by the age of 3 weeks; consistently, in spinal cord neurons, axonal transport disruption was associated with accumulation of neurofilament and axonal spheroids formation; furthermore, peripheral nerves showed signs of Wallerian degeneration with fiber loss and myelin debris followed by drastic neurogenic muscle atrophy. It is interesting to note that despite massive functional and structural defects, only oligomeric tau and no formation of insoluble tau aggregates or tangles could have been detected; in fact, the presence of toxic tau oligomers alone is a strong hint that the neurotoxic cascade leading to neurodegeneration might not depend on filamentous tau inclusions.

Remarkably, the pronounced drastic neurotoxicity in P301SxTAU62$^{on}$ mice was phenotypically and pathohistologically reversible: despite continuous expression of full- length P301S tau, we could confirm the reversibility of Δtau induced neuronal dysfunction in severely affected P301SxTAU62$^{on}$ mice. When only Δtau expression was halted, former paralyzed P301SxTAU62$^{on\text{-}off}$ mice rapidly regained full motor control and re-established nerve fiber function and restored muscle fiber atrophy was observed. Moreover, the functional and structural recovery was paralleled by the disappearance of oligomeric tau species.

Second, given the artificial nature of P301S mutant tau, we aimed for an *in vivo* analysis of Δtau in presence of full-length wild-type tau. Indeed, we could reproduce the pronounced reversible neurotoxicity in double transgenic ALZ17xTAU62$^{on}$ mice co-expressing Δtau and full-length wild-type 2N4R tau.

Third, we analyzed TAU62xALZ31$^{on}$ mice expressing 3R Δtau and the shortest form of wild-type human 0N3R tau; however, these mice exhibited the most pronounced neurotoxic phenotype that was not reversible when Δtau expression was ceased. A possible explanation is that functional and structural recovery would require the presence of mixed 3R/4R ratio of tau oligomeric species.

Of note, co-expression of only full-length tau species was not sufficient to induce severe neurotoxicity: both, P301SxALZ31 and ALZ17xALZ31 double transgenic mice only exhibit pretangle tau pathology and did not display paralysis.

Overall, these findings highlight two essential aspects of tauopathies: tau fragmentation and oligomerization. In accordance with previous findings, we could highlight a neurotoxic potential of tau fragments as pathogenic mediators in tauopathies. Indeed, recent work has shown that truncation of tau not only facilitates tau assembly into filaments (Abraha et al., 2000; Mocanu et al., 2008; Sydow et al., 2011), but also exacerbates the toxicity of full-length tau (Fasulo et al., 2005). In parallel, we identified oligomeric forms of tau as a key neurotoxic species contributing to the neurodegenerative process in tauopathies; in fact, tau toxicity precedes the formation of insoluble aggregates in our mouse model and thus fibrillary tau formation appears to be not required for tau toxicity, similar to findings in other proteinopathies (Eisenberg and Jucker, 2012). Indeed, this confirms the recognized importance of soluble oligomeric tau species for the pathogenesis of tauopathies (Lasagna-Reeves et al., 2010; Spires-Jones et al., 2011; Spires-Jones et al., 2009).

## Targeting truncated tau species

The neurotoxic potential of protein fragments in the course of various neurodegenerative disorders remains to be established in detail. However, neurodegeneration-associated proteins are substrate to various proteolytic enzymes that cleave designated proteins at individually different sites (Figure 4.1). The neurotoxic effect of protein fragments has been shown i.e. for the intramebranous located APP (Selkoe, 2001a), the transmembranous located $BRI_2$ (Rostagno and Ghiso, 2008; Vidal et al., 1999; Vidal et al., 2000), intracellular and/or extracellular cleaved α-Syn (Dufty et al., 2007; Kim et al., 2012; Mishizen-Eberz et al., 2005) , intracellular cleaved htt (Graham et al., 2006; Waldron-Roby et al., 2012; Wellington et al., 2002) and ataxins (Guyenet et al., 2015; Hubener et al., 2013; Mookerjee et al., 2009), membrane anchored PrP (Altmeppen et al., 2012; Trevitt et al., 2014), and nuclear TDP-43 (Furukawa et al., 2011; Nonaka et al., 2009). Across the different neurodegenerative disorders, major enzymes involved in the proteolytic processes are caspases and calpains; in particular, tau protein is cleaved by caspases-3/6 (Fasulo et al., 2005; Guo et al., 2004; Metcalfe et al., 2012) and calpains (Ferreira and Bigio, 2011; Higuchi et al., 2012; Park et al., 2007).

In light of this, inhibition of caspases and calpains cleavage emerged as a potential target to prevent disease pathology and might be a promising therapeutic strategy considering the observed neurotoxicity in our mouse model. Indeed, calpain-specific inhibitors have been shown to attenuate AD-like pathology in 3xTgAD mice (Medeiros et al., 2012); further reduce ataxin cleavage (Haacke et al., 2007) and attenuate α-Syn induced synaptic impairments (Diepenbroek et al., 2014). In addition, caspase inhibition has also been shown to mitigate α-Syn pathology (Bassil et al., 2016).

Nevertheless, there is also evidence that cleavage of neurodegeneration-associated protein species may constitute a regular cellular process (Li et al., 2005). For instance, N-terminally truncated α-Syn species are present in cases with or without Lewy pathology and correlating with the total amount of α-Syn (Muntane et al., 2012).

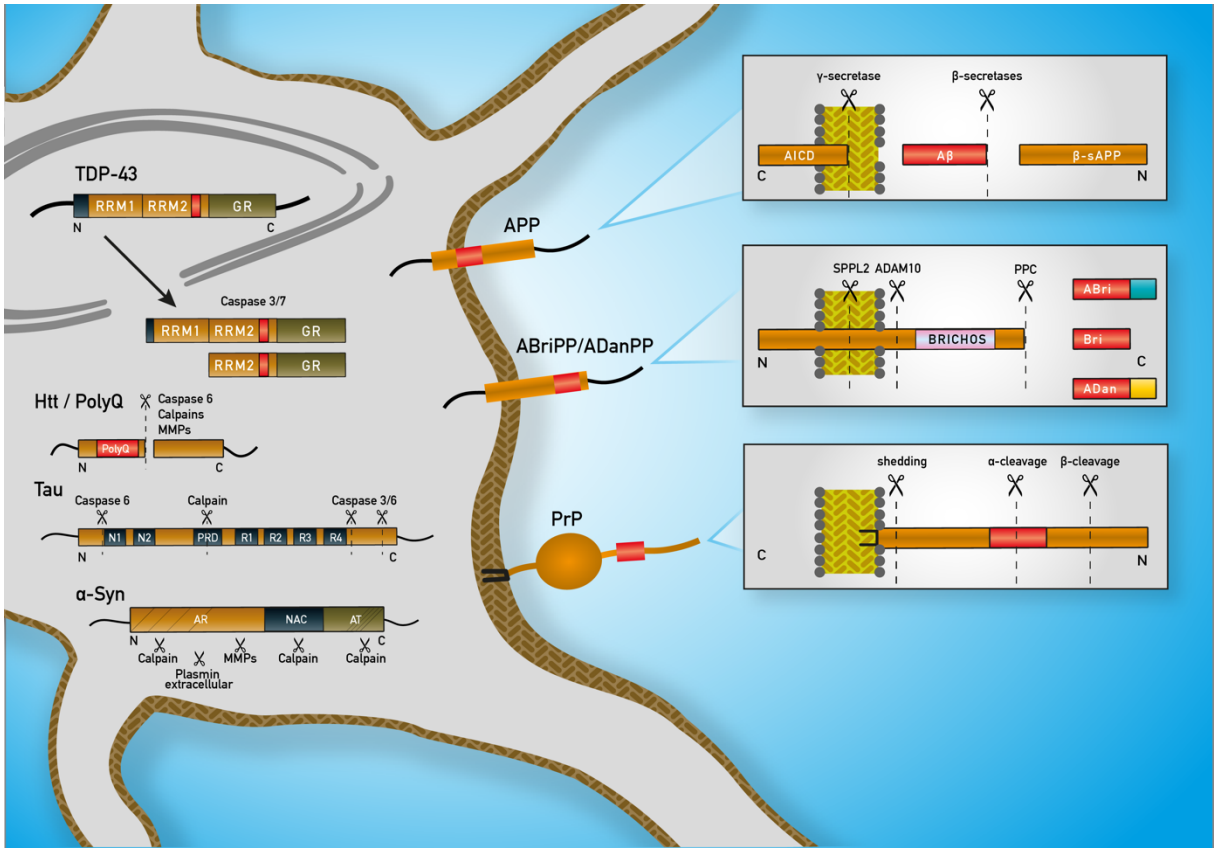


**Figure 4.1 Overview of the cellular location of neurodegeneration-associated proteins and their individual cleavage sites.**

## Targeting toxic oligomeric tau species

The spectrum of neurotoxic potentials of tau species is still under debate. Oligomeric tau formation occurs early in the progression of AD pathology (Patterson et al., 2011). In AD, late insoluble tau aggregates are believed to contribute to nerve cell death and closely correlate with cognitive decline (Arriagada et al., 1992; Gomez-Isla et al., 1997). In contrast, the toxicity of oligomeric tau has been shown to correlate better with neuronal dysfunction than the extent of filamentous tau (Berger et al., 2007).

Our data provide evidence that soluble oligomeric tau species play a key role in the neurotoxic cascade of tau pathology leading to neuronal loss (Blair et al., 2013; Brunden et al., 2008; Gerson and Kayed, 2013; Gerson et al., 2014; Usenovic et al., 2015). Indeed, progressive neuronal degeneration in absence of tau filament formation was reported not only in tauopathy mouse models (Oddo et al., 2003; Spires et al., 2006; Sydow and Mandelkow, 2010), but also in tau transgenic drosophila models (Cowan et al., 2010; Wittmann et al., 2001). Aside, oligomeric protein species have been implicated in the pathogenesis of various neurodegenerative diseases: in brains of AD patients, oligomeric Aβ peptides appeared to participate in the neurotoxic cascade even before the onset of symptoms (Lesne et al., 2013); moreover, toxic extracellular α-Syn oligomers have been shown to favour prion-like propagation in PD *in vitro* (Danzer et al., 2011); further, doperminergic loss in the substantia nigra caused by α-Syn oligomer formation rather than amyloid fibrils *in vivo* highlighted the toxicity of soluble oligomers (Winner et al., 2011); notably, oligomeric Aβ and α-Syn species were postulated to be competent to provoke neurotoxic tau oligomerization (Lasagna-Reeves et al., 2010); in addition, toxic oligomers forms of PrP have been suggested to mediate the infectious process in prion diseases (Silveira et al., 2005).

Oligomeric tau species are considerably interesting as a potential immune target. The observed severe neurotoxicity associated with abundant tau oligomer formation suggests our mouse model of special relevance for this type of pharmacological treatment. Indeed, a growing body of evidence supports the strategy of diminishing tau pathology with therapeutic antibodies. Studies on active immunization using phospho-tau peptides has been shown to

mitigate tau aggregation in P301L transgenic mice (Asuni et al., 2007). Moreover, passive immunization approaches with anti-tau directed monoclonal antibodies were shown to reduce tau pathology, when administrated prior to the disease onset (Boutajangout et al., 2011; Chai et al., 2011). However, the rapid onset of tau toxicity in our mouse model favours it greatly for immunotherapeutic approaches and investigating clearance mechanisms of pathological tau protein *in vivo*.

## Targeting the axonal transport system and oligomeric tau induced neurotoxicity

Here we report that fragmented tau exacerbates the toxicity of full-length tau *in vivo*. Our mouse model exhibit pronounced drastic, but remarkably, reversible toxic effect of oligomeric tau species associated with extensive neuronal dysfunction and a severe neurological phenotype. In P301SxTAU62$^{on}$ mice, apparent mitochondrial dislocation and clumping, disruption of the Golgi network and missorting of synaptic proteins strongly suggests a widespread disruption of the cellular transport system (Kopeikina et al., 2011; Liazoghli et al., 2005). Interestingly, comparable perinuclear mitochondrial clumping associated with the presence of only soluble tau species was reflected in studies on rTg4510 transgenic mice (Kopeikina et al., 2011). Fragmentation of the Golgi apparatus (GA) disturbs the central sorting machinery for all newly synthesized proteins destined for fast axonal transport and is believed to be an early event in various neurodegenerative disorders (Gonatas et al., 2006; Hammerschlag et al., 1982; Liazoghli et al., 2005). In AD, given that the GA was found to be fragmented upon cdk5 dysregulation, this process appears to directly precede cell death (Sun et al., 2008). Of note, overexpression of α-Syn has been shown to cause Golgi fragmentation and block ER-Golgi trafficking *in vitro* and *in vivo* (Cooper et al., 2006; Winslow et al., 2010). However, somatic accumulation of synaptophysin in the hippocampus of P301SxTAU62$^{on}$ mice and degradation of VAMP2, a binding partner of synaptophysin, indicate congested Golgi pathways and synaptic transmission disturbances (Nakashiba et al., 2008; Pennuto et al., 2003).

In accordance with our findings, damage to the axonal transport system have been described in multiple neurodegenerative disorders including AD (Kopeikina et al., 2011), ALS (De Vos et

al., 2007), PD (Saha et al., 2004), and HD (Chang et al., 2006). Further, in AD, Aβ was reported to interfere with mitochondrial transport in cultured hippocampal neurons (Rui et al., 2006). In tauopathies, over-expression of the shortest tau isoform has been shown to impair axonal transport *in vivo*; in addition, this was paralleled with insoluble tau inclusions (Ishihara et al., 1999). In contrast, soluble tau species were sufficient to induce disruption of the microtubule cytoskeleton in drosophila (Cowan et al., 2010).

In physiological conditions, tau is tightly associated with microtubules and critically involved in the dynamically assembly and stability of this cytoskeleton component; and thus, instrumental for viability of the intracellular transport system (Kosik, 1993). However, modifications of tau are likely responsible for the dysregulation of the microtubule network. There are two possible explanations for the disruption of polarized microtubule tracks: one source of interference might constitute abnormal high levels of tau and its concomitant excessive binding to microtubules results in the detachment of kinesin; thus, ultimately prevents anterograde transport of individual cargoes (Baas and Qiang, 2005; Dixit et al., 2008; Dubey et al., 2008). In this case, hyperphosphorylation and subsequent dissociation of tau, typically responsible for the destabilization of microtubules in the first place, might be even of benefit for the microtubule network operability. Of note, co-expression of various full-lengths forms of tau in our P301SxALZ31 and ALZ17xALZ31 revealed comparable levels of tau hyperphosphorylation, without a pronounced motor phenotype; thus, tau hyperphosphorylation appear not to correlate directly with nerve cell death in our mouse models and strengthen the possibility that abnormal phosphorylation might not be a primary pathoglogical event.

Microtubule network disruption is a major pathogenic event in the evolution of tauopathies. Our findings in P301SxTAU62$^{on}$ mice suggest that, initiated by Δtau overexpression, highly toxic oligomeric tau species interfere with microtubule assembly and stabilization, ultimately contribute to axonal transport disruption; however, the underlying mechanisms remain to be established in detail. A possible approach to dissect the process of axonal transport disruption would be to assess various potent microtubule stabilizing compounds such as epothilone D

and paclitaxel that have been shown to partly rescue tau induced axonal transport dysfunction (Ballatore et al., 2012; Barten et al., 2012; Brunden et al., 2012; Das and Miller, 2012).
Another approach would be to target tau oligomeric formation directly through aggregation inhibitors including methylene blue (MB) (Violet et al., 2015; Wischik et al., 1996) and curcumin (Ma et al., 2013). However, while MB has been shown to block tau protein assembly through the repeat domain and being competent to reverse early tau aggregation, however, it failed to remove robust tangle pathology in the rTG4510 mouse model of tauopathy (Spires-Jones et al., 2014). In addition, a reduction of Aβ levels and improved cognitive deficits upon MB treatment was reported (Medina et al., 2011).

## Protective effects of early tau burden on late neurotoxic distress level

This work originates from our most recent published observation that overexpression of Δtau in presence of full-length tau causes drastic, but reversible neurotoxicity *in vivo* (Ozcelik et al., 2016). Based on our results, we set out to investigate the long-term consequences of the extensive neurotoxic stress during early postnatal life in formerly paralyzed P301SxTAU62$^{on-off}$ mice. Remarkably, we found that these mice exhibit a less pronounced motor phenotype at 14 to 16 months of age compared to their heterozygous P301S littermates that did not experience compelling neurotoxicity early in life. This is paralleled by significant reduced tau pathology in aged P301SxTAU62$^{on-off}$ mice: the histopathological phenotype of formerly paralyzed mice showed mitigated tau hyperphosphorylation and almost no signs of insoluble tau inclusions. In line with these findings, significant less total, insoluble, and soluble tau protein levels could be detected.
Our observations advocate a late preventive effect of early Δtau induced neurotoxicity and raises the possibility of diverse sources, alone or in combination, being responsible for the underlying delayed tau pathology in P301SxTAU62$^{on-off}$ mice. As aforementioned, various active immunization attempts using recombinant tau peptides have been shown to reduce tau pathology in various tau transgenic mouse models (Asuni et al., 2007; Bi et al., 2011; Boutajangout et al., 2010). A possible scenario is that the excessive toxic tau oligomerization in young P301SxTAU62$^{on-off}$ mice would trigger an autoimmune reaction in the form of arising anti-tau antibodies. Alternatively, other clearance machineries may be involved in removing

oligomeric or hyperphosphorylated tau from the cell. For instance, cytosolic proteases such as puromycin sensitive aminopeptidase (PSA) were observed to attenuate tau levels and motor deficits in various models of tauopathy including Drosophila (Karsten et al., 2006) and mice (Kudo et al., 2011). Considering this, PSA might regulate tau degradation in two ways: directly via proteolytic degradation of tau as reported in other *in vitro* studies (Sengupta et al., 2006), or indirectly by inducing autophagy (Menzies et al., 2010); specifically, the inhibition of PSA has led to increased levels of toxic polyQ-containing htt and ataxin-3 fragments as well as mutant α-Syn associated with a decrease in autophagosome formation. Indeed, the protective effects of early tau stress in P301SxTAU62$^{on\text{-}off}$ mice could point towards the induction of autophagic pathways in general. The removal of aggregation-prone proteins through basal autophagy has been shown to be of importance for cell survival; indeed, the consensus in the field is that impairment of the autophagy process and subsequent loss of a cytoprotective function of autophagy leads to neurodegeneration (Hara et al., 2006; Komatsu et al., 2006). Protein clearance systems and autophagy dysfunction in AD have been subject to numerous studies (Nixon, 2013; Nixon et al., 2005; Piras et al., 2016); specifically, the reduction of Beclin1 expression has been shown to increase Aβ pathology and disrupt in the autophagy flux *in vivo* (Pickford et al., 2008). In PD, α-Syn overexpression causes mislocalization of the autophagy protein Atg9, which controls the formation of phagophore in the process of autophagy, through Rab1a inhibition; however, Rab1a overexpression has been shown to reverse α-Syn induced autophagy impairment (Winslow et al., 2010). In addition, stimulation of insulin and insulin-like growth factor 1 signaling cascades results in increased autophagic clearance of toxic huntingtin aggregates (Yamamoto et al., 2006). Furthermore, mTORC1-independent activation of autophagy by trehalose and inhibition of the mTORC1 pathway by rapamycin haven been shown to promote the clearance of mutant huntingtin and α-Syn *in vitro* (Sarkar et al., 2007). In line with these findings, our group could previously show that treatment with these autophagy-inducing agents results in delayed progression of tau pathology and signs of a restored autophagic flux associated with reduced accumulation of autophagy related proteins p62 and LC3 in P301S mutant mice (Ozcelik et al., 2013; Schaeffer et al., 2012). Of note, microtubule-associated protein 1 light chain 3 protein (LC3) is required in the autophagosome formation process (Mizushima and Komatsu, 2011); and p62 is an ubiquitin-LC3-binding protein that links various substrates including protein aggregates to the

autophagosome-lysosome degradation machinery (Kim et al., 2008). However, we lack a complete understanding of the autophagy machinery in our mouse models at this time point; thus, it would be interesting to investigate a potential autophagic, rectifying response to Δtau induced severe neurotoxicity associated with the formation of toxic tau oligomers. For this, experiments with autophagy inducing agents including rapamycin would yield new insight into the degradation process of toxic tau species and the potential late preventive, neuroprotective effect of early tau stress in aged P301SxTAU62$^{on\text{-}off}$ mice. In particular, the assessment of autophagic markers including LC3, p62, and Beclin1 would allow to analyze and define a clearer picture of the autophagy flux phenomenon.

## Mouse CSF derived Aβ species do not induce prion-like amyloidogenic propagation in APP23 transgenic host mice

This work extends recent published findings reported on brain and CSF derived Aβ seeding (Fritschi et al., 2014). Here we set out to inoculate forebrain homogenate or CSF in the hippocampus of APP23 transgenic mice, and analyse the seeding effect of Aβ in the CSF and brain. Consistent with this previous report, we found that Aβ species in brain homogenates harbours seed-like potential, whereas CSF derived Aβ species lack prion-like propagation activity (Skachokova et al., 2015). Indeed, APP23 transgenic mice seeded with brain derived Aβ for 20 months exhibited and increased plaque-load in the hippocampus; in contrast, in the same experimental set-up, CSF derived Aβ did not result in a change in plaque-load. A possible explanation might constitute the absence or structural difference of seed-potent Aβ species in the CSF. Whereas small and soluble Aβ species derived from APP23 mice have been demonstrated to be highly seed-potent (Langer et al., 2011), these Aβ species appear not to be present in the CSF; possibly due to downregulated transport to the CSF compartment, or upregulated degradation within the CSF compartment. Further, N-terminal truncated Aβ species have been found largely in the brain, but less in the CSF of AD patients (Langer et al., 2011). However, if its structural diversity affects the seeding potential of Aβ remains elusive. In addition, analysis of the selective Aβ transport and potential co-factors involved might be needed to explain the lack of seed-potent Aβ species in AD CSF.

## Conclusion and perspectives

Our data show that truncated tau, when co-expressed with full-length forms of tau, results in drastic, but reversible early tau stress. We further have identified soluble tau oligomers as toxic key species, rather than insoluble tau aggregates, in the neuropathological cascade of tauopathies. This information is in line with the neurotoxic potential of protein cleavage products and oligomeric species observed in diverse neurodegenerative disorders and strengthens the idea that truncated tau indeed contributes to the pathogenesis of tauopathies (Hanger and Wray, 2010; Ross and Poirier, 2004).

In fact, our mouse model offers a remarkable setting to asses therapeutic strategies and elucidate further the pathomechanisms leading to tauopathy. For instance, modulation of tau fragmentation and associated formation of oligomeric tau species may potentially prevent neurodegenerative processes; ultimately, being of crucial relevance for the development of novel therapeutic approaches.

We further show that CSF derived Aβ species is not competent enough to induce prion-like propagation. Instead, an interesting issue emerged from our work is that abundant toxic oligomeric tau species present in our mouse model might actually exhibit prion-like potential. This hypothesis raises the possibility to better understand prion-like processes in tauopathies and needs to be corroborated by further experiments.

In conclusion, our work underlines the role of fragmented tau and soluble oligomeric tau aggregation in the neurodegenerative process of tauopathies.

# 5 Materials and Methods

## 5.1 Animals

All transgenic mice were heterozygous for the transgenes of interest, unless specifically mentioned otherwise. The number of mice used was minimized according to the Swiss regulation on Animal Experimentation. All animal experiments were conducted in accordance with the Swiss guidelines for animal care and approved by the local legal authorities.

### 5.1.1 Housing of transgenic mice

Female mice were group-housed with a maximum of five individuals per cage. Male mice were housed individually as to avoid aggressive interactions. Free access to food and water was provided and animals were kept on a 12 hour/12 hour inverted light cycle.

### 5.1.2 TAU62 mice

Inducible and neuron-specific 3R $tau_{151–421}$ (Δtau) expressing TAU62 mice were generated by co-injection of two Thy 1.2 minigene-based constructs into C57BL/6J oocytes. The Thy 1.2 tTS construct was obtained by replacing exon 2 of the murine Thy

1.2 promoter by a tetracycline controlled transcriptional silencer element (tTS). The Thy 1.2-TRE-Δtau construct contained a tetracycline responsive element (TRE) ~800bp upstream of the human wild-type Δtau cDNA encoding amino acids 151 to 421 of a 3-repeat domain spanning human wild-type tau fragment (0N3R $tau_{151-421}$). A total of six positive transgenic founder TAU62 mice (C57BL/6J-TgN(tTS-Thy1-$\Delta tau_{151-421}$) were identified and the inducible expression of human Δtau was assessed by western blot and immunohistochemistry. The Lines 62-2 and 62-48 expressed comparable and robust Δtau ('*on*') and stopped expression following the removal of doxycycline ('*on-off*'). Most experiments were performed using the TAU62/48 line, abbreviated TAU62. TAU62/2 mice were used to rule out an insertion site effect.

### 5.1.3 P301S mice

The production of P301S mutant 0N4R tau transgenic mice (C57BL/6J-TgN (Thy1 hTauP301S)) has been previously described (Allen et al., 2002). Mice were generated by subcloning P301S mutated cDNA encoding the shortest human four-repeat tau isoform (383 amino acids isoforms of human tau) into a murine Thy 1.2 genomic expression vector using *Xho*I restriction site. Transgenic mice were generated by microinjection into pronuclei of (C57BL/6J x CBA/ca) F1 generation. PCR analysis was performed to identify the founders, which then were interbred with C57BL/6J mice. Homozygous and heterozygous P301S mice were selected according to specific experiment.

### 5.1.4 ALZ17 mice

The production of full-length wild-type 2N4R tau transgenic ALZ17 mice (C57BL/6J-TgN (Thy1hTau)17) has been previously described (Probst et al., 2000). Mice were generated by subcloning cDNA encoding the longest human tau isoform into the *Xho*I restriction site of the murine Thy 1.2 minigene. After microinjection into pronuclei of B6D2F1 x B6D2F1 embryos, the founders were analyzed by PCR and then interbred with C57BL/6J mice.

### 5.1.5 ALZ31 mice

For the generation of ALZ31 wild-type human 0N3R tau transgenic mice (C57BL/6J-TgN (Thy1hTau)31), 0N3R human tau complementary DNA was cloned into the neuron-specific Thy 1.2 promoter element and injected into C57BL/6J oocytes.

### 5.1.6 P301SxTAU62 mice

P301SxTAU62 double transgenic mice co-express a $tau_{151-421}$ fragment (Δtau) with full-length mutant P301S (0N4R) tau as long as 500 mg $kg^{-1}$ doxycycline was provided ad libitum.

### 5.1.7 ALZ17xTAU62 mice

ALZ17xTAU62 double transgenic mice co-express a $tau_{151-421}$ fragment (Δtau) with full-length wildtype (2N4R) tau as long as 500 mg $kg^{-1}$ doxycycline was provided ad libitum.

### 5.1.8 ALZ31xTAU62 mice

ALZ31xTAU62 double transgenic mice co-express a $tau_{151-421}$ fragment (Δtau) with full-length wildtype (0N3R) tau as long as 500 mg $kg^{-1}$ doxycycline was provided ad libitum.

### 5.1.9 P301SxALZ31 mice

P301SxALZ31 double transgenic mice have been obtained by crossing full-length mutant P301S (0N4R) tau with full-length wildtype (0N3R) tau expressing mice.

### 5.1.10 ALZ17xALZ31 mice

ALZ17xALZ31 double transgenic mice have been obtained by crossing full-length wildtype (2N4R) tau with full-length wildtype (0N3R) tau expressing mice.

### 5.1.11 APP23 mice

APP23 mice overexpress the human full-length *APP* gene (751-aa isoform) harbouring the Swedish double mutation at positions 670/671 (KM->NL), under control of the Thy 1.2 promoter. The $APP_{751}$ cDNA was inserted into the blunt-ended *Xho*I restriction site of the murine Thy 1.2 minigene that was microinjected into C57BL/6J oocytes. The founders were analyzed by PCR and then interbred with C57BL/6J mice.

## 5.2 DNA isolation and genotyping

Genomic DNA isolated from toe biopsies was used to identify and analyze the transgene inheritance of the respective mouse line. Biopsies were incubated in lysis buffer containing 0.1 mg/ml Proteinase K (Macherey-Nagel, Germany) incubated over night (O/N at 55 °C and 600 rpm in Eppendorf Thermomixer comfort shaker. The solution was centrifuged (13000rpm, 5 min) and 750 µl of the supernatant was mixed with 750 µl isopropanol by inverting the tubes. The solution was centrifuged (13000 rpm, 10 min), the supernatant was discarded and the pellet was washed with 200 µl of 75% ethanol (EtOH). After the solution was centrifuged again (13000 rpm, 10 min), the remaining DNA pellet was dried on Eppendorf Thermomixer comfort shaker (55°C, 5-10 min) and dissolved in 250 µl $dH_2O$ (50°C, 1h). DNA samples were kept at 4°C until analysis of transgene inheritance by PCR.

| Reagent | Concentration | Supplier |
|---|---|---|
| Tris | 100 mM (pH 8.0) | Biomol # 08003 |
| EDTA | 5 mM | Fluka BioChemika # 03690 |
| NaCl | 200 mM | Merck # 1.06404.10 000 |
| SDS | 0.20% | Bio Rad # 161 0301 |

Table 5.1: Lysis buffer composition

PCR conditions were determined independently for each transgenes of interest and each individual PCR program was run on a PTC100 machine (MJ Research, Canada). PCR products were run on 1.5% agarose gels at 150V for 90 min.

| Reagent | Volume |
|---|---|
| Forward primer (10 pmol/µl) | 2 µl |
| Reverse primer (10 pmol/µl) | 2 µl |
| TopTaq Master mix (Qiagen, Germany) | 12.5 µl |
| Sterile $H_2O$ | 6.5 µl |
| DNA | 2 µl |

Table 5.2: PCR mixture

| Temperature | Time | Cycles |
|---|---|---|
| 95°C | 2 min | 1 |
| 95°C | 1 min | 30 |
| 60°C | 1 min | |
| 72°C | 2 min | |
| 72°C | 10 min | 1 |
| 4°C | ∞ | |

Table 5.3: TAUF151 PCR program

| Temperature | Time | Cycles |
|---|---|---|
| 95°C | 4 min | 1 |
| 95°C | 1 min | 30 |
| 60°C | 1 min | |
| 72°C | 3 min | |
| 72°C | 10 min | 1 |
| 4°C | ∞ | |

Table 5.4: P301S PCR program

| Temperature | Time | Cycles |
|---|---|---|
| 95°C | 10 min | 1 |
| 95°C | 20 s | 30 |
| 54°C | 15 s | |
| 72°C | 1 min | |
| 72°C | 10 min | 1 |
| 4°C | ∞ | |

Table 5.5: P301SxALZ31 PCR program

| Temperature | Time | Cycles |
|---|---|---|
| 94°C | 2 min | 1 |
| 94°C | 45 s | 1 |
| 60°C | 1 min | 35 |
| 72°C | 45 s | |
| 94°C | 45 s | |
| 72°C | 5 min | 1 |
| 4°C | ∞ | |

Table 5.6: APP23 PCR program

Primers used for genotyping were designed individually for transgene of interest.

| PCR program | Forward primer | Reverse primer |
|---|---|---|
| TAUF151 | GTG GAT CTC AAG CCC TCA AG | GGC GAC TTG GGT GGA GTA |
| P301S | GGT TTT TGC TGG AAT CCT GG | GGA GTT CGA AGT GAT GGA AG |
| ALZ31xP301S | CCT CTC CCG TCC TCG CCT CTG TCG | AAG ACA GAC CAC GGG GCG GAG ATC |
| APP23 | CCG ATG GGT AGT GAA GCA ATG GTT | GAA TTC CGA CAT GAC TCA GG |

Table 5.7: Designed primer sequences (5' - 3')

## 5.3 Histology and immunohistochemistry

Mice were anesthetized with a mixture of 100 mg $kg^{-1}$ ketamine (Ketalar®, Pfizer) and 10 mg $kg^{-1}$ xylazine (Rompun® 2%, Bayer) intraperitoneally and after deep sleeping, mice were injected by 100 mg $kg^{-1}$ sodium pentobarbital (Pentothal® 0.5g, Ospedalia AG) and transcardially perfused with 0.01M cold phosphate-buffered saline (PBS).

### 5.3.1 Tissue preparation and processing: Brain, Spinal cord and Sciatic nerve

After perfusion, the spinal cord, sciatic nerve and the brain were quickly removed, immersion fixed in 4% paraformaldehyde O/N, and embedded in paraffin. Brains were cut either sagittally (4–20 µm transverse serial sections) or in coronal plane anterior to the hippocampus (4–20 µm transverse serial sections starting at -2 Bregma to -3 Bregma, as defined by the Mouse Brain Atlas by G. Paxinos and K. Franklin) by a sliding

microtome (Leica SM2000R, Leica, Germany). Paraffin sections were transferred on a floating bath (60°C), mounted on histological slides (Leica IP S, Leica, Germany) and dried O/N at 37 °C before further usage. Paraffin sections were deparaffinised in Xylol (20 min; from Biosystems, Switzerland), rehydrated in 100% EtOH (3 min), 96% EtOH (2x3 min) and 70% EtOH (2x3 min), followed by washing in PBS. In order to mask antigenic sites, antigen retrieval was performed in Citric acid buffer pH 6.0 (Pro Taps®) for 30 min at 90 °C. After blocking in 2.5% normal horse serum (Vector Laboratories) for 30 min at room temperature (RT), sections were incubated with primary antibody diluted in PBS O/N at 4°C. The next day, the sections were washed in Tris/PBS solution (3x5 min) and then incubated with ImmPRES™ Reagent peroxidase for anti-mouse antibody (Vector Laboratories, USA) for 1h at RT. After the incubation, sections were washed with Tris/PBS (3x5 min) and developed by using chromogen ImmPACT™ NovaRED™ Peroxidase substrate kit (Vector Laboratories, USA). The developing time was controlled under a microscope and sections washed with $H_2O$ to stop the reaction. Additionally, slides were then counterstained with hematoxyline (J.T. Baker). Finally, sections were rehydrated in 70% EtOH (1 min), 96% and 100% EtOH (each 2x1 min) and kept in xylol, before using Pertex® mounting medium (Biosystems, Switzerland). Pictures of section were taken using an Olympus DP73 (Olympus, USA) microscope. The content of the original images was not neglected by changes of processed images.

### 5.3.2 Hematoxylin and Eosin Staining

After deparaffinising and rehydration, sections were rinsed in cold tap water and stained in hematoxylin for 5-8 min. After washing in cold tap water and decolorizing shortly in alcohol-HCl, the slides were washed again in cold tap water and kept in warm water until blue colour appears. Then, sections were immersed in 1% erythrosine B solution (RAL diagnosis) for 2-3 min, washed again shortly in cold tap water, followed by dehydration in EtOH (70%, 96% and 100%) and mounting as previously described.

### 5.3.3 Gallyas silver staining

Sections were silver-impregnated by a previously described method (Braak et al., 1988; Gallyas, 1971). After deparaffinization and rehydration the sections were incubated in 3% Periodic Acid (Sigma-Aldrich, USA) for 30 min at RT. Slides then were washed in $dH_2O$ (2 min) and incubated in 1% Alkaline Silver solution (1M sodium hydroxide; 0.6M potassium iodide; 1% silver nitrate solution; all from Merck, Germany), for 10 min at RT. After incubation in ABC solution and simultaneous monitoring of the reaction time, sections were treated with 0.5% Acetic Acid (Merck, Germany) to block the reaction during 30 min in RT. Treated slides were washed in $dH_2O$ and incubated in 5% Sodium thiosulfate (Merck, Germany) for 5 min at RT. Then, slides were washed in cold tap water and nuclei stained (hematoxylin eosin staining), followed by dehydration in EtOH (70%, 96% and 100%) and mounting as previously described.

| Solution | Composition | Concentration | Supplier |
|---|---|---|---|
| **A** | Sodium Carbonate Anhydride | 0.5 M | Merck, Germany |
| **B** | Ammonium nitrate | 24 mM | Merck, Germany |
| | Silver Nitrate | 0.01 M | Merck, Germany |
| | Tungstosilicic Acid Hydrate | 3.5 mM | Sigma-Aldrich, USA |
| **C** | Ammonium nitrate | 24 mM | Merck, Germany |
| | Silver Nitrate | 0.01 M | Merck, Germany |
| | Tungstosilicic Acid Hydrate | 3.5 mM | Sigma-Aldrich, USA |
| | Formalin Solution | 0,26% | Merck, Germany |

Table 5.8: ABC solution

### 5.3.4 Holmes Silver Nitrate-Luxol Fast Blue staining

| Reagents | | Concentration | Supplier |
|---|---|---|---|
| **Impregnation solution** | Boric acid | 1,24% | Merck, Germany |
| | Dinatriumtetraborat (Borax) | 1,90% | Merck, Germany |
| | Silver nitrate | 1% | Merck, Germany |
| | Pyridin solution | 10% | J.T.Baker |
| **Reduction solution** | Sodium sulfite | 0.8M | Merck, Germany |
| | Hydrochinon | 90mM | Merck, Germany |
| | Gold chloride | 0,25% | Sigma-Aldrich, USA |
| | Acid oxalic | 2% | Merck, Germany |
| | Sodium thiosulfate | 5% | Merck, Germany |
| **Luxol Fast Blue solution** | Luxol fast blue | 24 mM | Medite |
| | Ethanol | 0.01 M | Pharmacy USB |
| | Acetic acid | 3.5 mM | Merck, Germany |

Table 5.9: Holmes Silver Nitrate-Luxol Fast Blue staining solutions

Sections were deparaffinised and rehydrated as previously described and placed in 20% Silver nitrate solution (Merck, Germany), for 90 min in the dark at RT. Slides then were washed in $dH_2O$ (3x) and incubated in impregnation solution at 37°C O/N. Next day, sections were placed onto filter paper to remove superfluous fluid and transferred directly in reduction solution for 10 min. The sections were then washed in tap water (5 min) and placed in dH2O. After, the sections were moved in 0.25% Gold chloride solution (5 min) and then rinsed in dH2O (10 min). Washed slides were incubated in 2% Acid oxalic (10 min) and the reaction were stopped by rinsing the sections in dH2O. Slides were then placed in 5% sodium thiosulfate solution for 5 min and rinsed in tap water before placing the slides briefly in 70% (1x) and 96% EtOH (2x). Next, the sections were incubated for 2 hours at 60°C in Luxol fast blue solution and briefly washed in 96% EtOH (2x) to remove excess stain, then placed in running cold tap water for 5 min and transferred into dH2O. Slides then were placed in 0.1% Lithium carbonate for few seconds and distained in 70% EtOH before to be washed in dH2O. Finally, the slides were immersed in Cresyl violet solution (10 min; at RT) and washed in 96% EtOH (2x) to remove excess stain and then in 100% EtOH (2x) before to place in xylol and apply Pertex mounting medium.

### 5.3.5 Masson Trichrome staining (Sciatic nerve)

| Reagents | | | Concentration | Supplier |
|---|---|---|---|---|
| **Weigert's Iron Hematoxylin solution I** | Solution I | Hematoxyline | 33 mM | Merck, Germany |
| | | Ethanol | 96% | Pharmacy USB |
| **Ferric chloride solution** | Solution II | Iron (III) chloride | 32 mM | Merck, Germany |
| | | Acid-HCl | 25% | Merck, Germany |
| **Acid fuchsin Ponceau** | Solution I | Fuchsin acid | 17 mM | Merck, Germany |
| | | Acetic acid | 1% | Merck, Germany |
| | Solution II | Ponceau | 23 mM | Chroma, Germany |
| | | Acetic acid | 1% | Merck, Germany |
| **Aniline blue solution** | | Aniline blue | 34 mM | Chroma, Germany |
| | | Acetic acid | 2,5% | Merck, Germany |

Table 5.10: Masson Trichrome staining solutions

The sections were deparaffinised and incubated in Weigert's Iron Hematoxylin solution (1 min) and washed in running cold water followed by warm water (5-10 min). Next, slides were placed in Acid fuchsin Ponceau solution (5 min), followed by washing in tap water. The sections were then incubated in 1% Acid Phosphomolibdic (Merck, Germany) for 5 min and Aniline blue solution was added directly on the slides for 3 min (without discarding the 1% Acid Phosphomolibdic) under shaking. Then, the sections were rinsed three-five times in dH2O and transferred in 1% acetic acid (5 sec). Finally, the rinsed slides were dehydrated in absolute EtOH (2x), then in xylol, and coverslipped.

### 5.3.6 Muscles preparation

After perfusion, gastrocnemius (GC), soleus (Sol), tibialis anterior (TA) and extensor digitorum longus (EDL) were removed and snap frozen in liquid nitrogen cooled isopentane. Muscles were embedded on a cork disc on O.C.T™ compound (Tissue-Tek®

Sakura™, USA) and stored at -80°C. Coronal cryosections (10-12 µm) were cut with a cryostat (HydraxC, Histocom AG, Switzerland) maintained at - 20°C.

### 5.3.7 Myosin-ATPase (Adenosintriphosphatase) staining (pH4.2)

| Reagents | | Concentration | Supplier |
|---|---|---|---|
| **Veronalacetate buffer (stock solution)** | Sodium acetate | 0.1M | Merck, Germany |
| | Sodium barbiturate (Veronal) | 0.1M | Sigma-Aldrich, USA |
| **ATP pH 4.2 solution** | Veronalacetate buffer pH 4.2 | 0.1M | Sigma-Aldrich, USA |
| | HCl | 0.1M | |
| **Veronal Ca buffer (stock solution)** | Sodium barbiturate (Veronal) | 0.1M | Sigma-Aldrich, USA |
| | CaCl2 | 0.03M | Merck, Germany |
| **Veronal Ca ATP pH 9.4 solution** | Adenosin-5-triphosphate disodium (ATP) | 4.5mM | Fluka # 02060 |
| **Cobalt chloride** | | 2% | Merck, Germany |
| **HCl** | | 0.1M | |
| **NaOH** | | 1M | Merck, Germany |
| **Ammonium sulfide solution** | | 21% | Sigma-Aldrich, USA |

Table 5.11: Myosin-ATPase staining solutions

Frozen sections of O.C.T embedded samples were equilibrated O/N at -20°C, and then placed into the cryostat for minimum 20 minutes. The samples were mounted on the cryostat with O.C.T and 10 µm sections were cut and collected on warm slides at RT. Before to proceed the staining, the sections must be dry at least 1h at RT. The slides were transferred in ATP pH 4.2 solution (10 min; RT) and placed shortly for washing in Veronal-Ca pH 9.4 buffer. Next, the sections were incubated in Veronal-Ca- ATP pH 9.4 solution (45 min at RT). The slides were then washed in tap water (2x) and moved in

dH2O before transferring in 2% Cobalt Chloride for 5 min. After washing in tap water (3x), the sections were placed in Ammoniumsulfide solution (14 sec) and rinsed before to be rehydrated in ascending EtOH (1x in 70%, 2x in 96% and 2x in 100%) and transferred in xylol and apply Pertex mounting medium.

### 5.3.8 Semithin sections (Sciatic nerve)

Sciatic nerves were dissected and fixed for at least 2h in 2.5% of Glutaraldehyde at RT, followed by washing samples in 10 mM PBS O/N. The tissues were reduced in 1 % Osmium tetroxide (Oxkem Limited 10x1g) for 2h at RT. After a dehydration step in histological grade EtOH (70%, 80%, 90% and 2x100%) for 20 min each and 2x in Acetone for 30 min, the tissue was incubated, first, in Acetone-Durcupan (1:1) solution for 60 min and, second, in Acetone-Durcupane (1:3) O/N at 4°C. Then, the tissues were mounted in Durcupan resin, containing 150ml of Durcupan A (Fluka), 150 ml of Durcupan B (Fluka), 3.1 ml of Durcupan C (Fluka), 4 ml of Durcupan D (Fluka), and cooked at 60°C for 2-3 days, before processed for light microscopy. Semithin sections were cut (1.5 µm) using a glass trip that was equipped with a Reichert-Jung apparatus.

### 5.3.9 *Para*-Phenylendiamine (Sciatic nerve)

Ultrathin cryosections on the slides were dried on a warm plate before incubated in 1% *p*-Phenylenediamine (Sigma-Aldrich, USA) solution for 2-3h. The slides then were rinsed 6-10 times in $dH_2O$ and dried at RT.

### 5.3.10 Electron microscopy

Mice were anesthetized as previously desrcibed. After transcardially perfusion with PBS for 2-4 min, animals were perfused further with a fixative solution composed of with 2% paraformaldehyde, 2% glutaraldehyde and 10 mM PBS (pH 7.4) for 1h. Brains and spinal cords were removed and postfixed for 1 h, followed by rinsing of the tissues in 10 mM PBS.

The tissues were reduced in 1 % Osmium tetroxide and 1.5% Potassium Ferrocyanide for 40 min; after, the tissues were transferred in 1% Osmiumtetroxid for 40 min. The tissues were dehydrated as previously described and embedded in Epon. During dehydration, the sections were treated with 1% uranyl acetate in 70% EtOH for 1h. Ultrathin sections from selected areas were cut with a microtome (Ultracut E; Leica Microsystems GmbH, Wetzlar, Germany), collected on single-shot grids, stained in 6% uranyl acetate for 1h. Sections were examined and photographed with a Morgagni FEI 80kV electron microscope (FEI Company, Eindhoven, The Netherlands).

## 5.4 Sarkosyl extraction

| **Reagent** | **Concentration** | **Supplier** |
|---|---|---|
| Tris | 25 mM (pH 7.4) | Biomol |
| NaCl | 150 mM | Merck, Germany |
| EDTA | 1 mM | Fluka BioChemika |
| EGTA | 1 mM | Sigma-Aldrich, USA |
| Sodium pyrophosphate | 5 mM | Sigma-Aldrich, USA |
| PhosSTOP®, Phosphatase inhibitor cocktail tablet | 1 tablet | Roche, Switzerland |
| Sodium fluoride | 30 mM | Merck, Germany |
| Complete Mini, Protease inhibitor cocktail tablets | 1 tablet | Roche, Switzerland |
| Phenylmethyl sulfonyl fluoride (PMSF) | 1 mM | Sigma-Aldrich, USA |
| Leupeptine | 10 µg/ml | Sigma-Aldrich, USA |
| Aprotinine | 10 µg/ml | Sigma-Aldrich, USA |
| Pepstatine | 10 µg/ml | Sigma-Aldrich, USA |

Table 5.12: Extraction buffer

| Reagent | Concentration | Supplier |
|---|---|---|
| Tris | 10 mM (pH 7.4) | Biomol |
| NaCl | 800 mM | Merck, Germany |
| Sucrose | 10% | Fluka BioChemika |
| EGTA | 1 mM | Sigma-Aldrich, USA |
| Phenylmethyl sulfonyl fluoride (PMSF) | 1 mM | Sigma-Aldrich, USA |
| Leupeptine | 10 µg/ml | Sigma-Aldrich, USA |
| Aprotinine | 10 µg/ml | Sigma-Aldrich, USA |
| Pepstatine | 10 µg/ml | Sigma-Aldrich, USA |

Table 5.13: A68 buffer

Phosphatase and protease inhibitor cocktail tablets were freshly added to each buffer.

Sarkosyl extraction was performed as described previously (Delobel et al., 2008). Following PBS perfusion, one half of the mouse brain was dissected into forebrain and brainstem and frozen in liquid nitrogen or on dry ice. Brain tissue was homogenized in cold Extraction buffer 1:3 (w/v) by using Ultraturrax T8 (IKA labortechnik) and briefly sonicated (Bandelin SONOPULS, 90
% power, 10 % cycle, 10 sec pulses). The samples were centrifuged at 4 000g (5 000 rpm) for 15 min and 10% of the supernatant (= total tau) was collected and aliquoted. Then, samples were further centrifuged at 80 000g (28 000 rpm) for 15 min by using ultracentrifuge (Beckman Coulter, Optima$^{TM}$ L-70K Ultracentrifuge) by using SW55Ti rotor (Beckman Coulter). The supernatant (= soluble tau) was collected and aliquoted. The remaining pellets were homogenized in A68 buffer 1:3 (w/v) and centrifuged at 4 000 g (5 000 rpm) for 20 min and 1% of sarkosyl (N-laurylsarcosine, Sigma-Aldrich, USA) added for 1h30 at 37 °C in thermoshaker (Eppendorf Thermomixer comfort shaker) under shaking (max rpm). The samples were further centrifuged at 80 000g (28 000rpm) for 30 min and the pellets was resuspended in 150 µl $g^{-1}$ of 50 mM Tris-HCl, pH 7.4 and aliquoted (= sarkosyl insoluble tau).

## 5.5 Western Blot

| Reagent | Concentration | Supplier |
|---|---|---|
| Tris | 20 mM (pH 7.5) | Biomol |
| NaCl | 137 mM | Merck, Germany |
| Complete Mini, Protease inhibitor cocktail tablets | 1 tablet | Roche, Switzerland |

Table 5.14: TBS-Complete buffer

| Reagent | Reduced sample (µl) | Non-reduced sample (µl) |
|---|---|---|
| Sample | x | x |
| NuPAGE® LDS Sample Buffer (4X) | 5 | x |
| NuPAGE® Reducing Agent (10X) | 2 | — |
| Deionized Water | x | x |
| Total Volume | 20 | 20 |

Table 5.15: Reduced and non-reduced sample preparation

Following PBS perfusion, one half of the mouse brain was dissected into forebrain and brainstem and frozen in liquid nitrogen or on dry ice. The brain tissue was homogenized in 1:10 volume of TBS-Complete buffer by using Ultraturrax T8 (IKA labortechnik) and briefly sonicated (Bandelin SONOPULS, 90 % power, 10 % cycle, 10 sec pulses). The samples were spun down at 4 000 g (5 000 rpm) for 30 min and the supernatant was collected and aliquoted. Western blots were performed either under reducing or non-reducing conditions (see Table 5.15). Following appropriate preparation, samples were heated for 5 min at 95°C and shortly spin down and loaded onto a 7% NuPAGE® Tris-acetate gel. Gels were run first at 100V for 30 min, then subsequently at 120V for additional 60 min. After the removal of gels from the cassette and activation of PVDF membrane (Amersham Biosciences) for first, 30 sec in methanol and then, 5 min in transfer buffer, samples were transferred on the PVDF membrane at 30V for 2h by using the XCell II™ Blot Module. Next, Unspecific binding epitopes were blocked with 5% non-fat milk in PBS-T (0.01M PBS pH 7.4; 0.05 % Tween-20) for 1h at RT, followed by incubation with primary antibody O/N at 4°C on a shaker. After washing with PBS-T (3x5 min) at RT, the membrane was incubated with horseradish peroxidase (HRP)-conjugated anti-mouse or -rabbit secondary antibody for 1h at RT. Then, the membrane was washed again in PBS-T (3x5 min) at RT and detected by electrochemiluminescence (ECL) (GE Healthcare, USA). Western blot was performed with the NuPAGE® System from Invitrogen.

## 5.6 Antibodies

| Antibody | Target | Dilution | Source |
|---|---|---|---|
| HT7 | human tau<br>aa 159-163 | WB 1:4000<br>IHC 1:800 | Pierce, Rockford, IL<br>#MN1000 |
| BR134 | human tau | WB 1:1000 | (Goedert et al., 1989) |
| Tau-C3 | Tau cleaved at residue Asp421 | WB 1:1000<br>IHC 1:1000 | Santa Cruz Biotechnology, Inc, Dallas, TX<br>#sc-32240 |
| AT8 | Tau<br>pSer202/Thr205 | WB 1:1000<br>IHC 1:800 | Pierce, Rockford, IL #MN1020 |
| AT100 | Tau<br>pThr212/Ser214 | WB 1:1000<br>IHC 1:500 | Pierce, Rockford, IL #MN1060 |
| PHF-1 | Tau<br>pSer396/404 | WB 1:2000<br>IHC 1:1000 | Peter Davies, Albert Einstein College of Medecine, Bronx, NY |
| MC1 | Tau<br>aa 5-15, 312-322 | IHC 1:100 | Peter Davies, Albert Einstein College of Medecine, Bronx, NY |
| 2F11 | neurofilament (NF)<br>NF-L, NF-H (70kD) | IHC 1:800 | Dako, Glostrup, DK #M0762 |
| NF200 | neurofilament (200kD | IHC 1:100 | (Probst et al., 2000) |
| GFAP | glial fibrillary acidic protein | IHC 1:500 | Thermo Fisher Scientific Inc., Kalamazoo, MI #MS-1407-R7 |
| Synaptophysin | synaptophysin | IHC 1:1000 | Millipore Corporation, Billerica, MA #MAB5258 |
| MG160 (rabbit) | Golgi apparatus | IHC 1:1000 | Nicholas Gonatas, Pathology and Laboratory Medicine, University of Pennsylvania, PA |
| VAMP2/Synaptobrevin 2 (rabbit) | transport vesicles | IHC 1:1000 | Synaptic system, Goettingen, Germany<br># 104 202 |
| GAPDH (6C5) | GAPDH | WB 1:1000 | Santa Cruz Biotechnology, Santa Cruz, CA, #32233 |
| ß-actin | actin | WB 1:5000 | Sigma-Aldrich, Saint Louis, MO #A5316 |
| Cox subunit 1a | mitochondrial staining | IHC 1:200 | Abcam plc, Cambridge, UK #ab14705 |
| RD3, clone 8E6/C11 | Human tau, recognize 3R, residue 209-224 | WB 1:4000;<br>IHC 1:3000 | Millipore Corporation, Billerica, MA #05-803 |
| RD4, clone1E1/A6 | Human tau and mouse, recognize 4R, aa 275-291 | WB 1:4000;<br>IHC 1:100 | Millipore Corporation, Billerica, MA #05-804 |
| T49 | Specific for rodent tau | WB 1:10 000 | Virginia Lee, CNDR, University of Pennsylvania School of Medicine, Philadelphia, PA |

Table 5.16: Antibodies used for immunohistochemistry (IHC) and Western blotting (WB). Species is mouse, unless indicated otherwise)

## 5.7 Behavioral assessment

### 5.7.1 Grid-test

Grid reflex and motor strength of mice was assessed by the grid test. Animals were placed on a vertical mesh grid and the latency to fall off from the grid was recorded during a maximum time of 180 sec. Each mouse was tested 3 times with at least a 5 min rest interval in between trails. An average score per day was made.

### 5.7.2 Rotarod test

The motor coordination and balance of mice were assessed using the Panlab Harvard Rotarod. The Rotarod starts at a speed of 4 rpm and accelerates consistently with 1 rpm every 3 sec. The testing phase consisted of 4 consecutive days. With each animal, an acclimation period consisting of 3 sessions with a rest interval of at least 5 min in between trails was performed. Subsequently, mice were tested for 3 consecutive days with 3 trials each day and a rest interval of 5 min minimum and the mean latency to fall was documented.

### 5.7.3 Object recognition test

Short term memory was assessed by the object recognition test. Animals were placed in a squared open field box (48 × 48 × 40 cm) under dim light conditions. Mice were allowed to freely explore the box during a habituation phase over 3 consecutive days for 15 min, until no signs of stress were present. During a training phase over 2 days, two identical objects were introduced at diagonal corners of the field for training sessions of 10 min duration. The training was halted when the mice had closely explored the objects for 20 sec, for a maximum training duration of 10 min (Leger et al., 2013)). In the test phase, the animals' short-term memory was tested by replacing one of the familiar objects with

a novel one, and the time spent exploring each object during a period of 6 min was video recorded. Video scoring VLC video player, VideoLAN, France) was done by a researcher blind to the genotype, and as exploration criteria nose sniffing/touching of the object at 2 cm or less distance (Leger et al., 2013)) were used. For both training and test phases, 10 cm high objects composed of the same material were used, and the position of the novel and familiar objects were randomized across groups.

## 5.8 Statistics

All statistical analysis was performed using one-way analysis of variance followed by Bonferroni's multiple comparison test and Student's t-tests with GraphPad Prism Software Version 5.0a (GraphPad Software, La Jolla, CA, USA). P-values are established and outlined as follows: $*P<0.05$, $**P<0.01$ and $***P<0.001$. The mean and s.d. are indicated.

# 6 References

Abraha, A., Ghoshal, N., Gamblin, T.C., Cryns, V., Berry, R.W., Kuret, J., and Binder, L.I. (2000). C-terminal inhibition of tau assembly in vitro and in Alzheimer's disease. J Cell Sci *113 Pt 21*, 3737-3745.

Aguzzi, A., and O'Connor, T. (2010). Protein aggregation diseases: pathogenicity and therapeutic perspectives. Nat Rev Drug Discov *9*, 237-248.

Akter, R., Cao, P., Noor, H., Ridgway, Z., Tu, L.H., Wang, H., Wong, A.G., Zhang, X., Abedini, A., Schmidt, A.M.*, et al.* (2016). Islet Amyloid Polypeptide: Structure, Function, and Pathophysiology. J Diabetes Res *2016*, 2798269.

Allen, B., Ingram, E., Takao, M., Smith, M.J., Jakes, R., Virdee, K., Yoshida, H., Holzer, M., Craxton, M., Emson, P.C.*, et al.* (2002). Abundant tau filaments and nonapoptotic neurodegeneration in transgenic mice expressing human P301S tau protein. J Neurosci *22*, 9340-9351.

Altmeppen, H.C., Puig, B., Dohler, F., Thurm, D.K., Falker, C., Krasemann, S., and Glatzel, M. (2012). Proteolytic processing of the prion protein in health and disease. Am J Neurodegener Dis *1*, 15-31.

Alzheimer, A. (1906). Über einen eigenartigen schweren Erkrankungsprozess der Hirnrinde. Neurologisches Centralblatt *25*, 1134.

Alzheimer, A. (1907). Über eine eigenartige Erkrankung der Hirnrinde. Allg Z Psychiat Psych-Gerichtl Med *64*, 146-148.

Andreadis, A., Brown, W.M., and Kosik, K.S. (1992). Structure and novel exons of the human tau gene. Biochemistry *31*, 10626-10633.

Anglade, P., Vyas, S., Javoy-Agid, F., Herrero, M.T., Michel, P.P., Marquez, J., Mouatt-Prigent, A., Ruberg, M., Hirsch, E.C., and Agid, Y. (1997). Apoptosis and autophagy in nigral neurons of patients with Parkinson's disease. Histol Histopathol *12*, 25-31.

Arai, T., Guo, J.P., and McGeer, P.L. (2005). Proteolysis of non-phosphorylated and phosphorylated tau by thrombin. J Biol Chem *280*, 5145-5153.

Arai, T., Hasegawa, M., Akiyama, H., Ikeda, K., Nonaka, T., Mori, H., Mann, D., Tsuchiya, K., Yoshida, M., Hashizume, Y.*, et al.* (2006). TDP-43 is a component of ubiquitin-positive tau-negative inclusions in frontotemporal lobar degeneration and amyotrophic lateral sclerosis. Biochem Biophys Res Commun *351*, 602-611.

Arai, T., Hasegawa, M., Nonoka, T., Kametani, F., Yamashita, M., Hosokawa, M., Niizato, K., Tsuchiya, K., Kobayashi, Z., Ikeda, K.*, et al.* (2010). Phosphorylated and cleaved TDP-43 in ALS, FTLD and other neurodegenerative disorders and in cellular models of TDP-43 proteinopathy. Neuropathology *30*, 170-181.

Arriagada, P.V., Growdon, J.H., Hedley-Whyte, E.T., and Hyman, B.T. (1992). Neurofibrillary tangles but not senile plaques parallel duration and severity of Alzheimer's disease. Neurology *42*, 631-639.

Asuni, A.A., Boutajangout, A., Quartermain, D., and Sigurdsson, E.M. (2007). Immunotherapy targeting pathological tau conformers in a tangle mouse model reduces brain pathology with associated functional improvements. J Neurosci *27*, 9115-9129.

Augustinack, J.C., Schneider, A., Mandelkow, E.M., and Hyman, B.T. (2002). Specific tau phosphorylation sites correlate with severity of neuronal cytopathology in Alzheimer's disease. Acta Neuropathol *103*, 26-35.

Avila, J. (2010). Alzheimer disease: caspases first. Nat Rev Neurol *6*, 587-588.

Baas, P.W., and Qiang, L. (2005). Neuronal microtubules: when the MAP is the roadblock. Trends Cell Biol *15*, 183-187.

Baba, M., Nakajo, S., Tu, P.H., Tomita, T., Nakaya, K., Lee, V.M., Trojanowski, J.Q., and Iwatsubo, T. (1998). Aggregation of alpha-synuclein in Lewy bodies of sporadic Parkinson's disease and dementia with Lewy bodies. Am J Pathol *152*, 879-884.

Ballatore, C., Brunden, K.R., Huryn, D.M., Trojanowski, J.Q., Lee, V.M., and Smith, A.B., 3rd (2012). Microtubule stabilizing agents as potential treatment for Alzheimer's disease and related neurodegenerative tauopathies. J Med Chem *55*, 8979-8996.

Barten, D.M., Fanara, P., Andorfer, C., Hoque, N., Wong, P.Y., Husted, K.H., Cadelina, G.W., Decarr, L.B., Yang, L., Liu, V.*, et al.* (2012). Hyperdynamic microtubules, cognitive deficits, and pathology are improved in tau transgenic mice with low doses of the microtubule-stabilizing agent BMS-241027. J Neurosci *32*, 7137-7145.

Bassil, F., Fernagut, P.O., Bezard, E., Pruvost, A., Leste-Lasserre, T., Hoang, Q.Q., Ringe, D., Petsko, G.A., and Meissner, W.G. (2016). Reducing C-terminal truncation mitigates synucleinopathy and neurodegeneration in a transgenic model of multiple system atrophy. Proc Natl Acad Sci U S A *113*, 9593-9598.

Basurto-Islas, G., Luna-Munoz, J., Guillozet-Bongaarts, A.L., Binder, L.I., Mena, R., and Garcia-Sierra, F. (2008). Accumulation of Aspartic Acid421- and Glutamic Acid391-Cleaved Tau in Neurofibrillary Tangles Correlates With Progression in Alzheimer Disease. J Neuropathol Exp Neurol *67*, 470-483.

Bayer, T.A., and Wirths, O. (2010). Intracellular accumulation of amyloid-Beta - a predictor for synaptic dysfunction and neuron loss in Alzheimer's disease. Front Aging Neurosci *2*, 8.

Bence, N.F., Sampat, R.M., and Kopito, R.R. (2001). Impairment of the ubiquitin-proteasome system by protein aggregation. Science *292*, 1552-1555.

Berger, Z., Roder, H., Hanna, A., Carlson, A., Rangachari, V., Yue, M., Wszolek, Z., Ashe, K., Knight, J., Dickson, D.*, et al.* (2007). Accumulation of pathological tau species and memory loss in a conditional model of tauopathy. J Neurosci *27*, 3650-3662.

Bi, M., Ittner, A., Ke, Y.D., Gotz, J., and Ittner, L.M. (2011). Tau-targeted immunization impedes progression of neurofibrillary histopathology in aged P301L tau transgenic mice. PLoS One *6*, e26860.

Biernat, J., Mandelkow, E.M., Schroter, C., Lichtenberg-Kraag, B., Steiner, B., Berling, B., Meyer, H., Mercken, M., Vandermeeren, A., Goedert, M.*, et al.* (1992). The switch of tau protein to an Alzheimer-like state includes the phosphorylation of two serine-proline motifs upstream of the microtubule binding region. EMBO J *11*, 1593-1597.

Binder, L.I., Frankfurter, A., and Rebhun, L.I. (1985). The distribution of tau in the mammalian central nervous system. J Cell Biol *101*, 1371-1378.

Blair, L.J., Nordhues, B.A., Hill, S.E., Scaglione, K.M., O'Leary, J.C., 3rd, Fontaine, S.N., Breydo, L., Zhang, B., Li, P., Wang, L.*, et al.* (2013). Accelerated neurodegeneration through chaperone-mediated oligomerization of tau. J Clin Invest *123*, 4158-4169.

Blennow, K., de Leon, M.J., and Zetterberg, H. (2006). Alzheimer's disease. Lancet *368*, 387-403.

Bohm, K.J., Vater, W., Steinmetzer, P., Kusnetsov, S.A., Rodionov, V.I., Gelfand, V.I., and Unger, E. (1990). Effect of MAP 1, MAP 2, and tau-proteins on structural parameters of tubulin assemblies. Acta Histochem Suppl *39*, 357-364.

Boland, B., Kumar, A., Lee, S., Platt, F.M., Wegiel, J., Yu, W.H., and Nixon, R.A. (2008). Autophagy induction and autophagosome clearance in neurons: relationship to autophagic pathology in Alzheimer's disease. J Neurosci *28*, 6926-6937.

Boutajangout, A., Ingadottir, J., Davies, P., and Sigurdsson, E.M. (2011). Passive immunization targeting pathological phospho-tau protein in a mouse model reduces functional decline and clears tau aggregates from the brain. J Neurochem *118*, 658-667.

Boutajangout, A., Quartermain, D., and Sigurdsson, E.M. (2010). Immunotherapy targeting pathological tau prevents cognitive decline in a new tangle mouse model. J Neurosci *30*, 16559-16566.

Braak, H., and Braak, E. (1989). Cortical and subcortical argyrophilic grains characterize a disease associated with adult onset dementia. Neuropathol Appl Neurobiol *15*, 13-26.

Braak, H., Braak, E., Ohm, T., and Bohl, J. (1988). Silver impregnation of Alzheimer's neurofibrillary changes counterstained for basophilic material and lipofuscin pigment. Stain Technol *63*, 197-200.

Braak, H., and Del Tredici, K. (2011). The pathological process underlying Alzheimer's disease in individuals under thirty. Acta Neuropathol *121*, 171-181.

Bramblett, G.T., Goedert, M., Jakes, R., Merrick, S.E., Trojanowski, J.Q., and Lee, V.M. (1993). Abnormal tau phosphorylation at Ser396 in Alzheimer's disease recapitulates development and contributes to reduced microtubule binding. Neuron *10*, 1089-1099.

Brandt, R., and Lee, G. (1993). Functional organization of microtubule-associated protein tau. Identification of regions which affect microtubule growth, nucleation, and bundle formation in vitro. J Biol Chem *268*, 3414-3419.

Brandt, R., Leger, J., and Lee, G. (1995). Interaction of tau with the neural plasma membrane mediated by tau's amino-terminal projection domain. J Cell Biol *131*, 1327-1340.

Browne, S.E. (2008). Mitochondria and Huntington's disease pathogenesis: insight from genetic and chemical models. Ann N Y Acad Sci *1147*, 358-382.

Brunden, K.R., Ballatore, C., Lee, V.M., Smith, A.B., 3rd, and Trojanowski, J.Q. (2012). Brain-penetrant microtubule-stabilizing compounds as potential therapeutic agents for tauopathies. Biochem Soc Trans *40*, 661-666.

Brunden, K.R., Trojanowski, J.Q., and Lee, V.M. (2008). Evidence that non-fibrillar tau causes pathology linked to neurodegeneration and behavioral impairments. J Alzheimers Dis *14*, 393-399.

Buee, L., Bussiere, T., Buee-Scherrer, V., Delacourte, A., and Hof, P.R. (2000). Tau protein isoforms, phosphorylation and role in neurodegenerative disorders. Brain Res Brain Res Rev *33*, 95-130.

Buratti, E., and Baralle, F.E. (2008). Multiple roles of TDP-43 in gene expression, splicing regulation, and human disease. Front Biosci *13*, 867-878.

Cantlon, A., Frigerio, C.S., and Walsh, D.M. (2015). Lessons from a Rare Familial Dementia: Amyloid and Beyond. J Parkinsons Dis Alzheimers Dis *2*.

Canu, N., Dus, L., Barbato, C., Ciotti, M.T., Brancolini, C., Rinaldi, A.M., Novak, M., Cattaneo, A., Bradbury, A., and Calissano, P. (1998). Tau cleavage and dephosphorylation in cerebellar granule neurons undergoing apoptosis. J Neurosci *18*, 7061-7074.

Castellani, R.J., Rolston, R.K., and Smith, M.A. (2010). Alzheimer disease. Dis Mon *56*, 484-546.

Caughey, B., Raymond, G.J., and Bessen, R.A. (1998). Strain-dependent differences in beta-sheet conformations of abnormal prion protein. J Biol Chem *273*, 32230-32235.

Cente, M., Filipcik, P., Pevalova, M., and Novak, M. (2006). Expression of a truncated tau protein induces oxidative stress in a rodent model of tauopathy. Eur J Neurosci *24*, 1085-1090.

Chai, X., Wu, S., Murray, T.K., Kinley, R., Cella, C.V., Sims, H., Buckner, N., Hanmer, J., Davies, P., O'Neill, M.J*., et al.* (2011). Passive immunization with anti-Tau antibodies in two transgenic models: reduction of Tau pathology and delay of disease progression. J Biol Chem *286*, 34457-34467.

Chang, D.T., Rintoul, G.L., Pandipati, S., and Reynolds, I.J. (2006). Mutant huntingtin aggregates impair mitochondrial movement and trafficking in cortical neurons. Neurobiol Dis *22*, 388-400.

Chen, C.D., Huff, M.E., Matteson, J., Page, L., Phillips, R., Kelly, J.W., and Balch, W.E. (2001). Furin initiates gelsolin familial amyloidosis in the Golgi through a defect in Ca(2+) stabilization. EMBO J *20*, 6277-6287.

Chen, J., Kanai, Y., Cowan, N.J., and Hirokawa, N. (1992). Projection domains of MAP2 and tau determine spacings between microtubules in dendrites and axons. Nature *360*, 674-677.

Chesebro, B., Trifilo, M., Race, R., Meade-White, K., Teng, C., LaCasse, R., Raymond, L., Favara, C., Baron, G., Priola, S*., et al.* (2005). Anchorless prion protein results in infectious amyloid disease without clinical scrapie. Science *308*, 1435-1439.

Chesser, A.S., Pritchard, S.M., and Johnson, G.V. (2013). Tau clearance mechanisms and their possible role in the pathogenesis of Alzheimer disease. Front Neurol *4*, 122.

Cho, D.H., Nakamura, T., Fang, J., Cieplak, P., Godzik, A., Gu, Z., and Lipton, S.A. (2009). S-nitrosylation of Drp1 mediates beta-amyloid-related mitochondrial fission and neuronal injury. Science *324*, 102-105.

Citron, M., Teplow, D.B., and Selkoe, D.J. (1995). Generation of amyloid beta protein from its precursor is sequence specific. Neuron *14*, 661-670.

Clavaguera, F., Akatsu, H., Fraser, G., Crowther, R.A., Frank, S., Hench, J., Probst, A., Winkler, D.T., Reichwald, J., Staufenbiel, M*., et al.* (2013). Brain homogenates from human tauopathies induce tau inclusions in mouse brain. Proc Natl Acad Sci U S A *110*, 9535-9540.

Clavaguera, F., Bolmont, T., Crowther, R.A., Abramowski, D., Frank, S., Probst, A., Fraser, G., Stalder, A.K., Beibel, M., Staufenbiel, M*., et al.* (2009). Transmission and spreading of tauopathy in transgenic mouse brain. Nat Cell Biol *11*, 909-913.

Cleveland, D.W., Hwo, S.Y., and Kirschner, M.W. (1977). Physical and chemical properties of purified tau factor and the role of tau in microtubule assembly. J Mol Biol *116*, 227-247.

Cohen, T.J., Guo, J.L., Hurtado, D.E., Kwong, L.K., Mills, I.P., Trojanowski, J.Q., and Lee, V.M. (2011). The acetylation of tau inhibits its function and promotes pathological tau aggregation. Nat Commun *2*, 252.

Coleman, P.D., and Yao, P.J. (2003). Synaptic slaughter in Alzheimer's disease. Neurobiol Aging *24*, 1023-1027.

Conceicao, I., Gonzalez-Duarte, A., Obici, L., Schmidt, H.H., Simoneau, D., Ong, M.L., and Amass, L. (2016). "Red-flag" symptom clusters in transthyretin familial amyloid polyneuropathy. J Peripher Nerv Syst *21*, 5-9.

Constantinidis, J., Richard, J., and Tissot, R. (1974). Pick's disease. Histological and clinical correlations. Eur Neurol *11*, 208-217.

Coomaraswamy, J., Kilger, E., Wolfing, H., Schafer, C., Kaeser, S.A., Wegenast-Braun, B.M., Hefendehl, J.K., Wolburg, H., Mazzella, M., Ghiso, J*., et al.* (2010). Modeling familial Danish dementia in mice supports the concept of the amyloid hypothesis of Alzheimer's disease. Proc Natl Acad Sci U S A *107*, 7969-7974.

Cooper, A.A., Gitler, A.D., Cashikar, A., Haynes, C.M., Hill, K.J., Bhullar, B., Liu, K., Xu, K., Strathearn, K.E., Liu, F*., et al.* (2006). Alpha-synuclein blocks ER-Golgi traffic and Rab1 rescues neuron loss in Parkinson's models. Science *313*, 324-328.

Correas, I., Diaz-Nido, J., and Avila, J. (1992). Microtubule-associated protein tau is phosphorylated by protein kinase C on its tubulin binding domain. J Biol Chem *267*, 15721-15728.

Cowan, C.M., Bossing, T., Page, A., Shepherd, D., and Mudher, A. (2010). Soluble hyper-phosphorylated tau causes microtubule breakdown and functionally compromises normal tau in vivo. Acta Neuropathol *120*, 593-604.

Cras, P., Smith, M.A., Richey, P.L., Siedlak, S.L., Mulvihill, P., and Perry, G. (1995). Extracellular neurofibrillary tangles reflect neuronal loss and provide further evidence of extensive protein cross-linking in Alzheimer disease. Acta Neuropathol *89*, 291-295.

Cummings, J.L. (2004). Alzheimer's disease. N Engl J Med *351*, 56-67.

D'Arcangelo, G., Nakajima, K., Miyata, T., Ogawa, M., Mikoshiba, K., and Curran, T. (1997). Reelin is a secreted glycoprotein recognized by the CR-50 monoclonal antibody. J Neurosci *17*, 23-31.

Danzer, K.M., Ruf, W.P., Putcha, P., Joyner, D., Hashimoto, T., Glabe, C., Hyman, B.T., and McLean, P.J. (2011). Heat-shock protein 70 modulates toxic extracellular alpha-synuclein oligomers and rescues trans-synaptic toxicity. FASEB J *25*, 326-336.

Das, V., and Miller, J.H. (2012). Microtubule stabilization by peloruside A and paclitaxel rescues degenerating neurons from okadaic acid-induced tau phosphorylation. Eur J Neurosci *35*, 1705-1717.

David, D.C., Layfield, R., Serpell, L., Narain, Y., Goedert, M., and Spillantini, M.G. (2002). Proteasomal degradation of tau protein. J Neurochem *83*, 176-185.

de Calignon, A., Fox, L.M., Pitstick, R., Carlson, G.A., Bacskai, B.J., Spires-Jones, T.L., and Hyman, B.T. (2010). Caspase activation precedes and leads to tangles. Nature *464*, 1201-1204.

De Strooper, B., and Annaert, W. (2010). Novel research horizons for presenilins and gamma-secretases in cell biology and disease. Annu Rev Cell Dev Biol *26*, 235-260.

De Strooper, B., Annaert, W., Cupers, P., Saftig, P., Craessaerts, K., Mumm, J.S., Schroeter, E.H., Schrijvers, V., Wolfe, M.S., Ray, W.J*., et al.* (1999). A presenilin-1-dependent gamma-secretase-like protease mediates release of Notch intracellular domain [see comments]. Nature *398*, 518-522.

De Vos, K.J., Chapman, A.L., Tennant, M.E., Manser, C., Tudor, E.L., Lau, K.F., Brownlees, J., Ackerley, S., Shaw, P.J., McLoughlin, D.M*., et al.* (2007). Familial amyotrophic lateral sclerosis-linked SOD1 mutants perturb fast axonal transport to reduce axonal mitochondria content. Hum Mol Genet *16*, 2720-2728.

De Vos, K.J., Grierson, A.J., Ackerley, S., and Miller, C.C. (2008). Role of axonal transport in neurodegenerative diseases. Annu Rev Neurosci *31*, 151-173.

DeArmond, S.J., McKinley, M.P., Barry, R.A., Braunfeld, M.B., McColloch, J.R., and Prusiner, S.B. (1985). Identification of prion amyloid filaments in scrapie-infected brain. Cell *41*, 221-235.

Del Campo, M., Oliveira, C.R., Scheper, W., Zwart, R., Korth, C., Muller-Schiffmann, A., Kostallas, G., Biverstal, H., Presto, J., Johansson, J*., et al.* (2015). BRI2 ectodomain affects Abeta42 fibrillation and tau truncation in human neuroblastoma cells. Cell Mol Life Sci *72*, 1599-1611.

Delobel, P., Lavenir, I., Fraser, G., Ingram, E., Holzer, M., Ghetti, B., Spillantini, M.G., Crowther, R.A., and Goedert, M. (2008). Analysis of tau phosphorylation and truncation in a mouse model of human tauopathy. Am J Pathol *172*, 123-131.

Diepenbroek, M., Casadei, N., Esmer, H., Saido, T.C., Takano, J., Kahle, P.J., Nixon, R.A., Rao, M.V., Melki, R., Pieri, L*., et al.* (2014). Overexpression of the calpain-specific inhibitor calpastatin reduces human alpha-Synuclein processing, aggregation and synaptic impairment in [A30P]alphaSyn transgenic mice. Hum Mol Genet *23*, 3975-3989.

Dixit, R., Ross, J.L., Goldman, Y.E., and Holzbaur, E.L. (2008). Differential regulation of dynein and kinesin motor proteins by tau. Science *319*, 1086-1089.

Dorval, V., and Fraser, P.E. (2006). Small ubiquitin-like modifier (SUMO) modification of natively unfolded proteins tau and alpha-synuclein. J Biol Chem *281*, 9919-9924.

Dubey, M., Chaudhury, P., Kabiru, H., and Shea, T.B. (2008). Tau inhibits anterograde axonal transport and perturbs stability in growing axonal neurites in part by displacing kinesin cargo: neurofilaments attenuate tau-mediated neurite instability. Cell Motil Cytoskeleton *65*, 89-99.

Dufty, B.M., Warner, L.R., Hou, S.T., Jiang, S.X., Gomez-Isla, T., Leenhouts, K.M., Oxford, J.T., Feany, M.B., Masliah, E., and Rohn, T.T. (2007). Calpain-cleavage of alpha-synuclein: connecting proteolytic processing to disease-linked aggregation. Am J Pathol *170*, 1725-1738.

Duyckaerts, C., Potier, M.C., and Delatour, B. (2008). Alzheimer disease models and human neuropathology: similarities and differences. Acta Neuropathol *115*, 5-38.

Egashira, M., Takase, H., Yamamoto, I., Tanaka, M., and Saito, H. (2011). Identification of regions responsible for heparin-induced amyloidogenesis of human serum amyloid A using its fragment peptides. Arch Biochem Biophys *511*, 101-106.

Eisenberg, D., and Jucker, M. (2012). The amyloid state of proteins in human diseases. Cell *148*, 1188-1203.

El-Agnaf, O.M., Nagala, S., Patel, B.P., and Austen, B.M. (2001). Non-fibrillar oligomeric species of the amyloid ABri peptide, implicated in familial British dementia, are more potent at inducing apoptotic cell death than protofibrils or mature fibrils. J Mol Biol *310*, 157-168.

Emanuele, M., and Chieregatti, E. (2015). Mechanisms of alpha-synuclein action on neurotransmission: cell-autonomous and non-cell autonomous role. Biomolecules *5*, 865-892.

Fan, H.C., Ho, L.I., Chi, C.S., Chen, S.J., Peng, G.S., Chan, T.M., Lin, S.Z., and Harn, H.J. (2014). Polyglutamine (PolyQ) diseases: genetics to treatments. Cell Transplant *23*, 441-458.

Fasulo, L., Ugolini, G., and Cattaneo, A. (2005). Apoptotic effect of caspase-3 cleaved tau in hippocampal neurons and its potentiation by tau FTDP-mutation N279K. J Alzheimers Dis *7*, 3-13.

Ferreira, A., and Bigio, E.H. (2011). Calpain-mediated tau cleavage: a mechanism leading to neurodegeneration shared by multiple tauopathies. Mol Med *17*, 676-685.

Filipcik, P., Zilka, N., Bugos, O., Kucerak, J., Koson, P., Novak, P., and Novak, M. (2012). First transgenic rat model developing progressive cortical neurofibrillary tangles. Neurobiol Aging *33*, 1448-1456.

Forno, L.S. (1996). Neuropathology of Parkinson's disease. J Neuropathol Exp Neurol *55*, 259-272.

Frappier, T.F., Georgieff, I.S., Brown, K., and Shelanski, M.L. (1994). tau Regulation of microtubule-microtubule spacing and bundling. J Neurochem *63*, 2288-2294.

Fritschi, S.K., Langer, F., Kaeser, S.A., Maia, L.F., Portelius, E., Pinotsi, D., Kaminski, C.F., Winkler, D.T., Maetzler, W., Keyvani, K*., et al.* (2014). Highly potent soluble amyloid-beta seeds in human Alzheimer brain but not cerebrospinal fluid. Brain *137*, 2909-2915.

Furukawa, Y., Kaneko, K., and Nukina, N. (2011). Molecular properties of TAR DNA binding protein-43 fragments are dependent upon its cleavage site. Biochim Biophys Acta *1812*, 1577-1583.

Gallyas, F. (1971). Silver staining of Alzheimer's neurofibrillary changes by means of physical development. Acta Morphol Acad Sci Hung *19*, 1-8.

Gamblin, T.C., Chen, F., Zambrano, A., Abraha, A., Lagalwar, S., Guillozet, A.L., Lu, M., Fu, Y., Garcia-Sierra, F., LaPointe, N*., et al.* (2003). Caspase cleavage of tau: linking amyloid and neurofibrillary tangles in Alzheimer's disease. Proc Natl Acad Sci U S A *100*, 10032-10037.

Garringer, H.J., Murrell, J., Sammeta, N., Gnezda, A., Ghetti, B., and Vidal, R. (2013). Increased tau phosphorylation and tau truncation, and decreased synaptophysin levels in mutant BRI2/tau transgenic mice. PLoS One *8*, e56426.

Gauthier-Kemper, A., Weissmann, C., Golovyashkina, N., Sebo-Lemke, Z., Drewes, G., Gerke, V., Heinisch, J.J., and Brandt, R. (2011). The frontotemporal dementia mutation R406W blocks tau's interaction with the membrane in an annexin A2-dependent manner. J Cell Biol *192*, 647-661.

Gerson, J.E., and Kayed, R. (2013). Formation and propagation of tau oligomeric seeds. Front Neurol *4*, 93.

Gerson, J.E., Sengupta, U., Lasagna-Reeves, C.A., Guerrero-Munoz, M.J., Troncoso, J., and Kayed, R. (2014). Characterization of tau oligomeric seeds in progressive supranuclear palsy. Acta Neuropathol Commun *2*, 73.

Ghazi-Noori, S., Froud, K.E., Mizielinska, S., Powell, C., Smidak, M., Fernandez de Marco, M., O'Malley, C., Farmer, M., Parkinson, N., Fisher, E.M.*, et al.* (2012). Progressive neuronal inclusion formation and axonal degeneration in CHMP2B mutant transgenic mice. Brain *135*, 819-832.

Ghidoni, R., Benussi, L., Glionna, M., Franzoni, M., and Binetti, G. (2008). Low plasma progranulin levels predict progranulin mutations in frontotemporal lobar degeneration. Neurology *71*, 1235-1239.

Ghiso, J., Holton, J., Miravalle, L., Calero, M., Lashley, T., Vidal, R., Houlden, H., Wood, N., Neubert, T., Rostagno, A*., et al.* (2001). Systemic amyloid deposits in familial British dementia. J Biol Chem *13*, 13.

Giannakopoulos, P., von Gunten, A., Kovari, E., Gold, G., Herrmann, F.R., Hof, P.R., and Bouras, C. (2007). Stereological analysis of neuropil threads in the hippocampal formation: relationships with Alzheimer's disease neuronal pathology and cognition. Neuropathol Appl Neurobiol *33*, 334-343.

Giasson, B.I., Duda, J.E., Quinn, S.M., Zhang, B., Trojanowski, J.Q., and Lee, V.M. (2002). Neuronal alpha-synucleinopathy with severe movement disorder in mice expressing A53T human alpha-synuclein. Neuron *34*, 521-533.

Goate, A., Chartier-Harlin, M.C., Mullan, M., Brown, J., Crawford, F., Fidani, L., Giuffra, L., Haynes, A., Irving, N., James, L*., et al.* (1991). Segregation of a missense mutation in the amyloid precursor protein gene with familial Alzheimer's disease. Nature *349*, 704-706.

Goedert, M. (2015). NEURODEGENERATION. Alzheimer's and Parkinson's diseases: The prion concept in relation to assembled Abeta, tau, and alpha-synuclein. Science *349*, 1255555.

Goedert, M., Spillantini, M.G., Cairns, N.J., and Crowther, R.A. (1992). Tau proteins of Alzheimer paired helical filaments: abnormal phosphorylation of all six brain isoforms. Neuron *8*, 159-168.

Goedert, M., Spillantini, M.G., Jakes, R., Rutherford, D., and Crowther, R.A. (1989). Multiple isoforms of human microtubule-associated protein tau: sequences and localization in neurofibrillary tangles of Alzheimer's disease. Neuron *3*, 519-526.

Goedert, M., Wischik, C.M., Crowther, R.A., Walker, J.E., and Klug, A. (1988). Cloning and sequencing of the cDNA encoding a core protein of the paired helical filament of Alzheimer disease: identification as the microtubule-associated protein tau. Proc Natl Acad Sci U S A *85*, 4051-4055.

Gomez-Isla, T., Hollister, R., West, H., Mui, S., Growdon, J.H., Petersen, R.C., Parisi, J.E., and Hyman, B.T. (1997). Neuronal loss correlates with but exceeds neurofibrillary tangles in Alzheimer's disease. Ann Neurol *41*, 17-24.

Gonatas, N.K., Stieber, A., and Gonatas, J.O. (2006). Fragmentation of the Golgi apparatus in neurodegenerative diseases and cell death. J Neurol Sci *246*, 21-30.

Gong, C.X., Liu, F., Grundke-Iqbal, I., and Iqbal, K. (2005). Post-translational modifications of tau protein in Alzheimer's disease. J Neural Transm *112*, 813-838.

Gong, C.X., Singh, T.J., Grundke-Iqbal, I., and Iqbal, K. (1993). Phosphoprotein phosphatase activities in Alzheimer disease brain. J Neurochem *61*, 921-927.

Goode, B.L., Denis, P.E., Panda, D., Radeke, M.J., Miller, H.P., Wilson, L., and Feinstein, S.C. (1997). Functional interactions between the proline-rich and repeat regions of tau enhance microtubule binding and assembly. Mol Biol Cell *8*, 353-365.

Gotz, J., Probst, A., Spillantini, M.G., Schafer, T., Jakes, R., Burki, K., and Goedert, M. (1995). Somatodendritic localization and hyperphosphorylation of tau protein in transgenic mice expressing the longest human brain tau isoform. Embo J *14*, 1304-1313.

Gotz, J., Streffer, J.R., David, D., Schild, A., Hoerndli, F., Pennanen, L., Kurosinski, P., and Chen, F. (2004). Transgenic animal models of Alzheimer's disease and related disorders: histopathology, behavior and therapy. Mol Psychiatry *9*, 664-683.

Graham, R.K., Deng, Y., Slow, E.J., Haigh, B., Bissada, N., Lu, G., Pearson, J., Shehadeh, J., Bertram, L., Murphy, Z*., et al.* (2006). Cleavage at the caspase-6 site is required for neuronal dysfunction and degeneration due to mutant huntingtin. Cell *125*, 1179-1191.

Gregori, L., Fuchs, C., Figueiredo-Pereira, M.E., Van Nostrand, W.E., and Goldgaber, D. (1995). Amyloid beta-protein inhibits ubiquitin-dependent protein degradation in vitro. J Biol Chem *270*, 19702-19708.

Grundke-Iqbal, I., Iqbal, K., Tung, Y.C., Quinlan, M., Wisniewski, H.M., and Binder, L.I. (1986). Abnormal phosphorylation of the microtubule-associated protein tau (tau) in Alzheimer cytoskeletal pathology. Proc Natl Acad Sci U S A *83*, 4913-4917.

Guillot-Sestier, M.V., Sunyach, C., Druon, C., Scarzello, S., and Checler, F. (2009). The alpha-secretase-derived N-terminal product of cellular prion, N1, displays neuroprotective function in vitro and in vivo. J Biol Chem *284*, 35973-35986.

Guillozet-Bongaarts, A.L., Garcia-Sierra, F., Reynolds, M.R., Horowitz, P.M., Fu, Y., Wang, T., Cahill, M.E., Bigio, E.H., Berry, R.W., and Binder, L.I. (2005). Tau truncation during neurofibrillary tangle evolution in Alzheimer's disease. Neurobiol Aging *26*, 1015-1022.

Guo, H., Albrecht, S., Bourdeau, M., Petzke, T., Bergeron, C., and LeBlanc, A.C. (2004). Active caspase-6 and caspase-6-cleaved tau in neuropil threads, neuritic plaques, and neurofibrillary tangles of Alzheimer's disease. Am J Pathol *165*, 523-531.

Guyenet, S.J., Mookerjee, S.S., Lin, A., Custer, S.K., Chen, S.F., Sopher, B.L., La Spada, A.R., and Ellerby, L.M. (2015). Proteolytic cleavage of ataxin-7 promotes SCA7 retinal degeneration and neurological dysfunction. Hum Mol Genet *24*, 3908-3917.

Haacke, A., Hartl, F.U., and Breuer, P. (2007). Calpain inhibition is sufficient to suppress aggregation of polyglutamine-expanded ataxin-3. J Biol Chem *282*, 18851-18856.

Haass, C., Hung, A.Y., Selkoe, D.J., and Teplow, D.B. (1994). Mutations associated with a locus for familial Alzheimer's disease result in alternative processing of amyloid beta-protein precursor. J Biol Chem *269*, 17741-17748.

Hammerschlag, R., Stone, G.C., Bolen, F.A., Lindsey, J.D., and Ellisman, M.H. (1982). Evidence that all newly synthesized proteins destined for fast axonal transport pass through the Golgi apparatus. J Cell Biol *93*, 568-575.

Hanger, D.P., and Wray, S. (2010). Tau cleavage and tau aggregation in neurodegenerative disease. Biochem Soc Trans *38*, 1016-1020.

Hara, T., Nakamura, K., Matsui, M., Yamamoto, A., Nakahara, Y., Suzuki-Migishima, R., Yokoyama, M., Mishima, K., Saito, I., Okano, H.*, et al.* (2006). Suppression of basal autophagy in neural cells causes neurodegenerative disease in mice. Nature *441*, 885-889.

Harada, A., Takei, Y., Kanai, Y., Tanaka, Y., Nonaka, S., and Hirokawa, N. (1998). Golgi vesiculation and lysosome dispersion in cells lacking cytoplasmic dynein. J Cell Biol *141*, 51-59.

Harry, G.J., Lefebvre d'Hellencourt, C., Bruccoleri, A., and Schmechel, D. (2000). Age-dependent cytokine responses: trimethyltin hippocampal injury in wild-type, APOE knockout, and APOE4 mice. Brain Behav Immun *14*, 288-304.

Higuchi, M., Iwata, N., Matsuba, Y., Takano, J., Suemoto, T., Maeda, J., Ji, B., Ono, M., Staufenbiel, M., Suhara, T.*, et al.* (2012). Mechanistic involvement of the calpain-calpastatin system in Alzheimer neuropathology. FASEB J *26*, 1204-1217.

Hirai, K., Aliev, G., Nunomura, A., Fujioka, H., Russell, R.L., Atwood, C.S., Johnson, A.B., Kress, Y., Vinters, H.V., Tabaton, M.*, et al.* (2001). Mitochondrial abnormalities in Alzheimer's disease. J Neurosci *21*, 3017-3023.

Hollenbeck, P.J., and Saxton, W.M. (2005). The axonal transport of mitochondria. J Cell Sci *118*, 5411-5419.

Horowitz, P.M., Patterson, K.R., Guillozet-Bongaarts, A.L., Reynolds, M.R., Carroll, C.A., Weintraub, S.T., Bennett, D.A., Cryns, V.L., Berry, R.W., and Binder, L.I. (2004). Early N-terminal changes and caspase-6 cleavage of tau in Alzheimer's disease. J Neurosci *24*, 7895-7902.

Hubener, J., Vauti, F., Funke, C., Wolburg, H., Ye, Y., Schmidt, T., Wolburg-Buchholz, K., Schmitt, I., Gardyan, A., Driessen, S.*, et al.* (2011). N-terminal ataxin-3 causes neurological symptoms with inclusions, endoplasmic reticulum stress and ribosomal dislocation. Brain *134*, 1925-1942.

Hubener, J., Weber, J.J., Richter, C., Honold, L., Weiss, A., Murad, F., Breuer, P., Wullner, U., Bellstedt, P., Paquet-Durand, F.*, et al.* (2013). Calpain-mediated ataxin-3 cleavage in the molecular pathogenesis of spinocerebellar ataxia type 3 (SCA3). Hum Mol Genet *22*, 508-518.

Hussain, I., Powell, D., Howlett, D.R., Tew, D.G., Meek, T.D., Chapman, C., Gloger, I.S., Murphy, K.E., Southan, C.D., Ryan, D.M.*, et al.* (1999). Identification of a novel aspartic protease (Asp 2) as beta-secretase. Mol Cell Neurosci *14*, 419-427.

Hutton, M., Lendon, C.L., Rizzu, P., Baker, M., Froelich, S., Houlden, H., Pickering-Brown, S., Chakraverty, S., Isaacs, A., Grover, A.*, et al.* (1998). Association of missense and 5'-splice-site mutations in tau with the inherited dementia FTDP-17. Nature *393*, 702-705.

Igaz, L.M., Kwong, L.K., Chen-Plotkin, A., Winton, M.J., Unger, T.L., Xu, Y., Neumann, M., Trojanowski, J.Q., and Lee, V.M. (2009). Expression of TDP-43 C-terminal Fragments in Vitro Recapitulates Pathological Features of TDP-43 Proteinopathies. J Biol Chem *284*, 8516-8524.

Ihse, E., Rapezzi, C., Merlini, G., Benson, M.D., Ando, Y., Suhr, O.B., Ikeda, S., Lavatelli, F., Obici, L., Quarta, C.C.*, et al.* (2013). Amyloid fibrils containing fragmented ATTR may be the standard fibril composition in ATTR amyloidosis. Amyloid *20*, 142-150.

Ishihara, T., Hong, M., Zhang, B., Nakagawa, Y., Lee, M.K., Trojanowski, J.Q., and Lee, V.M. (1999). Age-dependent emergence and progression of a tauopathy in transgenic mice overexpressing the shortest human tau isoform. Neuron *24*, 751-762.

Ittner, L.M., Ke, Y.D., Delerue, F., Bi, M., Gladbach, A., van Eersel, J., Wolfing, H., Chieng, B.C., Christie, M.J., Napier, I.A.*, et al.* (2010). Dendritic function of tau mediates amyloid-beta toxicity in Alzheimer's disease mouse models. Cell *142*, 387-397.

Jancsik, V., Filliol, D., Felter, S., and Rendon, A. (1989). Binding of microtubule-associated proteins (MAPs) to rat brain mitochondria: a comparative study of the binding of MAP2, its microtubule-binding and projection domains, and tau proteins. Cell Motil Cytoskeleton *14*, 372-381.

Jucker, M., and Walker, L.C. (2013). Self-propagation of pathogenic protein aggregates in neurodegenerative diseases. Nature *501*, 45-51.

Jung, J., Xu, K., Lessing, D., and Bonini, N.M. (2009). Preventing Ataxin-3 protein cleavage mitigates degeneration in a Drosophila model of SCA3. Hum Mol Genet *18*, 4843-4852.

Kampers, T., Friedhoff, P., Biernat, J., Mandelkow, E.M., and Mandelkow, E. (1996). RNA stimulates aggregation of microtubule-associated protein tau into Alzheimer-like paired helical filaments. FEBS Lett *399*, 344-349.

Kanda, S., Bishop, J.F., Eglitis, M.A., Yang, Y., and Mouradian, M.M. (2000). Enhanced vulnerability to oxidative stress by alpha-synuclein mutations and C-terminal truncation. Neuroscience *97*, 279-284.

Kane, M.D., Lipinski, W.J., Callahan, M.J., Bian, F., Durham, R.A., Schwarz, R.D., Roher, A.E., and Walker, L.C. (2000). Evidence for seeding of beta -amyloid by intracerebral infusion of Alzheimer brain extracts in beta -amyloid precursor protein-transgenic mice. J Neurosci *20*, 3606-3611.

Kang, J., Lemaire, H.G., Unterbeck, A., Salbaum, J.M., Masters, C.L., Grzeschik, K.H., Multhaup, G., Beyreuther, K., and Muller-Hill, B. (1987). The precursor of Alzheimer's disease amyloid A4 protein resembles a cell-surface receptor. Nature *325*, 733-736.

Karsten, S.L., Sang, T.K., Gehman, L.T., Chatterjee, S., Liu, J., Lawless, G.M., Sengupta, S., Berry, R.W., Pomakian, J., Oh, H.S.*, et al.* (2006). A genomic screen for modifiers of tauopathy identifies puromycin-sensitive aminopeptidase as an inhibitor of tau-induced neurodegeneration. Neuron *51*, 549-560.

Keck, S., Nitsch, R., Grune, T., and Ullrich, O. (2003). Proteasome inhibition by paired helical filament-tau in brains of patients with Alzheimer's disease. J Neurochem *85*, 115-122.

Keller, J.N., Hanni, K.B., and Markesbery, W.R. (2000). Impaired proteasome function in Alzheimer's disease. J Neurochem *75*, 436-439.

Kenessey, A., Nacharaju, P., Ko, L.W., and Yen, S.H. (1997). Degradation of tau by lysosomal enzyme cathepsin D: implication for Alzheimer neurofibrillary degeneration. J Neurochem *69*, 2026-2038.

Kent, L., Vizard, T.N., Smith, B.N., Topp, S.D., Vance, C., Gkazi, A., Miller, J., Shaw, C.E., and Talbot, K. (2014). Autosomal dominant inheritance of rapidly progressive amyotrophic lateral sclerosis due to a truncation mutation in the fused in sarcoma (FUS) gene. Amyotroph Lateral Scler Frontotemporal Degener *15*, 557-562.

Kessler, J.C., Rochet, J.C., and Lansbury, P.T., Jr. (2003). The N-terminal repeat domain of alpha-synuclein inhibits beta-sheet and amyloid fibril formation. Biochemistry *42*, 672-678.

Kim, K.S., Choi, Y.R., Park, J.Y., Lee, J.H., Kim, D.K., Lee, S.J., Paik, S.R., Jou, I., and Park, S.M. (2012). Proteolytic cleavage of extracellular alpha-synuclein by plasmin: implications for Parkinson disease. J Biol Chem *287*, 24862-24872.

Kim, P.K., Hailey, D.W., Mullen, R.T., and Lippincott-Schwartz, J. (2008). Ubiquitin signals autophagic degradation of cytosolic proteins and peroxisomes. Proc Natl Acad Sci U S A *105*, 20567-20574.

Kim, S.H., Wang, R., Gordon, D.J., Bass, J., Steiner, D.F., Lynn, D.G., Thinakaran, G., Meredith, S.C., and Sisodia, S.S. (1999). Furin mediates enhanced production of fibrillogenic ABri peptides in familial British dementia. Nat Neurosci *2*, 984-988.

Kim, Y.J., Yi, Y., Sapp, E., Wang, Y., Cuiffo, B., Kegel, K.B., Qin, Z.H., Aronin, N., and DiFiglia, M. (2001). Caspase 3-cleaved N-terminal fragments of wild-type and mutant huntingtin are present in normal and Huntington's disease brains, associate with membranes, and undergo calpain-dependent proteolysis. Proc Natl Acad Sci U S A *98*, 12784-12789.

Komatsu, M., Waguri, S., Chiba, T., Murata, S., Iwata, J., Tanida, I., Ueno, T., Koike, M., Uchiyama, Y., Kominami, E.*, et al.* (2006). Loss of autophagy in the central nervous system causes neurodegeneration in mice. Nature *441*, 880-884.

Kondo, J., Honda, T., Mori, H., Hamada, Y., Miura, R., Ogawara, M., and Ihara, Y. (1988). The carboxyl third of tau is tightly bound to paired helical filaments. Neuron *1*, 827-834.

Kopeikina, K.J., Carlson, G.A., Pitstick, R., Ludvigson, A.E., Peters, A., Luebke, J.I., Koffie, R.M., Frosch, M.P., Hyman, B.T., and Spires-Jones, T.L. (2011). Tau accumulation causes mitochondrial distribution deficits in neurons in a mouse model of tauopathy and in human Alzheimer's disease brain. Am J Pathol *179*, 2071-2082.

Kosik, K.S. (1993). The molecular and cellular biology of tau. Brain Pathol *3*, 39-43.

Kosik, K.S., Joachim, C.L., and Selkoe, D.J. (1986). Microtubule-associated protein tau (tau) is a major antigenic component of paired helical filaments in Alzheimer disease. Proc Natl Acad Sci U S A *83*, 4044-4048.

Ksiezak-Reding, H., Liu, W.K., and Yen, S.H. (1992). Phosphate analysis and dephosphorylation of modified tau associated with paired helical filaments. Brain Res *597*, 209-219.

Kudo, L.C., Parfenova, L., Ren, G., Vi, N., Hui, M., Ma, Z., Lau, K., Gray, M., Bardag-Gorce, F., Wiedau-Pazos, M.*, et al.* (2011). Puromycin-sensitive aminopeptidase (PSA/NPEPPS) impedes development of neuropathology in hPSA/TAU(P301L) double-transgenic mice. Hum Mol Genet *20*, 1820-1833.

Kwiatkowski, T.J., Jr., Bosco, D.A., Leclerc, A.L., Tamrazian, E., Vanderburg, C.R., Russ, C., Davis, A., Gilchrist, J., Kasarskis, E.J., Munsat, T.*, et al.* (2009). Mutations in the FUS/TLS gene on chromosome 16 cause familial amyotrophic lateral sclerosis. Science *323*, 1205-1208.

Landau, S.M., Horng, A., Fero, A., Jagust, W.J., and Alzheimer's Disease Neuroimaging, I. (2016). Amyloid negativity in patients with clinically diagnosed Alzheimer disease and MCI. Neurology.

Langer, F., Eisele, Y.S., Fritschi, S.K., Staufenbiel, M., Walker, L.C., and Jucker, M. (2011). Soluble Abeta seeds are potent inducers of cerebral beta-amyloid deposition. J Neurosci *31*, 14488-14495.

Larson, M.E., and Lesne, S.E. (2012). Soluble Abeta oligomer production and toxicity. J Neurochem *120 Suppl 1*, 125-139.

Lasagna-Reeves, C.A., Castillo-Carranza, D.L., Guerrero-Muoz, M.J., Jackson, G.R., and Kayed, R. (2010). Preparation and characterization of neurotoxic tau oligomers. Biochemistry *49*, 10039-10041.

Law, W.J., Cann, K.L., and Hicks, G.G. (2006). TLS, EWS and TAF15: a model for transcriptional integration of gene expression. Brief Funct Genomic Proteomic *5*, 8-14.

Leavitt, B.R., Guttman, J.A., Hodgson, J.G., Kimel, G.H., Singaraja, R., Vogl, A.W., and Hayden, M.R. (2001). Wild-type huntingtin reduces the cellular toxicity of mutant huntingtin in vivo. Am J Hum Genet *68*, 313-324.

Leavitt, B.R., van Raamsdonk, J.M., Shehadeh, J., Fernandes, H., Murphy, Z., Graham, R.K., Wellington, C.L., Raymond, L.A., and Hayden, M.R. (2006). Wild-type huntingtin protects neurons from excitotoxicity. J Neurochem *96*, 1121-1129.

Ledesma, M.D., Bonay, P., Colaco, C., and Avila, J. (1994). Analysis of microtubule-associated protein tau glycation in paired helical filaments. J Biol Chem *269*, 21614-21619.

Lee, B.H., Lee, M.J., Park, S., Oh, D.C., Elsasser, S., Chen, P.C., Gartner, C., Dimova, N., Hanna, J., Gygi, S.P.*, et al.* (2010). Enhancement of proteasome activity by a small-molecule inhibitor of USP14. Nature *467*, 179-184.

Lee, G., Cowan, N., and Kirschner, M. (1988). The primary structure and heterogeneity of tau protein from mouse brain. Science *239*, 285-288.

Lee, G., Neve, R.L., and Kosik, K.S. (1989). The microtubule binding domain of tau protein. Neuron *2*, 1615-1624.

Lee, G., Newman, S.T., Gard, D.L., Band, H., and Panchamoorthy, G. (1998). Tau interacts with src-family non-receptor tyrosine kinases. J Cell Sci *111 ( Pt 21)*, 3167-3177.

Leger, M., Quiedeville, A., Bouet, V., Haelewyn, B., Boulouard, M., Schumann-Bard, P., and Freret, T. (2013). Object recognition test in mice. Nat Protoc *8*, 2531-2537.

Lesne, S.E., Sherman, M.A., Grant, M., Kuskowski, M., Schneider, J.A., Bennett, D.A., and Ashe, K.H. (2013). Brain amyloid-beta oligomers in ageing and Alzheimer's disease. Brain *136*, 1383-1398.

Levin, J., Giese, A., Boetzel, K., Israel, L., Hogen, T., Nubling, G., Kretzschmar, H., and Lorenzl, S. (2009). Increased alpha-synuclein aggregation following limited cleavage by certain matrix metalloproteinases. Exp Neurol *215*, 201-208.

Lewis, V., Hill, A.F., Haigh, C.L., Klug, G.M., Masters, C.L., Lawson, V.A., and Collins, S.J. (2009). Increased proportions of C1 truncated prion protein protect against cellular M1000 prion infection. J Neuropathol Exp Neurol *68*, 1125-1135.

Li, Q., Yokoshi, M., Okada, H., and Kawahara, Y. (2015). The cleavage pattern of TDP-43 determines its rate of clearance and cytotoxicity. Nat Commun *6*, 6183.

Li, W., West, N., Colla, E., Pletnikova, O., Troncoso, J.C., Marsh, L., Dawson, T.M., Jakala, P., Hartmann, T., Price, D.L.*, et al.* (2005). Aggregation promoting C-terminal truncation of alpha-synuclein is a normal cellular process and is enhanced by the familial Parkinson's disease-linked mutations. Proc Natl Acad Sci U S A *102*, 2162-2167.

Liazoghli, D., Perreault, S., Micheva, K.D., Desjardins, M., and Leclerc, N. (2005). Fragmentation of the Golgi apparatus induced by the overexpression of wild-type and mutant human tau forms in neurons. Am J Pathol *166*, 1499-1514.

Liu, C.W., Giasson, B.I., Lewis, K.A., Lee, V.M., Demartino, G.N., and Thomas, P.J. (2005). A precipitating role for truncated alpha-synuclein and the proteasome in alpha-synuclein aggregation: implications for pathogenesis of Parkinson disease. J Biol Chem *280*, 22670-22678.

Loomis, P.A., Howard, T.H., Castleberry, R.P., and Binder, L.I. (1990). Identification of nuclear tau isoforms in human neuroblastoma cells. Proc Natl Acad Sci U S A *87*, 8422-8426.

Lustbader, J.W., Cirilli, M., Lin, C., Xu, H.W., Takuma, K., Wang, N., Caspersen, C., Chen, X., Pollak, S., Chaney, M.*, et al.* (2004). ABAD directly links Abeta to mitochondrial toxicity in Alzheimer's disease. Science *304*, 448-452.

Ma, Q.L., Zuo, X., Yang, F., Ubeda, O.J., Gant, D.J., Alaverdyan, M., Teng, E., Hu, S., Chen, P.P., Maiti, P.*, et al.* (2013). Curcumin suppresses soluble tau dimers and corrects molecular chaperone, synaptic, and behavioral deficits in aged human tau transgenic mice. J Biol Chem *288*, 4056-4065.

Maia, L.F., Kaeser, S.A., Reichwald, J., Hruscha, M., Martus, P., Staufenbiel, M., and Jucker, M. (2013). Changes in Amyloid-beta and Tau in the Cerebrospinal Fluid of Transgenic Mice Overexpressing Amyloid Precursor Protein. Sci Transl Med *5*, 194re192.

Mandybur, T.I. (1986). Cerebral amyloid angiopathy: the vascular pathology and complications. J Neuropathol Exp Neurol *45*, 79-90.

Mangiarini, L., Sathasivam, K., Seller, M., Cozens, B., Harper, A., Hetherington, C., Lawton, M., Trottier, Y., Lehrach, H., Davies, S.W*., et al.* (1996). Exon 1 of the HD gene with an expanded CAG repeat is sufficient to cause a progressive neurological phenotype in transgenic mice. Cell *87*, 493-506.

Marchetti, L., Klein, M., Schlett, K., Pfizenmaier, K., and Eisel, U.L. (2004). Tumor necrosis factor (TNF)-mediated neuroprotection against glutamate-induced excitotoxicity is enhanced by N-methyl-D-aspartate receptor activation. Essential role of a TNF receptor 2-mediated phosphatidylinositol 3-kinase-dependent NF-kappa B pathway. J Biol Chem *279*, 32869-32881.

Marcora, M.S., Fernandez-Gamba, A.C., Avendano, L.A., Rotondaro, C., Podhajcer, O.L., Vidal, R., Morelli, L., Ceriani, M.F., and Castano, E.M. (2014). Amyloid peptides ABri and ADan show differential neurotoxicity in transgenic Drosophila models of familial British and Danish dementia. Mol Neurodegener *9*, 5.

Margolis, R.L., and Ross, C.A. (2001). Expansion explosion: new clues to the pathogenesis of repeat expansion neurodegenerative diseases. Trends Mol Med *7*, 479-482.

Martin, L., Fluhrer, R., Reiss, K., Kremmer, E., Saftig, P., and Haass, C. (2008). Regulated intramembrane proteolysis of Bri2 (Itm2b) by ADAM10 and SPPL2a/SPPL2b. J Biol Chem *283*, 1644-1652.

Masters, C.L., and Selkoe, D.J. (2012). Biochemistry of amyloid beta-protein and amyloid deposits in Alzheimer disease. Cold Spring Harb Perspect Med *2*, a006262.

McKhann, G.M., Knopman, D.S., Chertkow, H., Hyman, B.T., Jack, C.R., Jr., Kawas, C.H., Klunk, W.E., Koroshetz, W.J., Manly, J.J., Mayeux, R*., et al.* (2011). The diagnosis of dementia due to Alzheimer's disease: recommendations from the National Institute on Aging-Alzheimer's Association workgroups on diagnostic guidelines for Alzheimer's disease. Alzheimers Dement *7*, 263-269.

McMillan, P.J., Kraemer, B.C., Robinson, L., Leverenz, J.B., Raskind, M., and Schellenberg, G. (2011). Truncation of tau at E391 promotes early pathologic changes in transgenic mice. J Neuropathol Exp Neurol *70*, 1006-1019.

Mead, S., James-Galton, M., Revesz, T., Doshi, R.B., Harwood, G., Pan, E.L., Ghiso, J., Frangione, B., and Plant, G. (2000). Familial British dementia with amyloid angiopathy: early clinical, neuropsychological and imaging findings. Brain *123*, 975-991.

Medeiros, R., Kitazawa, M., Chabrier, M.A., Cheng, D., Baglietto-Vargas, D., Kling, A., Moeller, A., Green, K.N., and LaFerla, F.M. (2012). Calpain inhibitor A-705253 mitigates Alzheimer's disease-like pathology and cognitive decline in aged 3xTgAD mice. Am J Pathol *181*, 616-625.

Medina, D.X., Caccamo, A., and Oddo, S. (2011). Methylene blue reduces abeta levels and rescues early cognitive deficit by increasing proteasome activity. Brain Pathol *21*, 140-149.

Mena, R., Edwards, P.C., Harrington, C.R., Mukaetova-Ladinska, E.B., and Wischik, C.M. (1996). Staging the pathological assembly of truncated tau protein into paired helical filaments in Alzheimer's disease. Acta Neuropathol *91*, 633-641.

Menzies, F.M., Hourez, R., Imarisio, S., Raspe, M., Sadiq, O., Chandraratna, D., O'Kane, C., Rock, K.L., Reits, E., Goldberg, A.L*., et al.* (2010). Puromycin-sensitive aminopeptidase protects against aggregation-prone proteins via autophagy. Hum Mol Genet *19*, 4573-4586.

Metcalfe, M.J., Huang, Q., and Figueiredo-Pereira, M.E. (2012). Coordination between proteasome impairment and caspase activation leading to TAU pathology: neuroprotection by cAMP. Cell Death Dis *3*, e326.

Meyer-Luehmann, M., Coomaraswamy, J., Bolmont, T., Kaeser, S., Schaefer, C., Kilger, E., Neuenschwander, A., Abramowski, D., Frey, P., Jaton, A.L*., et al.* (2006). Exogenous induction of cerebral beta-amyloidogenesis is governed by agent and host. Science *313*, 1781-1784.

Miller, J.P., Holcomb, J., Al-Ramahi, I., de Haro, M., Gafni, J., Zhang, N., Kim, E., Sanhueza, M., Torcassi, C., Kwak, S*., et al.* (2010). Matrix metalloproteinases are modifiers of huntingtin proteolysis and toxicity in Huntington's disease. Neuron *67*, 199-212.

Mishizen-Eberz, A.J., Norris, E.H., Giasson, B.I., Hodara, R., Ischiropoulos, H., Lee, V.M., Trojanowski, J.Q., and Lynch, D.R. (2005). Cleavage of alpha-synuclein by calpain: potential role in degradation of fibrillized and nitrated species of alpha-synuclein. Biochemistry *44*, 7818-7829.

Mitchison, T., and Kirschner, M. (1984). Dynamic instability of microtubule growth. Nature *312*, 237-242.

Mizushima, N., and Komatsu, M. (2011). Autophagy: renovation of cells and tissues. Cell *147*, 728-741.

Mocanu, M.M., Nissen, A., Eckermann, K., Khlistunova, I., Biernat, J., Drexler, D., Petrova, O., Schonig, K., Bujard, H., Mandelkow, E.*, et al.* (2008). The potential for beta-structure in the repeat domain of tau protein determines aggregation, synaptic decay, neuronal loss, and coassembly with endogenous Tau in inducible mouse models of tauopathy. J Neurosci *28*, 737-748.

Mondragon-Rodriguez, S., Basurto-Islas, G., Santa-Maria, I., Mena, R., Binder, L.I., Avila, J., Smith, M.A., Perry, G., and Garcia-Sierra, F. (2008). Cleavage and conformational changes of tau protein follow phosphorylation during Alzheimer's disease. Int J Exp Pathol *89*, 81-90.

Mookerjee, S., Papanikolaou, T., Guyenet, S.J., Sampath, V., Lin, A., Vitelli, C., DeGiacomo, F., Sopher, B.L., Chen, S.F., La Spada, A.R.*, et al.* (2009). Posttranslational modification of ataxin-7 at lysine 257 prevents autophagy-mediated turnover of an N-terminal caspase-7 cleavage fragment. J Neurosci *29*, 15134-15144.

Mori, H., Kondo, J., and Ihara, Y. (1987). Ubiquitin is a component of paired helical filaments in Alzheimer's disease. Science *235*, 1641-1644.

Muntane, G., Ferrer, I., and Martinez-Vicente, M. (2012). alpha-synuclein phosphorylation and truncation are normal events in the adult human brain. Neuroscience *200*, 106-119.

Murphy, J.M., Henry, R.G., Langmore, S., Kramer, J.H., Miller, B.L., and Lomen-Hoerth, C. (2007). Continuum of frontal lobe impairment in amyotrophic lateral sclerosis. Arch Neurol *64*, 530-534.

Murray, I.V., Giasson, B.I., Quinn, S.M., Koppaka, V., Axelsen, P.H., Ischiropoulos, H., Trojanowski, J.Q., and Lee, V.M. (2003). Role of alpha-synuclein carboxy-terminus on fibril formation in vitro. Biochemistry *42*, 8530-8540.

Nakashiba, T., Young, J.Z., McHugh, T.J., Buhl, D.L., and Tonegawa, S. (2008). Transgenic inhibition of synaptic transmission reveals role of CA3 output in hippocampal learning. Science *319*, 1260-1264.

Neary, D., Snowden, J.S., Gustafson, L., Passant, U., Stuss, D., Black, S., Freedman, M., Kertesz, A., Robert, P.H., Albert, M.*, et al.* (1998). Frontotemporal lobar degeneration: a consensus on clinical diagnostic criteria. Neurology *51*, 1546-1554.

Neumann, M., Sampathu, D.M., Kwong, L.K., Truax, A.C., Micsenyi, M.C., Chou, T.T., Bruce, J., Schuck, T., Grossman, M., Clark, C.M.*, et al.* (2006). Ubiquitinated TDP-43 in frontotemporal lobar degeneration and amyotrophic lateral sclerosis. Science *314*, 130-133.

Nixon, R.A. (2007). Autophagy, amyloidogenesis and Alzheimer disease. J Cell Sci *120*, 4081-4091.

Nixon, R.A. (2013). The role of autophagy in neurodegenerative disease. Nat Med *19*, 983-997.

Nixon, R.A., Wegiel, J., Kumar, A., Yu, W.H., Peterhoff, C., Cataldo, A., and Cuervo, A.M. (2005). Extensive involvement of autophagy in Alzheimer disease: an immuno-electron microscopy study. J Neuropathol Exp Neurol *64*, 113-122.

Nonaka, T., Kametani, F., Arai, T., Akiyama, H., and Hasegawa, M. (2009). Truncation and pathogenic mutations facilitate the formation of intracellular aggregates of TDP-43. Hum Mol Genet *18*, 3353-3364.

Notari, S., Strammiello, R., Capellari, S., Giese, A., Cescatti, M., Grassi, J., Ghetti, B., Langeveld, J.P., Zou, W.Q., Gambetti, P.*, et al.* (2008). Characterization of truncated forms of abnormal prion protein in Creutzfeldt-Jakob disease. J Biol Chem *283*, 30557-30565.

Novak, M., Kabat, J., and Wischik, C.M. (1993). Molecular characterization of the minimal protease resistant tau unit of the Alzheimer's disease paired helical filament. EMBO J *12*, 365-370.

Novak, M.J., and Tabrizi, S.J. (2011). Huntington's disease: clinical presentation and treatment. Int Rev Neurobiol *98*, 297-323.

Oddo, S. (2008). The ubiquitin-proteasome system in Alzheimer's disease. J Cell Mol Med *12*, 363-373.

Oddo, S., Caccamo, A., Shepherd, J.D., Murphy, M.P., Golde, T.E., Kayed, R., Metherate, R., Mattson, M.P., Akbari, Y., and LaFerla, F.M. (2003). Triple-transgenic model of Alzheimer's disease with plaques and tangles: intracellular Abeta and synaptic dysfunction. Neuron *39*, 409-421.

Orr, A.L., Li, S., Wang, C.E., Li, H., Wang, J., Rong, J., Xu, X., Mastroberardino, P.G., Greenamyre, J.T., and Li, X.J. (2008). N-terminal mutant huntingtin associates with mitochondria and impairs mitochondrial trafficking. J Neurosci *28*, 2783-2792.

Ossenkoppele, R., Schonhaut, D.R., Scholl, M., Lockhart, S.N., Ayakta, N., Baker, S.L., O'Neil, J.P., Janabi, M., Lazaris, A., Cantwell, A.*, et al.* (2016). Tau PET patterns mirror clinical and neuroanatomical variability in Alzheimer's disease. Brain.

Ou, S.H., Wu, F., Harrich, D., Garcia-Martinez, L.F., and Gaynor, R.B. (1995). Cloning and characterization of a novel cellular protein, TDP-43, that binds to human immunodeficiency virus type 1 TAR DNA sequence motifs. J Virol *69*, 3584-3596.

Ozcelik, S., Fraser, G., Castets, P., Schaeffer, V., Skachokova, Z., Breu, K., Clavaguera, F., Sinnreich, M., Kappos, L., Goedert, M.*, et al.* (2013). Rapamycin Attenuates the Progression of Tau Pathology in P301S Tau Transgenic Mice. PLoS One *8*, e62459.

Ozcelik, S., Sprenger, F., Skachokova, Z., Fraser, G., Abramowski, D., Clavaguera, F., Probst, A., Frank, S., Muller, M., Staufenbiel, M.*, et al.* (2016). Co-expression of truncated and full-length tau induces severe neurotoxicity. Mol Psychiatry.

Palhan, V.B., Chen, S., Peng, G.H., Tjernberg, A., Gamper, A.M., Fan, Y., Chait, B.T., La Spada, A.R., and Roeder, R.G. (2005). Polyglutamine-expanded ataxin-7 inhibits STAGA histone acetyltransferase activity to produce retinal degeneration. Proc Natl Acad Sci U S A *102*, 8472-8477.

Pan, T., Wong, P., Chang, B., Li, C., Li, R., Kang, S.C., Wisniewski, T., and Sy, M.S. (2005). Biochemical fingerprints of prion infection: accumulations of aberrant full-length and N-terminally truncated PrP species are common features in mouse prion disease. J Virol *79*, 934-943.

Panda, D., Samuel, J.C., Massie, M., Feinstein, S.C., and Wilson, L. (2003). Differential regulation of microtubule dynamics by three- and four-repeat tau: implications for the onset of neurodegenerative disease. Proc Natl Acad Sci U S A *100*, 9548-9553.

Parchi, P., Castellani, R., Capellari, S., Ghetti, B., Young, K., Chen, S.G., Farlow, M., Dickson, D.W., Sima, A.A., Trojanowski, J.Q.*, et al.* (1996). Molecular basis of phenotypic variability in sporadic Creutzfeldt-Jakob disease. Ann Neurol *39*, 767-778.

Parchi, P., Chen, S.G., Brown, P., Zou, W., Capellari, S., Budka, H., Hainfellner, J., Reyes, P.F., Golden, G.T., Hauw, J.J.*, et al.* (1998). Different patterns of truncated prion protein fragments correlate with distinct phenotypes in P102L Gerstmann-Straussler-Scheinker disease. Proc Natl Acad Sci U S A *95*, 8322-8327.

Park, S.Y., Tournell, C., Sinjoanu, R.C., and Ferreira, A. (2007). Caspase-3- and calpain-mediated tau cleavage are differentially prevented by estrogen and testosterone in beta-amyloid-treated hippocampal neurons. Neuroscience *144*, 119-127.

Patterson, K.R., Remmers, C., Fu, Y., Brooker, S., Kanaan, N.M., Vana, L., Ward, S., Reyes, J.F., Philibert, K., Glucksman, M.J.*, et al.* (2011). Characterization of prefibrillar Tau oligomers in vitro and in Alzheimer disease. J Biol Chem *286*, 23063-23076.

Pennuto, M., Bonanomi, D., Benfenati, F., and Valtorta, F. (2003). Synaptophysin I controls the targeting of VAMP2/synaptobrevin II to synaptic vesicles. Mol Biol Cell *14*, 4909-4919.

Perez, M., Santa-Maria, I., Gomez de Barreda, E., Zhu, X., Cuadros, R., Cabrero, J.R., Sanchez-Madrid, F., Dawson, H.N., Vitek, M.P., Perry, G.*, et al.* (2009). Tau--an inhibitor of deacetylase HDAC6 function. J Neurochem *109*, 1756-1766.

Pickford, F., Masliah, E., Britschgi, M., Lucin, K., Narasimhan, R., Jaeger, P.A., Small, S., Spencer, B., Rockenstein, E., Levine, B.*, et al.* (2008). The autophagy-related protein beclin 1 shows reduced expression in early Alzheimer disease and regulates amyloid beta accumulation in mice. J Clin Invest *118*, 2190-2199.

Piras, A., Collin, L., Gruninger, F., Graff, C., and Ronnback, A. (2016). Autophagic and lysosomal defects in human tauopathies: analysis of post-mortem brain from patients with familial Alzheimer disease, corticobasal degeneration and progressive supranuclear palsy. Acta Neuropathol Commun *4*, 22.

Poorkaj, P., Bird, T.D., Wijsman, E., Nemens, E., Garruto, R.M., Anderson, L., Andreadis, A., Wiederholt, W.C., Raskind, M., and Schellenberg, G.D. (1998). Tau is a candidate gene for chromosome 17 frontotemporal dementia. Ann Neurol *43*, 815-825.

Pop, C., and Salvesen, G.S. (2009). Human caspases: activation, specificity, and regulation. J Biol Chem *284*, 21777-21781.

Probst, A., Gotz, J., Wiederhold, K.H., Tolnay, M., Mistl, C., Jaton, A.L., Hong, M., Ishihara, T., Lee, V.M., Trojanowski, J.Q.*, et al.* (2000). Axonopathy and amyotrophy in mice transgenic for human four-repeat tau protein. Acta Neuropathol *99*, 469-481.

Prusiner, S.B. (1991). Molecular biology of prion diseases. Science *252*, 1515-1522.

Prusiner, S.B., Scott, M.R., DeArmond, S.J., and Cohen, F.E. (1998). Prion protein biology. Cell *93*, 337-348.

Qin, Z.H., Wang, Y., Kegel, K.B., Kazantsev, A., Apostol, B.L., Thompson, L.M., Yoder, J., Aronin, N., and DiFiglia, M. (2003). Autophagy regulates the processing of amino terminal huntingtin fragments. Hum Mol Genet *12*, 3231-3244.

Rademakers, R., and Rovelet-Lecrux, A. (2009). Recent insights into the molecular genetics of dementia. Trends Neurosci *32*, 451-461.

Rebeiz, J.J., Kolodny, E.H., and Richardson, E.P., Jr. (1968). Corticodentatonigral degeneration with neuronal achromasia. Arch Neurol *18*, 20-33.

Rensink, A.A., de Waal, R.M., Kremer, B., and Verbeek, M.M. (2003). Pathogenesis of cerebral amyloid angiopathy. Brain Res Brain Res Rev *43*, 207-223.

Revesz, T., Holton, J.L., Doshi, B., Anderton, B.H., Scaravilli, F., and Plant, G.T. (1999). Cytoskeletal pathology in familial cerebral amyloid angiopathy (British type) with non-neuritic amyloid plaque formation. Acta Neuropathol (Berl) *97*, 170-176.

Revesz, T., Holton, J.L., Lashley, T., Plant, G., Rostagno, A., Ghiso, J., and Frangione, B. (2002). Sporadic and familial cerebral amyloid angiopathies. Brain Pathol *12*, 343-357.

Reynolds, C.H., Garwood, C.J., Wray, S., Price, C., Kellie, S., Perera, T., Zvelebil, M., Yang, A., Sheppard, P.W., Varndell, I.M.*, et al.* (2008). Phosphorylation regulates tau interactions with Src homology 3 domains of phosphatidylinositol 3-kinase, phospholipase Cgamma1, Grb2, and Src family kinases. J Biol Chem *283*, 18177-18186.

Reynolds, M.R., Reyes, J.F., Fu, Y., Bigio, E.H., Guillozet-Bongaarts, A.L., Berry, R.W., and Binder, L.I. (2006). Tau nitration occurs at tyrosine 29 in the fibrillar lesions of Alzheimer's disease and other tauopathies. J Neurosci *26*, 10636-10645.

Rissman, R.A., Poon, W.W., Blurton-Jones, M., Oddo, S., Torp, R., Vitek, M.P., LaFerla, F.M., Rohn, T.T., and Cotman, C.W. (2004). Caspase-cleavage of tau is an early event in Alzheimer disease tangle pathology. J Clin Invest *114*, 121-130.

Roberts, S.B., Ripellino, J.A., Ingalls, K.M., Robakis, N.K., and Felsenstein, K.M. (1994). Non-amyloidogenic cleavage of the beta-amyloid precursor protein by an integral membrane metalloendopeptidase. J Biol Chem *269*, 3111-3116.

Rogers, M., Yehiely, F., Scott, M., and Prusiner, S.B. (1993). Conversion of truncated and elongated prion proteins into the scrapie isoform in cultured cells. Proc Natl Acad Sci U S A *90*, 3182-3186.

Rohn, T.T., Rissman, R.A., Davis, M.C., Kim, Y.E., Cotman, C.W., and Head, E. (2002). Caspase-9 activation and caspase cleavage of tau in the Alzheimer's disease brain. Neurobiol Dis *11*, 341-354.

Rolfs, A., Koeppen, A.H., Bauer, I., Bauer, P., Buhlmann, S., Topka, H., Schols, L., and Riess, O. (2003). Clinical features and neuropathology of autosomal dominant spinocerebellar ataxia (SCA17). Ann Neurol *54*, 367-375.

Ross, C.A., and Poirier, M.A. (2004). Protein aggregation and neurodegenerative disease. Nat Med *10 Suppl*, S10-17.

Ross, C.A., and Tabrizi, S.J. (2011). Huntington's disease: from molecular pathogenesis to clinical treatment. Lancet Neurol *10*, 83-98.

Rostagno, A., and Ghiso, J. (2008). Preamyloid lesions and cerebrovascular deposits in the mechanism of dementia: lessons from non-beta-amyloid cerebral amyloidosis. Neurodegener Dis *5*, 173-175.

Rui, Y., Gu, J., Yu, K., Hartzell, H.C., and Zheng, J.Q. (2010). Inhibition of AMPA receptor trafficking at hippocampal synapses by beta-amyloid oligomers: the mitochondrial contribution. Mol Brain *3*, 10.

Rui, Y., Tiwari, P., Xie, Z., and Zheng, J.Q. (2006). Acute impairment of mitochondrial trafficking by beta-amyloid peptides in hippocampal neurons. J Neurosci *26*, 10480-10487.

Rui, Y.N., Xu, Z., Patel, B., Chen, Z., Chen, D., Tito, A., David, G., Sun, Y., Stimming, E.F., Bellen, H.J.*, et al.* (2015). Huntingtin functions as a scaffold for selective macroautophagy. Nat Cell Biol *17*, 262-275.

Saha, A.R., Hill, J., Utton, M.A., Asuni, A.A., Ackerley, S., Grierson, A.J., Miller, C.C., Davies, A.M., Buchman, V.L., Anderton, B.H.*, et al.* (2004). Parkinson's disease alpha-synuclein mutations exhibit defective axonal transport in cultured neurons. J Cell Sci *117*, 1017-1024.

Saito, M., Chakraborty, G., Mao, R.F., Paik, S.M., Vadasz, C., and Saito, M. (2010). Tau phosphorylation and cleavage in ethanol-induced neurodegeneration in the developing mouse brain. Neurochem Res *35*, 651-659.

Sarkar, S., Davies, J.E., Huang, Z., Tunnacliffe, A., and Rubinsztein, D.C. (2007). Trehalose, a novel mTOR-independent autophagy enhancer, accelerates the clearance of mutant huntingtin and alpha-synuclein. J Biol Chem *282*, 5641-5652.

Sato, T., Miura, M., Yamada, M., Yoshida, T., Wood, J.D., Yazawa, I., Masuda, M., Suzuki, T., Shin, R.M., Yau, H.J.*, et al.* (2009). Severe neurological phenotypes of Q129 DRPLA transgenic mice serendipitously created by en masse expansion of CAG repeats in Q76 DRPLA mice. Hum Mol Genet *18*, 723-736.

Scarmeas, N., Hadjigeorgiou, G.M., Papadimitriou, A., Dubois, B., Sarazin, M., Brandt, J., Albert, M., Marder, K., Bell, K., Honig, L.S.*, et al.* (2004). Motor signs during the course of Alzheimer disease. Neurology *63*, 975-982.

Schaeffer, V., Lavenir, I., Ozcelik, S., Tolnay, M., Winkler, D.T., and Goedert, M. (2012). Stimulation of autophagy reduces neurodegeneration in a mouse model of human tauopathy. Brain *135*, 2169-2177.

Scheltens, P., Blennow, K., Breteler, M.M., de Strooper, B., Frisoni, G.B., Salloway, S., and Van der Flier, W.M. (2016). Alzheimer's disease. Lancet.

Schilling, G., Becher, M.W., Sharp, A.H., Jinnah, H.A., Duan, K., Kotzuk, J.A., Slunt, H.H., Ratovitski, T., Cooper, J.K., Jenkins, N.A.*, et al.* (1999). Intranuclear inclusions and neuritic aggregates in transgenic mice expressing a mutant N-terminal fragment of huntingtin. Hum Mol Genet *8*, 397-407.

Schweers, O., Schonbrunn-Hanebeck, E., Marx, A., and Mandelkow, E. (1994). Structural studies of tau protein and Alzheimer paired helical filaments show no evidence for beta-structure. J Biol Chem *269*, 24290-24297.

Selkoe, D.J. (2001a). Alzheimer's disease: genes, proteins, and therapy. Physiol Rev *81*, 741-766.

Selkoe, D.J. (2001b). Presenilin, Notch, and the genesis and treatment of Alzheimer's disease. Proc Natl Acad Sci U S A *98*, 11039-11041.

Sengupta, S., Horowitz, P.M., Karsten, S.L., Jackson, G.R., Geschwind, D.H., Fu, Y., Berry, R.W., and Binder, L.I. (2006). Degradation of tau protein by puromycin-sensitive aminopeptidase in vitro. Biochemistry *45*, 15111-15119.

Sergeant, N., Delacourte, A., and Buee, L. (2005). Tau protein as a differential biomarker of tauopathies. Biochim Biophys Acta *1739*, 179-197.

Shahani, N., and Brandt, R. (2002). Functions and malfunctions of the tau proteins. Cell Mol Life Sci *59*, 1668-1680.

Sherrington, R., Rogaev, E.I., Liang, Y., Rogaeva, E.A., Levesque, G., Ikeda, M., Chi, H., Lin, C., Li, G., Holman, K.*, et al.* (1995). Cloning of a gene bearing missense mutations in early-onset familial Alzheimer's disease. Nature *375*, 754-760.

Silveira, J.R., Raymond, G.J., Hughson, A.G., Race, R.E., Sim, V.L., Hayes, S.F., and Caughey, B. (2005). The most infectious prion protein particles. Nature *437*, 257-261.

Sinha, S., Anderson, J.P., Barbour, R., Basi, G.S., Caccavello, R., Davis, D., Doan, M., Dovey, H.F., Frigon, N., Hong, J.*, et al.* (1999). Purification and cloning of amyloid precursor protein beta-secretase from human brain [see comments]. Nature *402*, 537-540.

Skachokova, Z., Sprenger, F., Breu, K., Abramowski, D., Clavaguera, F., Hench, J., Staufenbiel, M., Tolnay, M., and Winkler, D.T. (2015). Amyloid-beta in the Cerebrospinal Fluid of APP Transgenic Mice Does not Show Prion-like Properties. Curr Alzheimer Res *12*, 886-891.

Snyder, H., Mensah, K., Theisler, C., Lee, J., Matouschek, A., and Wolozin, B. (2003). Aggregated and monomeric alpha-synuclein bind to the S6' proteasomal protein and inhibit proteasomal function. J Biol Chem *278*, 11753-11759.

Sokolowski, J.D., Gamage, K.K., Heffron, D.S., Leblanc, A.C., Deppmann, C.D., and Mandell, J.W. (2014). Caspase-mediated cleavage of actin and tubulin is a common feature and sensitive marker of axonal degeneration in neural development and injury. Acta Neuropathol Commun *2*, 16.

Solomon, J.P., Page, L.J., Balch, W.E., and Kelly, J.W. (2012). Gelsolin amyloidosis: genetics, biochemistry, pathology and possible strategies for therapeutic intervention. Crit Rev Biochem Mol Biol *47*, 282-296.

Spillantini, M.G., and Goedert, M. (2013). Tau pathology and neurodegeneration. Lancet Neurol *12*, 609-622.

Spillantini, M.G., Murrell, J.R., Goedert, M., Farlow, M.R., Klug, A., and Ghetti, B. (1998). Mutation in the tau gene in familial multiple system tauopathy with presenile dementia. Proc Natl Acad Sci U S A *95*, 7737-7741.

Spillantini, M.G., Schmidt, M.L., Lee, V.M., Trojanowski, J.Q., Jakes, R., and Goedert, M. (1997). Alpha-synuclein in Lewy bodies. Nature *388*, 839-840.

Spires, T.L., Orne, J.D., SantaCruz, K., Pitstick, R., Carlson, G.A., Ashe, K.H., and Hyman, B.T. (2006). Region-specific dissociation of neuronal loss and neurofibrillary pathology in a mouse model of tauopathy. Am J Pathol *168*, 1598-1607.

Spires-Jones, T.L., Friedman, T., Pitstick, R., Polydoro, M., Roe, A., Carlson, G.A., and Hyman, B.T. (2014). Methylene blue does not reverse existing neurofibrillary tangle pathology in the rTg4510 mouse model of tauopathy. Neurosci Lett *562*, 63-68.

Spires-Jones, T.L., Kopeikina, K.J., Koffie, R.M., de Calignon, A., and Hyman, B.T. (2011). Are tangles as toxic as they look? J Mol Neurosci *45*, 438-444.

Spires-Jones, T.L., Stoothoff, W.H., de Calignon, A., Jones, P.B., and Hyman, B.T. (2009). Tau pathophysiology in neurodegeneration: a tangled issue. Trends Neurosci *32*, 150-159.

Steele, J.C., Richardson, J.C., and Olszewski, J. (1964). Progressive Supranuclear Palsy. A Heterogeneous Degeneration Involving the Brain Stem, Basal Ganglia and Cerebellum with Vertical Gaze and Pseudobulbar Palsy, Nuchal Dystonia and Dementia. Arch Neurol *10*, 333-359.

Strittmatter, W.J., Saunders, A.M., Schmechel, D., Pericak-Vance, M., Enghild, J., Salvesen, G.S., and Roses, A.D. (1993). Apolipoprotein E: high-avidity binding to beta-amyloid and increased frequency of type 4 allele in late-onset familial Alzheimer disease. Proc Natl Acad Sci U S A *90*, 1977-1981.

Stromgren, E., Dalby, A., Dalby, M.A., and Ranheim, B. (1970). Cataract, deafness, cerebellar ataxia, psychosis and dementia--a new syndrome. Acta Neurol Scand *46*, Suppl 43:261+.

Sultan, A., Nesslany, F., Violet, M., Begard, S., Loyens, A., Talahari, S., Mansuroglu, Z., Marzin, D., Sergeant, N., Humez, S.*, et al.* (2011). Nuclear tau, a key player in neuronal DNA protection. J Biol Chem *286*, 4566-4575.

Sun, K.H., de Pablo, Y., Vincent, F., Johnson, E.O., Chavers, A.K., and Shah, K. (2008). Novel genetic tools reveal Cdk5's major role in Golgi fragmentation in Alzheimer's disease. Mol Biol Cell *19*, 3052-3069.

Sunyach, C., Cisse, M.A., da Costa, C.A., Vincent, B., and Checler, F. (2007). The C-terminal products of cellular prion protein processing, C1 and C2, exert distinct influence on p53-dependent staurosporine-induced caspase-3 activation. J Biol Chem *282*, 1956-1963.

Sydow, A., and Mandelkow, E.M. (2010). 'Prion-like' propagation of mouse and human tau aggregates in an inducible mouse model of tauopathy. Neurodegener Dis *7*, 28-31.

Sydow, A., Van der Jeugd, A., Zheng, F., Ahmed, T., Balschun, D., Petrova, O., Drexler, D., Zhou, L., Rune, G., Mandelkow, E.*, et al.* (2011). Tau-induced defects in synaptic plasticity, learning, and memory are reversible in transgenic mice after switching off the toxic Tau mutant. J Neurosci *31*, 2511-2525.

Tabert, M.H., Liu, X., Doty, R.L., Serby, M., Zamora, D., Pelton, G.H., Marder, K., Albers, M.W., Stern, Y., and Devanand, D.P. (2005). A 10-item smell identification scale related to risk for Alzheimer's disease. Ann Neurol *58*, 155-160.

Tagliavini, F., Prelli, F., Porro, M., Salmona, M., Bugiani, O., and Frangione, B. (1992). A soluble form of prion protein in human cerebrospinal fluid: implications for prion-related encephalopathies. Biochem Biophys Res Commun *184*, 1398-1404.

Tang, B.L. (2009). Neuronal protein trafficking associated with Alzheimer disease: from APP and BACE1 to glutamate receptors. Cell Adh Migr *3*, 118-128.

Tanzi, R.E. (1999). A genetic dichotomy model for the inheritance of Alzheimer's disease and common age-related disorders. J Clin Invest *104*, 1175-1179.

Tanzi, R.E., Gusella, J.F., Watkins, P.C., Bruns, G.A., St George-Hyslop, P., Van Keuren, M.L., Patterson, D., Pagan, S., Kurnit, D.M., and Neve, R.L. (1987). Amyloid beta protein gene: cDNA, mRNA distribution, and genetic linkage near the Alzheimer locus. Science *235*, 880-884.

Tapiola, T., Alafuzoff, I., Herukka, S.K., Parkkinen, L., Hartikainen, P., Soininen, H., and Pirttila, T. (2009). Cerebrospinal fluid {beta}-amyloid 42 and tau proteins as biomarkers of Alzheimer-type pathologic changes in the brain. Arch Neurol *66*, 382-389.

Terry, R.D., Masliah, E., Salmon, D.P., Butters, N., DeTeresa, R., Hill, R., Hansen, L.A., and Katzman, R. (1991). Physical basis of cognitive alterations in Alzheimer's disease: synapse loss is the major correlate of cognitive impairment. Ann Neurol *30*, 572-580.

Thathiah, A., and De Strooper, B. (2011). The role of G protein-coupled receptors in the pathology of Alzheimer's disease. Nat Rev Neurosci *12*, 73-87.

Thies, E., and Mandelkow, E.M. (2007). Missorting of tau in neurons causes degeneration of synapses that can be rescued by the kinase MARK2/Par-1. J Neurosci *27*, 2896-2907.

Tofaris, G.K., and Spillantini, M.G. (2005). Alpha-synuclein dysfunction in Lewy body diseases. Mov Disord *20 Suppl 12*, S37-44.

Trevitt, C.R., Hosszu, L.L., Batchelor, M., Panico, S., Terry, C., Nicoll, A.J., Risse, E., Taylor, W.A., Sandberg, M.K., Al-Doujaily, H.*, et al.* (2014). N-terminal domain of prion protein directs its oligomeric association. J Biol Chem *289*, 25497-25508.

Trinczek, B., Biernat, J., Baumann, K., Mandelkow, E.M., and Mandelkow, E. (1995). Domains of tau protein, differential phosphorylation, and dynamic instability of microtubules. Mol Biol Cell *6*, 1887-1902.

Tseng, B.P., Green, K.N., Chan, J.L., Blurton-Jones, M., and Laferla, F.M. (2007). Abeta inhibits the proteasome and enhances amyloid and tau accumulation. Neurobiol Aging.

Turnbaugh, J.A., Unterberger, U., Saa, P., Massignan, T., Fluharty, B.R., Bowman, F.P., Miller, M.B., Supattapone, S., Biasini, E., and Harris, D.A. (2012). The N-terminal, polybasic region of PrP(C) dictates the efficiency of prion propagation by binding to PrP(Sc). J Neurosci *32*, 8817-8830.

Usenovic, M., Niroomand, S., Drolet, R.E., Yao, L., Gaspar, R.C., Hatcher, N.G., Schachter, J., Renger, J.J., and Parmentier-Batteur, S. (2015). Internalized Tau Oligomers Cause Neurodegeneration by Inducing Accumulation of Pathogenic Tau in Human Neurons Derived from Induced Pluripotent Stem Cells. J Neurosci *35*, 14234-14250.

Van Raamsdonk, J.M., Pearson, J., Slow, E.J., Hossain, S.M., Leavitt, B.R., and Hayden, M.R. (2005). Cognitive dysfunction precedes neuropathology and motor abnormalities in the YAC128 mouse model of Huntington's disease. J Neurosci *25*, 4169-4180.

Vassar, R., Bennett, B.D., Babu-Khan, S., Kahn, S., Mendiaz, E.A., Denis, P., Teplow, D.B., Ross, S., Amarante, P., Loeloff, R.*, et al.* (1999). Beta-secretase cleavage of Alzheimer's amyloid precursor protein by the transmembrane aspartic protease BACE. Science *286*, 735-741.

Vereecken, T.H., Vogels, O.J., and Nieuwenhuys, R. (1994). Neuron loss and shrinkage in the amygdala in Alzheimer's disease. Neurobiol Aging *15*, 45-54.

Vidal, R., Frangione, B., Rostagno, A., Mead, S., Revesz, T., Plant, G., and Ghiso, J. (1999). A stop-codon mutation in the BRI gene associated with familial British dementia. Nature *399*, 776-781.

Vidal, R., Revesz, T., Rostagno, A., Kim, E., Holton, J.L., Bek, T., Bojsen-Moller, M., Braendgaard, H., Plant, G., Ghiso, J.*, et al.* (2000). A decamer duplication in the 3' region of the BRI gene originates an amyloid peptide that is associated with dementia in a Danish kindred. Proc Natl Acad Sci U S A *97*, 4920-4925.

Violet, M., Chauderlier, A., Delattre, L., Tardivel, M., Chouala, M.S., Sultan, A., Marciniak, E., Humez, S., Binder, L., Kayed, R.*, et al.* (2015). Prefibrillar Tau oligomers alter the nucleic acid protective function of Tau in hippocampal neurons in vivo. Neurobiol Dis *82*, 540-551.

von Bergen, M., Barghorn, S., Biernat, J., Mandelkow, E.M., and Mandelkow, E. (2005). Tau aggregation is driven by a transition from random coil to beta sheet structure. Biochim Biophys Acta *1739*, 158-166.

Vonsattel, J.P., and DiFiglia, M. (1998). Huntington disease. J Neuropathol Exp Neurol *57*, 369-384.

Waldemar, G., Dubois, B., Emre, M., Georges, J., McKeith, I.G., Rossor, M., Scheltens, P., Tariska, P., Winblad, B., and Efns (2007). Recommendations for the diagnosis and management of Alzheimer's disease and other disorders associated with dementia: EFNS guideline. Eur J Neurol *14*, e1-26.

Waldron-Roby, E., Ratovitski, T., Wang, X., Jiang, M., Watkin, E., Arbez, N., Graham, R.K., Hayden, M.R., Hou, Z., Mori, S.*, et al.* (2012). Transgenic mouse model expressing the caspase 6 fragment of mutant huntingtin. J Neurosci *32*, 183-193.

Wali, G., Sutharsan, R., Fan, Y., Stewart, R., Tello Velasquez, J., Sue, C.M., Crane, D.I., and Mackay-Sim, A. (2016). Mechanism of impaired microtubule-dependent peroxisome trafficking and oxidative stress in SPAST-mutated cells from patients with Hereditary Spastic Paraplegia. Sci Rep *6*, 27004.

Wang, H.Y., Wang, I.F., Bose, J., and Shen, C.K. (2004). Structural diversity and functional implications of the eukaryotic TDP gene family. Genomics *83*, 130-139.

Wang, J.Z., Gong, C.X., Zaidi, T., Grundke-Iqbal, I., and Iqbal, K. (1995). Dephosphorylation of Alzheimer paired helical filaments by protein phosphatase-2A and -2B. J Biol Chem *270*, 4854-4860.

Wang, J.Z., Grundke-Iqbal, I., and Iqbal, K. (2007). Kinases and phosphatases and tau sites involved in Alzheimer neurofibrillary degeneration. Eur J Neurosci *25*, 59-68.

Wang, X., Su, B., Lee, H.G., Li, X., Perry, G., Smith, M.A., and Zhu, X. (2009a). Impaired balance of mitochondrial fission and fusion in Alzheimer's disease. J Neurosci *29*, 9090-9103.

Wang, Y., Martinez-Vicente, M., Kruger, U., Kaushik, S., Wong, E., Mandelkow, E.M., Cuervo, A.M., and Mandelkow, E. (2009b). Tau fragmentation, aggregation and clearance: the dual role of lysosomal processing. Hum Mol Genet *18*, 4153-4170.

Weingarten, M.D., Lockwood, A.H., Hwo, S.Y., and Kirschner, M.W. (1975). A protein factor essential for microtubule assembly. Proc Natl Acad Sci U S A *72*, 1858-1862.

Weissmann, C., Reyher, H.J., Gauthier, A., Steinhoff, H.J., Junge, W., and Brandt, R. (2009). Microtubule binding and trapping at the tip of neurites regulate tau motion in living neurons. Traffic *10*, 1655-1668.

Wellington, C.L., Ellerby, L.M., Gutekunst, C.A., Rogers, D., Warby, S., Graham, R.K., Loubser, O., van Raamsdonk, J., Singaraja, R., Yang, Y.Z.*, et al.* (2002). Caspase cleavage of mutant huntingtin precedes neurodegeneration in Huntington's disease. J Neurosci *22*, 7862-7872.

Wellington, C.L., Singaraja, R., Ellerby, L., Savill, J., Roy, S., Leavitt, B., Cattaneo, E., Hackam, A., Sharp, A., Thornberry, N.*, et al.* (2000). Inhibiting caspase cleavage of huntingtin reduces toxicity and aggregate formation in neuronal and nonneuronal cells. J Biol Chem *275*, 19831-19838.

West, M.J., Coleman, P.D., Flood, D.G., and Troncoso, J.C. (1994). Differences in the pattern of hippocampal neuronal loss in normal ageing and Alzheimer's disease. Lancet *344*, 769-772.

Westergard, L., Turnbaugh, J.A., and Harris, D.A. (2011). A naturally occurring C-terminal fragment of the prion protein (PrP) delays disease and acts as a dominant-negative inhibitor of PrPSc formation. J Biol Chem *286*, 44234-44242.

Wilhelmsen, K.C., Lynch, T., Pavlou, E., Higgins, M., and Nygaard, T.G. (1994). Localization of disinhibition-dementia-parkinsonism-amyotrophy complex to 17q21-22. Am J Hum Genet *55*, 1159-1165.

Winner, B., Jappelli, R., Maji, S.K., Desplats, P.A., Boyer, L., Aigner, S., Hetzer, C., Loher, T., Vilar, M., Campioni, S.*, et al.* (2011). In vivo demonstration that alpha-synuclein oligomers are toxic. Proc Natl Acad Sci U S A *108*, 4194-4199.

Winslow, A.R., Chen, C.W., Corrochano, S., Acevedo-Arozena, A., Gordon, D.E., Peden, A.A., Lichtenberg, M., Menzies, F.M., Ravikumar, B., Imarisio, S.*, et al.* (2010). alpha-Synuclein impairs macroautophagy: implications for Parkinson's disease. J Cell Biol *190*, 1023-1037.

Wischik, C.M., Edwards, P.C., Lai, R.Y., Roth, M., and Harrington, C.R. (1996). Selective inhibition of Alzheimer disease-like tau aggregation by phenothiazines. Proc Natl Acad Sci U S A *93*, 11213-11218.

Wischik, C.M., Novak, M., Edwards, P.C., Klug, A., Tichelaar, W., and Crowther, R.A. (1988a). Structural characterization of the core of the paired helical filament of Alzheimer disease. Proc Natl Acad Sci U S A *85*, 4884-4888.

Wischik, C.M., Novak, M., Thogersen, H.C., Edwards, P.C., Runswick, M.J., Jakes, R., Walker, J.E., Milstein, C., Roth, M., and Klug, A. (1988b). Isolation of a fragment of tau derived from the core of the paired helical filament of Alzheimer disease. Proc Natl Acad Sci U S A *85*, 4506-4510.

Wittmann, C.W., Wszolek, M.F., Shulman, J.M., Salvaterra, P.M., Lewis, J., Hutton, M., and Feany, M.B. (2001). Tauopathy in Drosophila: neurodegeneration without neurofibrillary tangles. Science *293*, 711-714.

Xu, B., Liu, W., Deng, Y., Yang, T.Y., Feng, S., and Xu, Z.F. (2015). Inhibition of calpain prevents manganese-induced cell injury and alpha-synuclein oligomerization in organotypic brain slice cultures. PLoS One *10*, e0119205.

Yamamoto, A., Cremona, M.L., and Rothman, J.E. (2006). Autophagy-mediated clearance of huntingtin aggregates triggered by the insulin-signaling pathway. J Cell Biol *172*, 719-731.

Yamamoto, H., Saitoh, Y., Fukunaga, K., Nishimura, H., and Miyamoto, E. (1988). Dephosphorylation of microtubule proteins by brain protein phosphatases 1 and 2A, and its effect on microtubule assembly. J Neurochem *50*, 1614-1623.

Young, J.E., Gouw, L., Propp, S., Sopher, B.L., Taylor, J., Lin, A., Hermel, E., Logvinova, A., Chen, S.F., Chen, S.*, et al.* (2007). Proteolytic cleavage of ataxin-7 by caspase-7 modulates cellular toxicity and transcriptional dysregulation. J Biol Chem *282*, 30150-30160.

Zhang, Q., Zhang, X., and Sun, A. (2009a). Truncated tau at D421 is associated with neurodegeneration and tangle formation in the brain of Alzheimer transgenic models. Acta Neuropathol *117*, 687-697.

Zhang, Y., Li, M., Drozda, M., Chen, M., Ren, S., Mejia Sanchez, R.O., Leavitt, B.R., Cattaneo, E., Ferrante, R.J., Hayden, M.R.*, et al.* (2003). Depletion of wild-type huntingtin in mouse models of neurologic diseases. J Neurochem *87*, 101-106.

Zhang, Y.J., Xu, Y.F., Cook, C., Gendron, T.F., Roettges, P., Link, C.D., Lin, W.L., Tong, J., Castanedes-Casey, M., Ash, P.*, et al.* (2009b). Aberrant cleavage of TDP-43 enhances aggregation and cellular toxicity. Proc Natl Acad Sci U S A *106*, 7607-7612.

Zhang, Y.J., Xu, Y.F., Dickey, C.A., Buratti, E., Baralle, F., Bailey, R., Pickering-Brown, S., Dickson, D., and Petrucelli, L. (2007). Progranulin mediates caspase-dependent cleavage of TAR DNA binding protein-43. J Neurosci *27*, 10530-10534.

Zhang, Y.W., Thompson, R., Zhang, H., and Xu, H. (2011). APP processing in Alzheimer's disease. Mol Brain *4*, 3.

Zou, W.Q., Capellari, S., Parchi, P., Sy, M.S., Gambetti, P., and Chen, S.G. (2003). Identification of novel proteinase K-resistant C-terminal fragments of PrP in Creutzfeldt-Jakob disease. J Biol Chem *278*, 40429-40436.

Prince et al. 2015: http://www.worldalzreport2015.org/downloads/world-alzheimer-report-2015.pdf

# 7 Abbreviations

| | |
|---|---|
| **α-Syn** | α-synuclein |
| **aa** | amino acids |
| **Aβ** | amyloid beta |
| **ABri** | amyloid-Bri |
| **ABriPP** | amyloid-Bri precursor |
| **ADAM** | adamalysin protease |
| **ADAM10** | a desintegrin and metalloproteinase 10 |
| **ADan** | amyloid-Dan |
| **ADanPP** | amyloid-Dan precursor |
| **AD** | Alzheimer's disease |
| **AgD** | argyrophilic grain disease |
| **AICD** | APP intracellular domain |
| **ALS** | amyotrophic lateral sclerosis |
| **AnxA2** | annexin A2 |
| **APH1** | anterior pharynx defective 1 |
| **ApoE4** | apolipoprotein E4 |
| **APP** | amyloid precursor protein |
| **Asp** | aspartic acid |
| **ATP** | adenosine triphosphate |
| **$BRI_2$** | BRICHOS domain containing 2B |
| **C-terminal** | carboxy terminal |
| **CAA** | cerebral amyloid angiopathy |
| **CAG** | cytosine-adenine-guanine trinucleotide repeats |
| **CaM** | calmodulin |
| **CBD** | corticobasal degeneration |
| **cdk;cdc** | cyclin-dependent kinase |
| **CHMP2B** | charged multivescular body protein 2B |
| **CjD** | Creutzfeldt-Jakob disease |
| **CK** | casein kinase |
| **CNS** | central nervous system |
| **CSF** | cerebrospinal fluid |
| **CTF** | C-terminal fragment |

| | |
|---|---|
| **DLB** | dementia with Lewy bodies |
| **DNA** | deoxyribonucleic acid |
| **DRPLA** | Dentatorubral-pallidoluysian atrophy |
| **E391** | C-terminal truncated tau at Glutamic Acid[391] |
| **ECL** | enhanced chemiluminescence |
| **EOAD** | early-onset AD |
| **ER** | endoplasmatic reticulum |
| **g** | gram |
| **GA** | golgi apparatus |
| **GGT** | globular glial tauopathy |
| **GPI** | glycosylphosphatidylinositol |
| **GSK3** | glycogen synthase kinase 3 |
| **GSS** | Gerstmann-Sträussler-Scheinker diseases |
| **FAD** | familial AD |
| **FBD** | familial British dementia |
| **FDD** | familial Danish dementia |
| **FTD** | frontotemporal dementia |
| **FTLD** | frontotemporal lobar degeneration |
| **FTDP-17T** | FTD and parkinsonism linked to chromosome 17 |
| **GSK3** | glycogen synthase kinase 3 |
| **h** | hour |
| **HD** | Huntington disease |
| **htt** | huntingtin |
| **IAPP** | hormone islet amyloid peptide |
| **IHC** | immunohistochemistry |
| **JNK** | c-Jun N-terminal kinase |
| **kDa** | kilo daltons |
| **LB** | Lewy bodies |
| **LN** | Lewy neurites |
| **LOAD** | late-onset AD |
| **MAPK** | microtubule associated protein kinase |
| **MAPT** | microtubule associated protein tau |
| **MARK** | microtubule-affinity regulating kinase |
| **mRNA** | messenger ribunucleic acid |
| **MSA** | multiple system atrophy |
| **MTB** | microtubule binding domain |
| **µm** | micrometer(s) |
| **mm** | millimeter(s) |
| **mM** | milli molar |
| **MMP** | matrix metalloproteinase |
| **Mn** | manganese |
| **N-terminal** | amino terminal |
| **NTF** | amino terminal fragment |
| **nm** | nanometer(s) |
| **nmol** | nanomolar |
| **NFT** | neurofibrillary tangle |
| **PBS** | phosphate buffered saline |
| **PCR** | polymerase chain reaction |

| | |
|---|---|
| **PCs** | proprotein convertases |
| **PD** | Parkinson's disease |
| **PEN-2** | presenilin enhancer 2 |
| **PGRN** | progranulin |
| **PHF** | paired helical filaments |
| **PiD** | Pick's disease |
| **PK** | protein kinase |
| **PolyQ** | Polyglutamine disease |
| **PP** | phosphatase |
| **PRNP** | PRioN Protein |
| **$PrP^C$** | cellular prion protein |
| **$PrP^{Sc}$** | scrapie prion protein |
| **PRR** | pronline-rich region |
| **PS1/2** | presenilin 1 and 2 |
| **PSA** | puromycin-sensitive aminopeptidase |
| **PSP** | progressive supranuclear palsy |
| **RRM** | RNA-recognition motifs |
| **sAPP** | soluble ectodomain of APP |
| **SAA** | serum amyloid A |
| **SCA** | spinocerebellar-ataxia |
| **SH3** | SCR Homology-3 |
| **SPPL2** | signal peptide peptidase-like 2 |
| **TARDBP** | transactive response DNA binding protein |
| **TDP-43** | transactive response DNA binding protein 43 kDA |
| **TRD** | Trinucleotide repeat expansion disorder |
| **TTR** | Globular protein transthyretin |
| **UPS** | ubiquitine proteasome system |
| **tTs** | tetracycline controlled transcriptional silencer element |
| **VAMP2** | vesicle associated membrane protein |